UNIVERSITY OF CALIFORNIA

SANTA CRUZ

CHARACTERIZING THE ROLE OF THE COUPLING PROTEINS CHEV1 AND CHEW IN *HELICOBACTER PYLORI* CHEMOTAXIS

A dissertation submitted in partial satisfaction
of the requirements for the degree of

DOCTOR OF PHILOSOPHY

in

MICROBIOLOGY AND ENVIRONMENTAL TOXICOLOGY

by

Samar Abedrabbo

December 2016

The Dissertation of Samar Abedrabbo is approved:

_____
Professor Karen M. Ottemann, Chair

_____
Professor Fitnat H. Yildiz

_____
Professor Manel Camps

_____
Professor Seth M. Rubin

_____
Tyrus Miller
Vice Provost and Dean of Graduate Studies

TABLE OF CONTENTS

LIST OF FIGURES

LIST OF TABLES

ABSTRACT

Characterizing the role of the coupling proteins CheV1 and CheW in *Helicobacter pylori* chemotaxis

By

Samar Abedrabbo

Many microbes use chemotaxis as a system for thriving and colonizing their various environmental niches. Chemotaxis is the ability of organisms to swim toward favorable environments and away from toxic environments. *Helicobacter pylori* is a chemotactic pathogen that infects over half the world's population and successfully colonizes the gastric mucosa of humans. Chemotaxis is an important virulence factor that helps *H. pylori* effectively colonize the human stomach.

The chemotaxis complex system consists of proteins: chemoreceptors, coupling proteins, and the CheA kinase. Chemoreceptors sense the environment and transmit the response to the CheA kinase through coupling proteins. Coupling proteins of the CheW or CheV type physically link chemoreceptors to the CheA kinase. *H. pylori* has a unique chemotaxis system that contains multiple coupling proteins, one CheW and three CheV proteins—CheV1, CheV2, and CheV3 respectively that all play a role in chemotaxis. It is unknown why some chemotaxis systems contain multiple types of coupling proteins.

In this thesis, the role and function of the coupling proteins CheV1 and CheW was investigated, as well as the stoichiometry of the chemotaxis proteins that

make up the chemoreceptor-CheA kinase complex in *H. pylori.* CheV1 and CheW have similar protein interaction networks *in vivo* and *in vitro* with the chemoreceptors, the CheA kinase, and themselves. Both proteins promoted CheA autophosphorylation activity with CheW having slightly better CheA activation than CheV1. CheV1 and CheW were also both needed to retain the CheA kinase at the cell membrane where the chemotaxis complex is found. Cellular localization of the chemoreceptors and CheA kinase required the presence of both CheV1 and CheW. Ultimately, these results indicate that CheV1 and CheW work together to promote super chemotaxis cluster formation at cell poles which is important for eliciting a chemotaxis response. Also reported here are the concentration and ratio of the chemotaxis proteins in *H. pylori*. *H. pylori* possessed significantly higher concentrations of chemoreceptors, coupling proteins, and the CheA kinase in comparison to *E. coli* and *B. subtilis*. Despite these differences, a chemoreceptor trimer of dimers to one CheA dimer was maintained in *H. pylori*. There was also a conserved ratio of 1.8 CheW to 1 CheA dimer like *B. subtilis* and *E. coli*. The stoichiometry of the chemotaxis proteins was also analyzed in *cheV1* and *cheW* mutants. While the amount of CheW or CheV1 did not vary without the other, we did find that there was a low amount of CheA without CheW or the chemoreceptors. Addition of a protease inhibitor restored CheA amounts in mutants, protein interactions within the chemotaxis complex protect proteins from degradation. Finally, we found that cheV1 mutants rapidly accumulate suppressor mutants in a soft agar assay.

I dedicate this Ph.D. in Microbiology to the children of Syria that continue to risk their lives to go to school and to the children that war has forced out of school to support their families tirelessly. I dedicate this to the children that still have faith in a brighter future despite losing everything from a tragic war.

"The pen is mightier than the sword."

ACKNOWLEDGEMENTS

I would like to thank many amazing people for their help during my Ph.D. journey. First and foremost, my deepest and sincerest gratitude goes to my Ph.D. advisor, Prof. Karen Ottemann. Karen is a compassionate supportive mentor. She has assisted me extensively throughout my project, both academically and emotionally, with encouraging wisdom and patience. Her cheerful words and optimism always brighten my days and inspire me to keep working hard and not give up. Thank you for being the best mentor.

I would also like to thank members of my Ph.D. committee who have provided critical insight into my project: Prof. Fitnat Yildiz, Prof. Manel Camps, and Prof. Seth Rubin. I am grateful for your support of my research project and the guidance you have provided. I also thank all the professors of the METX Department for their caring support during my PhD. I would also like to thank Prof. Johnson Zehr and Prof. Adam Martiny for the wonderful time I spent researching cyanobacteria in their labs.

I would like to thank my lab mates for their tremendous help during my research: Dr. Daniela Keilberg, Kieran Collins, Kevin Johnson, Christina Yang, and Jashwin Sagoo. Thank you for making our lab a fun supportive environment. I would also like to thank Juan Castellon for his patience and care in training me during the start of my research in the Ottemann Lab.

Finally, none of this would be possible without the continuous support of my family and friends. First, I would like to thank my family for teaching me to

always be kind, humble, and helpful towards anyone I meet. I would like to thank them for always believing in me and supporting everything I dream of. Thank you for always pushing me one step further than what I want for myself—I love you. I would like to thank my brother, Tarek Abedrabbo, for showing me what it means to be a fighter—your strength inspires me. I would like to thank my dad for teaching me to always be kind and respectful towards everyone I meet. I would like to thank my twin brother for telling me to keep going no matter how long it takes. I would like to thank my uncle Bassam Fadli for always supporting me tirelessly throughout my educational journey—I love you.

I would like to thank my fiancé for his wonderful encouragement and love during this journey and for always showing me the brighter side to every situation and always keeping me smiling. Lastly, to my friends who believed in me no matter how tough things became, thank you for pushing me to keep going despite the challenges and obstacles even if just to pour one more agar plate. Thank you for always pushing me to "keep swimming."

I dedicate this to my mom, Basima Fadli, for her tremendous love and care for our family—I love you and I hope you are in heaven smiling and proud. This is for you.

CHAPTER 1

Helicobacter pylori and bacterial chemotaxis signal transduction

1.1 Background

1.1.1 *H. pylori* morphology, physiology, & metabolism

Helicobacter pylori is a human pathogen that was identified in 1982 by Barry Marshall and Robin Warren and infects over half the world's population (Kusters, van Vliet and Kuipers, 2006). It is a gram negative spiral-shaped bacterium that belongs to the class Epsilonproteobacteria. Four *H. pylori* strain genomes have been completely sequenced: strains 26695, J99, HPAG1, and G27 (Yamaoka, 2008) (Baltrus *et al.*, 2009). Numerous genetically-diverse *H. pylori* strains exist with an approximate genome size of 1.7 million base pairs containing around 1500 genes (Mobley Harry L.T, 2001) (McClain *et al.*, 2009). *H. pylori* is 2-4 um in length and 0.5-1 um in width. *H. pylori* has five-seven flagella on one end of the microbe used for motility (Mobley Harry L.T, 2001). Despite being spiral-shaped, it can convert into a coccoid shape in possibly nutrient-limited environments; the coccoid form is thought to be viable but non-culturable.

H. pylori is a microaerophilic acid-tolerant microbe that inhabits the gastric mucosa of the human stomach (Kusters, van Vliet and Kuipers, 2006). This bacterium has a somewhat simple genome, and lacks genes that would allow a complex metabolism (Kusters, van Vliet and Kuipers, 2006). The human stomach is a very acidic environment and *H. pylori* acclimates to this acidic environment by

having the ability to neutralize its surroundings by the enzyme urease. Urease buffers the microbe's surrounding environment by converting urea into ammonia and bicarbonate; this is essential for *H. pylori* colonization (Mobley Harry L.T, 2001). *H. pylori* is also catalase and oxidase positive. Glucose is the only carbohydrate that *H. pylori* can use despite preferring amino acids for energy metabolism (Kusters, van Vliet and Kuipers, 2006).

H. pylori contains five major outer membrane protein families which include adhesions, transmembrane diffusion channel proteins, and iron-regulation proteins (Yamaoka, 2008). The outer membrane proteins containing lipopolysaccharides (LPS) are important virulence factors of *H. pylori* because they are used by the bacterium to both interact with its environment as well as respond to the host's immune response during infection (Yamaoka, 2008).

1.1.2 Pathology

H. pylori causes multiple diseases that include gastritis, peptic ulcers, gastric mucosa-associated lymphoid tissue lymphoma (MALT), as well as gastric cancer; all infected individuals develop chronic gastritis (Bauer and Meyer, 2011) (Cover and Blaser, 2009). It is the only known bacteria that is a risk factor for human cancer and is classified as a class I carcinogen (Polk and Peek, 2010). One of the factors that leads to *H. pylori*'s persistent infection and colonization in the human gastric mucosa is its ability to modulate adhesion to the mucosa through its outer membrane proteins (Clyne, Dolan and Reeves, 2007). Some virulence factors that

determine disease outcome include: the vaculating cytotoxin (VacA) and the type IV secretion system encoded in the Cag pathogenicity island found in various *H. pylori* strains (Mobley Harry L.T, 2001).

1.1.3 Bacterial survival strategy: chemotaxis

To survive in the human stomach niche, a fluctuating environment, *H. pylori* presumably must be able to sense environmental signals effectively to swim towards beneficial environments and away from harmful signals, a process called chemotaxis. Chemotaxis is a process used by many bacteria to survive in their environment. To fully successfully colonize and infect the gastric niche, *H. pylori* must be chemotactic as chemotaxis mutants infect less well than wild type in mice and piglet animal model systems (Foynes *et al.*, 2000) (Terry *et al.*, 2005). Thus a deeper understanding of chemotaxis as a two-component signal transduction is discussed below.

1.2 Two-component signal transduction system

Two-component systems are common signal transduction systems that are common in many organisms including bacteria (Hoch *et al.* 2000). Two-component systems (TCS) typically consist of a histidine kinase and a response regulator that affects the final bacterial response/activity. In general, a sensed signal activates histidine kinases leading to their autophosphorylation on a conserved histidine residue; the phosphoryl group is then transferred from the histidine kinase to a conserved aspartate residue on the response regulator that leads to a bacterial

response (Fig. 1). Response regulators typically act as transcriptional regulators that target specific genes following various signals sensed by the histidine kinase (Gao *et al.* 2009).

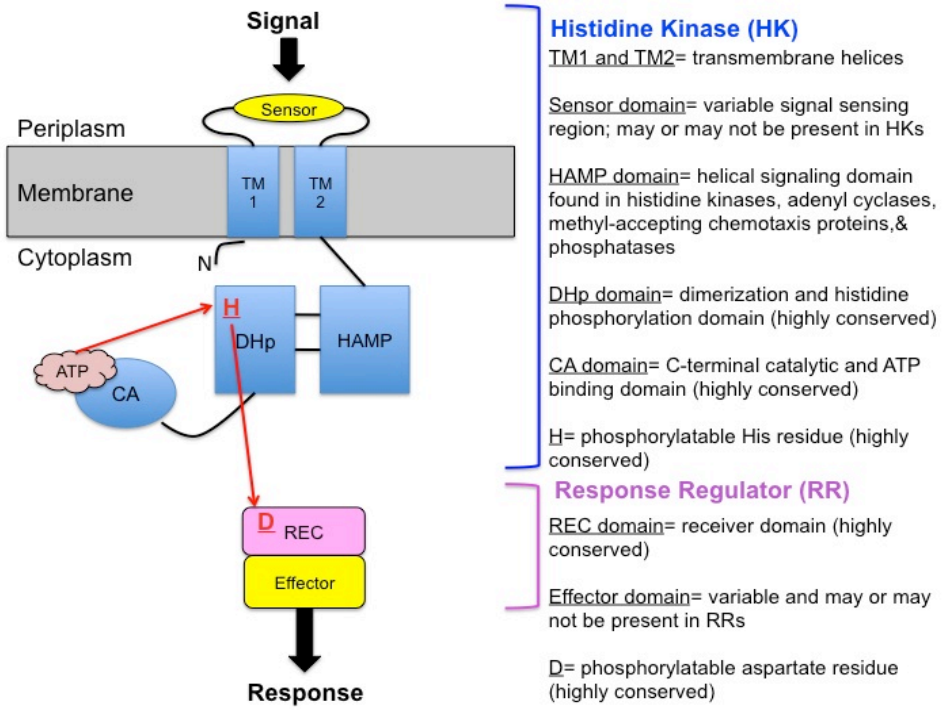

Figure 1.1. Two-component signal transduction system.

1.2.1 Histidine kinase

The histidine kinase is typically the component of the TCS that senses environmental stimuli and acts as the input for the signal transduction pathway. Histidine kinases are generally homodimeric integral membrane proteins that contain an extracellular sensor domain between two transmembrane (TM) helices (Fig. 1) (Mascher *et al.* 2006). A HAMP domain comes after the second transmembrane helix. The HAMP domain is connected to the dimerization and histidine phosphorylation domain (DHp) followed by a catalytic domain (CA) that

binds ATP at the C-terminus of the histidine kinase. Histidine kinases are dimers; homodimerization occurs between the TM helices, the HAMP domains, and DHp domains of the histidine kinase. A conserved histidine residue is found in the DHp domain and is phosphorylated by an ATP phosphoryl group transfer. The phosphoryl group is transferred to the response regulator (Fig. 1). The DHp and CA domains are highly conserved in the histidine kinase. The histidine kinase structure as a whole contains conserved sequences called the H, N, G1, F, and G2 boxes (Gao *et al.* 2009).

Sensor domains have very diverse sequences among various organisms and may or may not be present in histidine kinases (Gao *et al.* 2009). The most common annotations of sensor domains from various organisms have shown that they consist of PAS, GAF, or PDC domains (Wang *et al.* 2012). Sensor domains have mostly been found to consist of the following structural folds: mixed αß, all-helical, and ß-sandwich (Wang *et al.* 2012). The purpose of sensory domains is to sense environmental ligands/stimuli which explains why they are so variable among different organisms.

HAMP domains are found in histidine kinases, adenylyl cyclases, methyl accepting chemotaxis proteins, and phosphatases. They are also generally found in bacterial receptors and serve to connect the sensing domain to the signaling domain of the histidine kinase. HAMP domains are dimers that are made up of two alpha helices (Wang *et al.* 2012). They form dimers with the DHp domain.

The CA domain has catalytic activity and binds ATP and is also called HATPase_c domain (Finn *et al.* 2007). It is a conserved domain and has an αβ sandwich fold (Wang *et al.* 2012). The CA domain is a monomer and contains the N, G1, F, and G2 sequence motifs in which there is an ATP-binding cavity (Gao *et al.* 2009). Within these sequences, there exists a region that changes conformation when an ATP is bound in the CA domain called the ATP lid. The ATP lid covers the ATP binding site and protects a bound ATP from hydrolysis once it enters yet when no ATP is bound, the ATP lid is flexible (Wang *et al* 2012). When an ATP binds, the CA domain then transfers the phoshphoryl group from the bound ATP to the histidine residue in the DHp domain.

The DHp domain is made up of two alpha helices and contains the conserved phosphorylatable histidine residue on one alpha helix and is also called the His kinase A domain (Finn *et al.* 2007). This His residue is in the H box (Gao *et al.* 2009). The histidine reside is autophosphorylated by an ATP bound to the catalytic (CA) domain. The phosphorylated histidine residue then is able to transfer its phosphoryl group to the response regulator.

The exact mechanism of how histidine kinase signaling occurs is not quite known but it is thought that changes in the sensory domain structures during ATP binding leads to conformational changes of the histidine kinase that may allow changes in its protein-protein interactions (Gao *et al.* 2009).

1.2.2 Response regulator

Response regulators affect the final bacterial response and are the output response of the TCS that are affected by the histidine kinase. They typically contain two domains: a highly-conserved receiver (REC) domain and a less conserved effector domain (Fig. 1). The receiver domain has a conserved $(\beta\alpha)_5$ fold. It contains a conserved aspartate residue that is phosphorylated by a phosphoryl group transfer from the histidine kinase (Wang *et al.* 2012). It is thought that response regulators generally function as dimers when active (Wang *et al.* 2012). Phosphorylation changes the conformation of the response regulator leading to its affinity for its targets (Gao *et al.* 2009). Structural changes occur on the response regulator once phosphorylation occurs in which conserved residues switch orienting the aspartate residue for phosphorylation. Response regulators typically function as transcriptional activators and thus most effector domains are DNA binding domains or enzymatic domains (Gae *et al.* 2009).

1.3 Chemotaxis system

1.3.1 *Escherichia coli* model

One of the most studied signal transduction pathways is chemotaxis that functions by using a histidine kinase and response regulator system. The chemotaxis pathway is found in many bacteria but has been well-studied in *Escherichia coli* (Wadhams *et al.* 2004). In *E. coli,* the bacterial chemotaxis system includes multiple transmembrane chemoreceptors that sense environmental parameters, a coupling

protein that physically couples receptors to the histidine kinase, CheA, and the response regulator, CheY, that together drive the direction of flagellar rotation leading to different bacterial swimming responses (Fig. 2). There are three additional chemotaxis regulatory proteins—CheR, CheB, and CheZ—that influence the chemotactic swimming response and are discussed below (Porter, Wadhams and Armitage, 2011) (Kirby, 2009).

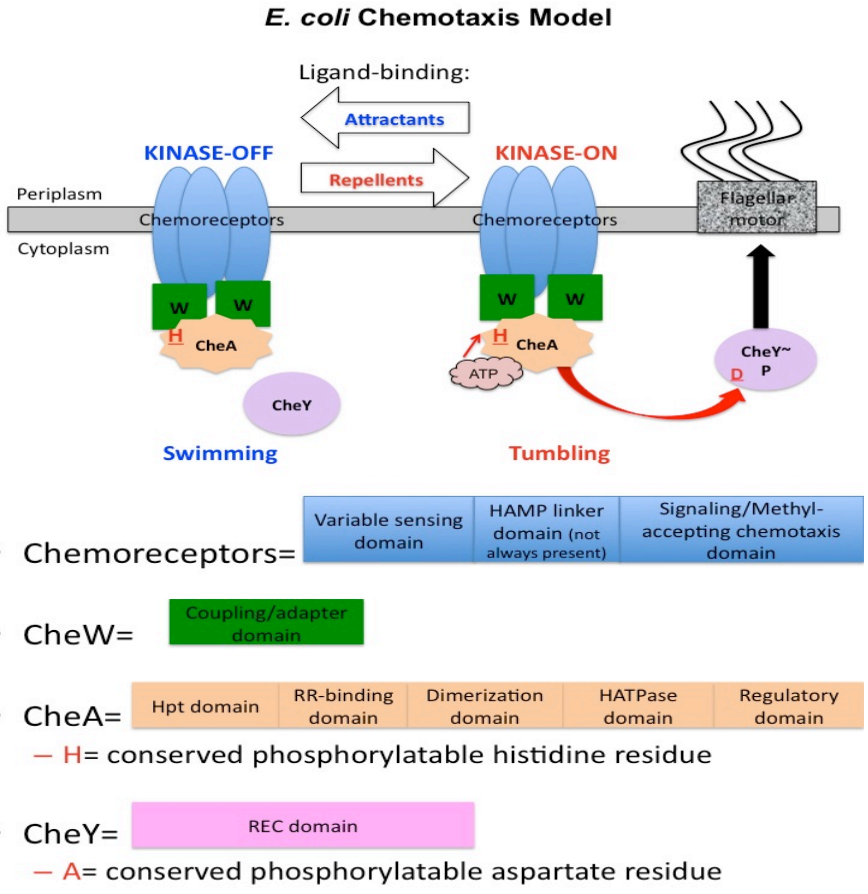

Figure 1.2. *E. coli* chemotaxis model & protein domains. In this system, signals are detected by the transmembrane chemoreceptors, CheW links the chemoreceptor with CheA kinase activity which influences CheY. The phosphorylation state of CheY ultimately affects motility by altering flagella motor rotation—CheY~P results in counterclockwise flagellar rotation (tumbling), CheY results in clockwise rotation (swimming).

The *E. coli* transmembrane chemoreceptors are made up of a periplasmic ligand binding sensory domain and a cytoplasmic methyl-accepting signaling domain. A signal is detected in the sensory domain and the response is transmitted to the cytoplasmic signaling domain of the chemoreceptor where a complex of chemoreceptor-associated proteins are found. Sensory domains are generally quite variable yet the cytoplasmic domain is conserved among chemoreceptors. The cytoplasmic domain typically contains four conserved domains: a HAMP domain, a methylated helix (MH1), a signaling domain, and a methylated helix 2 (MH2) domain (Baker *et al.* 2005). The structure of *E. coli*'s chemoreceptor has been shown to be a trimer of dimers that is involved in the ternary complex and has been shown to form clusters at the signaling domain (Kentner *et al.*, 2006). Chemoreceptors undergo a conformational change when a signal (attractant or repellant) is detected, either directly or indirectly through a periplasmic binding protein. This chemoreceptor conformational change drives the microbe's chemotactic response by altering the chemoreceptor—CheW—CheA ternary complex and overall transmitting a change in the flagellar rotation direction.

CheW plays a crucial role as a coupling, or scaffold, protein that physically links the chemoreceoptor with the histidine kinase CheA. This complex regulates the transfer of phosphoryl groups to other chemotaxis proteins with regard to the presence of positive or negative stimulants. CheW also plays a role in maintaining the stability of the trimers of dimers chemoreceptor complexes in *E. coli*(Kentner *et al.*, 2006) (Studdert and Parkinson, 2005). Bacteria are non-chemotactic without the

function of the CheW coupling protein linking the chemotaxis components because information cannot be signaled between the chemoreceptor and kinase (Boukhvalova *et al.* 2002).

Environmental signals affect swimming behavior by influencing CheA histidine kinase activity: positive signals (attractants) decrease kinase activity, resulting in swimming, and negative signals (repellants) increase kinase activity resulting in tumbling motility. In the presence of a negative signal binding to its appropriate transmembrane chemoreceptor, CheA autophosphorylates itself and passes the phosphoryl group to the response regulators CheY. Phosphorylated CheY (CheY~P) ultimately results in cell tumbling by Che Y~P binding the flagella motor proteins, FliM and FliN, and changes the rotation of flagella from counterclockwise to clockwise rotation .However, in the presence of a positive signal (attractant), CheA kinase activity is inhibited resulting in counterclockwise flagellar rotation and leading to smooth swimming activity. The phosphorylation state of CheY thus determines flagella rotation. This motility status of the bacteria, swimming or tumbling, is thus influenced by CheY phosphorylation status. The longevity of the bacteria's motile response to various signals is kept in check by the CheA kinase acting on CheY as well as a phosphatase protein, CheZ which plays a critical role in controlling CheY dephosphorylation. The CheZ phosphatase protein acclerates CheY's intrinsic autodephosphorylation, removes the phosphoryl group from CheY~P and so returns flagella to their default counterclockwise rotation.

Some bacterial cells, including *E. coli*, have an adaptation system, which controls the bacteria's ability to chemotactically respond to various distinct environmental signals. In the *E. coli* chemotaxis system, the adaptation response is maintained by the methylesterase CheB protein and the methyltransferase CheR protein. These proteins demethylate and methylate chemoreceptors in the adaptation process so the cell can respond to different stimulant chemical gradients. CheB can be phosphorylated by CheA which results in its increased methylesterase activity on the chemoreceptor and this ultimately returns the cells to its basal anticlockwise flagella rotation. Thus both kinase activity and chemoreceptor methylation state drive the overall chemotactic response through control of the flagellar motor rotation.

Signaling in the chemotaxis pathway leads to a piston-like movement in the chemoreceptor which is then transmitted to the cytoplasmic domains of the chemoreceptors that leads to the bacterial response through interaction with the coupling protein and the histidine kinase.

CheA Histidine Kinase

CheA is a soluble cytoplasmic homodimeric histidine kinase protein. CheA is generally made up of five conserved domains that include: a histidine phosphotransfer (Hpt) domain, the response regulator binding domain, a dimerization domain, the histidine kinase protein kinase catalytic (HATPase) domain, and the regulatory domain (Bilwes *et al*. 1999). The HATPase domain corresponds to the CA domain and the Hpt domain corresponds to the DHp domain

of the TCS histidine kinase. The *E. coli* CheA domain has a P2 domain that is capable of binding CheY (Wuichet *et al.* 2007). The Hpt domain, which contains the conserved histidine residue, is responsible for the transfer of the phosphoryl group from ATP to the aspartate residue contained in the response regulator CheY (Baker *et al.* 2005). Like general histidine kinase structures, the ATP lid of CheA changes conformation upon binding ATP leading to changes in protein interactions (Bilwes *et al.* 1999).

CheY Response Regulator

The CheY protein is a soluble monomer made up of a receiver (REC) domain only and is phosphorylatable. CheY is phosphorylated through interaction with the response regulator binding domain of CheA (Baker *et al.* 2005). Phosphorylated CheY (CheY~P) interacts with the bacterium's flagellar motor and alters flagellar rotation leading to bacterial tumbling. Phosphorylation occurs on an aspartate residue (Asp57) on CheY that causes a change in the CheY structural β/ α fold (Dyer *et al.* 2006). This change in structure allows CheY to bind to the flagellar motor protein, FliM, through exposure of one the CheY protein interfaces (Dyer *et al.* 2006).

CheW Coupling Protein

The CheW protein in *E. coli* consists of a coupling domain with conserved residues that bind the signaling domain of the chemoreceptor and alternate conserved residues for CheA histidine kinase binding (Boukhvalova *et al.* 2002).

CheW is a soluble protein that is a monomer made up of two five-stranded beta barrels plus two adjacent alpha helices (Alexander *et al.* 2010).

The *E. coli* chemotaxis system is very similar to those observed in other microbes that exhibit slightly more diversity and complexity in their respective chemotactic signaling systems. Common deviations observed in microbial chemotaxis systems include: the presence of alternative coupling proteins known as CheVs, differences in proteins involved in adaptation, various CheY~P phosphatase proteins, and other accessory chemotaxis proteins. These differences are illustrated in multiple bacterial species including *H. pylori, C. jejuni , B. subtilis,* and *S. typhimurium*, as described below.

1.3.2 *Helicobacter pylori* model

The chemotaxis signal transduction pathway of *H. pylori* is different from that found in *E. coli* in a few ways, including the presence of a hybrid CheAY histidine kinase, the presence of three CheV proteins in *H. pylori*, the absence of the adaptation proteins CheB and CheR, the presence of an atypical CheZ phosphatase, and a protein of unknown function called ChePep.

The chemotaxis system of *H. pylori* is made up of the core chemotaxis components—chemoreceptors, CheW, CheA, and CheY that all function similarly to orthologs in *E. coli* (Lertsethtakarn, Draper and Ottemann, 2012). *H. pylori* uses chemotaxis in response to environmental signals in its gastric niche. Attractants the bacteria swim towards include various amino acids, zinc, and cholesterol, whereas

repellants include low pH, autoinducer-2, and various toxic metals. *H. pylori* has four chemoreceptors: TlpA, TlpB, TlpC, and TlpD that sense various signals. Unlike the chemoreceptors found in *E. coli* that are all integral membrane chemoreceptors, the TlpD chemoreceptor of *H. pylori* is a soluble cytoplasmic chemoreceptor. With the exception of TlpC, these chemoreceptors have known responses to different signals: TlpA senses arginine and bicarbonate, TlpB senses low pH and autoinducer-2, and TlpD is involved in responding to cellular energy status (Lertsethtakarn, Draper and Ottemann, 2012).

In *H. pylori*, a chemoreceptor senses a signal and communicates the information to the CheA kinase through physical interaction maintained by the CheW coupling protein which plays a crucial role as seen in *E. coli* (Fig. 3). Unlike *E. coli* though, *H. pylori* has alternative CheW-like coupling proteins termed CheV proteins. *H. pylori* possesses three CheV proteins in addition to the CheW coupling protein. The CheV protein, which is thought to have similar function to the *E. coli* CheW coupling protein was first discovered in the gram-positive bacterium *Bacillus subtilis* (Rosario *et al.* 1994). As in *E. coli*, these coupling proteins link the chemoreceptors to the CheA kinase and possibly play have other role(s) in chemotaxis such as chemoreceptor—CheA cluster stabilization (Kentner *et. al.* 2006).

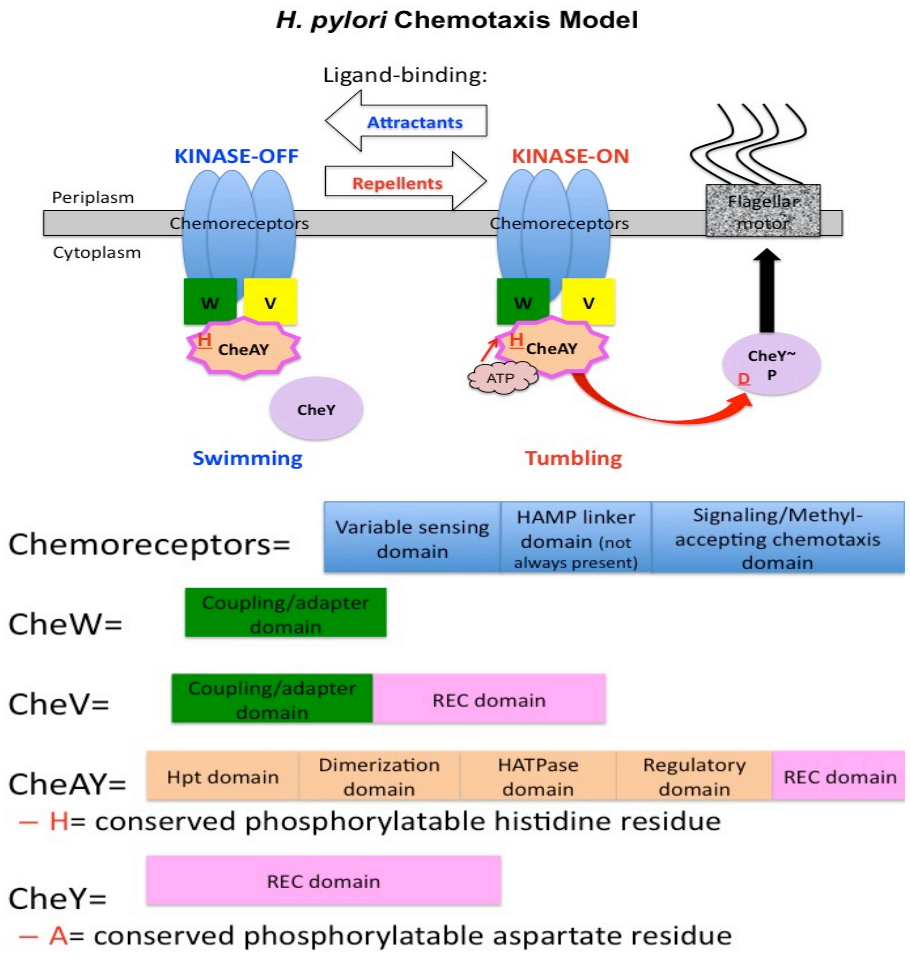

Figure 1.3. *H. pylori* chemotaxis model & protein domains. The chemotaxis system of *H. pylori* contains various chemoreceptors that are linked to the CheA histidine kinase through CheW or CheV coupling proteins. The CheAY kinase protein acts on the CheY response regulator shown.

CheA Histidine Kinase

H. pylori's CheA protein is a hybrid protein made up of both a histidine kinase-like domain and a response regulator (CheY, REC)-like domain thus giving it both kinase and phosphatase activity. Because of the additional response regulator domain, REC domain at its C-terminus, unlike that found in *E. coli*, the *H. pylori* CheA is often called "CheAY" (Foynes *et al.* 2000). The CheAY REC domain is

thought to play a role in the autophosphorylation of CheAY yet the exact function of the CheAY REC domain is not quite known (Lertsethtakaran *et al.* 2012). The CheAY REC domain, however, does shorten the half life of phosphorylated CheAY, as compared to CheA with the REC domain deleted (Jimenez-Pearson *et al.* 2005). The CheA-like domain of *H. pylori*'s CheAY protein is similar to the *E. coli* CheA and contains the same four core conserved domains as discussed in the *E. coli* section, except it lacks the P2 domain seen in *E. coli* (Wuichet *et al.* 2007). As observed in *E. coli, H. pylori*'s CheA is autophosphorylated at a conserved histidine residue by ATP. Autophosphorylated CheA passes its phosphoryl group to the CheY response regulator.

CheY Response Regulator

Similarly to *E. coli*, the response regulator, CheY, affects *H. pylori* flagellar rotation: phosphorylated CheY interacts with the flagellar motor proteins, FliM and FliN, resulting in bacterial tumbling (Sarkar *et al.* 2010). CheY is made up of a REC domain that is capable of being phosphorylated at a conserved aspartate residue (Jimenez-Pearson *et al.* 2005). The CheY structure is a $(\beta/\alpha)_5$ fold which is generally the structure observed in response regulators (Lam *et al.* 2010).

CheW & CheV Coupling Proteins

H. pylori has a CheW protein that is solely made up of a coupling domain similar to that observed in *E. coli* with the same conserved residues that allow CheW to bind to both chemoreceptor(s) and the CheA histidine kinase (Lowenthal *et al.* 2009; Alexander *et al.* 2010).

CheV is a hybrid protein made up of a CheW-like N-terminal domain and a phosphorylatable C-terminal domain that is homologous to response regulators (REC) (Fredrick *et al.* 1994). Unlike the CheW protein that only has a coupling domain, the three CheV proteins consist of both a coupling domain (CheW domain) and a phosphorylated REC domain (Alexander *et al.* 2010). REC domains are thought to allow for the modulation of CheV proteins by phosphorylation, similar to the role of the REC domain of the response regulator CheY.

H. pylori's coupling proteins—CheW and three CheVs (CheV1, CheV2, CheV3—all affect the chemotactic system to different degrees. Unlike the effect of CheV mutants, deletion of CheW renders the bacteria completely non-chemotactic with decreased mouse stomach colonization ability (Terry *et al.*, 2005). In a chemotaxis soft agar motility assay, the *cheV1* mutant was found to have a rather significant chemotaxis defect as reflected in a severe decrease in its motility and expanded colony formation rate compared to *cheV2* and *cheV3* mutants; *cheV2* and *cheV3* mutants had a slight chemotaxis defect with minor decrease in their migration abilities(Pittman, Goodwin and Kelly, 2001) (Lowenthal, Simon, *et al.*, 2009). *cheV1* and *cheV2* mutants also are smooth swimming behavior biased and a *cheV3* mutant is hyperswitching behavior biased as observed in a fixed-time diffusion model (Lowenthal, Simon, *et al.*, 2009). Lowenthal *et al*. has suggested that it is possible that CheV1 and CheV2 may thus activate CheA unlike CheV3 which seems to deactivate CheA(Lowenthal, Simon, *et al.*, 2009). It is clear that all three CheV proteins are involved in chemotaxis and have a similar function to the

CheW coupling protein. Whether *H. pylori* chemoreceptors prefer specific CheW or CheV coupling proteins is currently unknown.

CheV proteins may also play a role in adaptation in *H. pylori* because this microbe lacks the typical adaptation methylation system proteins—Che B methylesterase and CheR methyltransferase. CheV proteins in *H. pylori* have been shown to be possibly involved in adaptation because of their ability to remove a phosphoryl group from CheA as well as being able to control phosphorylation of themselves (Jiménez-Pearson *et al.*, 2005).

Dephosphorylation of CheY in *H. pylori* can be promoted by CheZ and possibly the FliY phosphatase (Lertsethtakarn, Draper and Ottemann, 2012). CheZ increase the autodephosphorylation activity of CheY. The CheZ phosphatase protein in *H. pylori* is unique in that it can also dephosphorylate the CheA REC domain and the CheV2 protein (Lertsethtakarn and Ottemann, 2010). The FliY phosphatase protein is part of the flagellar switch proteins of *H. pylori* not found in *E. coli.* The FliY does not have a CheY~P binding domain (Lowenthal, Hill, *et al.*, 2009). Whether *H. pylori* FliY is a phosphatase, however, remains to be determined.

Finally, ChePEP is a newly discovered accessory chemotaxis protein in *H. pylori* whose exact chemotaxis function has yet to be elucidated (Howitt and Lee, 2011). It has been shown to contain a N-terminal REC domain and possibly have a role similar to the CheZ phosphatase protein (Howitt and Lee, 2011).

1.3.3 *Campylobacter jejuni* model

A close relative of *H. pylori*, *Campylobacter jejuni* is also chemotactic. *C. jejuni* has ten chemoreceptors—seven integral membrane chemoreceptors and three soluble chemoreceptors which respond to similar stimulants as *H. pylori* including amino acids, carbohydrates, and organic acids as attractants(Lertsethtakarn, Ottemann and Hendrixson, 2011). Its chemotaxis system is very similar to that found in *H. pylori*, but it only has one CheV protein (Lertsethtakarn, Ottemann and Hendrixson, 2011) (Hartley-tassell *et al.*, 2010). It is suggested that the CheV protein of *C. jejuni* is similar to CheW because of similar defective phenotypes observed between both *cheV* and *cheW* mutants in a chemotaxis assay (Hartley-tassell *et al.*, 2010). This depleted nutrient chemotaxis assay showed that the *cheV* mutant had a slightly higher decrease in its motility rate in comparison to the *cheW* mutant. CheV protein has also been shown to be preferentially couple a specific *C. jejuni* chemoreceptor with CheA in comparison to the CheW coupling protein (Hartley-tassell *et al.*, 2010).

1.3.4 *Bacillus subtilis* model

The chemotaxis system of *B. subtilis* exhibits more complexity than that observed in *E. coli* by having a CheV protein as well as additional adaptation proteins—CheC and CheD (Fig. 4) (Porter, Wadhams and Armitage, 2011). CheC is a phosphatase similar to the CheZ phosphatase of *H. pylori* that functions in *B. subtilis* adaptation; CheD acts as a CheA kinase (Rao, Glekas and Ordal, 2008).

There are 10 chemoreceptors present in this organism in comparison to the 5 *E. coli* transmembrane chemoreceptors. In this bacterium, the default flagellar rotation is clockwise rotation that promotes tumbling movement and is the reverse of the *E. coli* default counterclockwise flagellar rotation.

CheW and CheV are required for a full chemotactic response in *B. subtilis* (Karatan *et al.*, 2001). *cheW* and *cheV* mutants both display smooth swimming behavior bias due to counterclockwise flagellar rotation (Karatan *et al.*, 2001). CheV also plays a role in mediating the adaptation response in addition to functioning as a CheW-like coupling protein(Karatan *et al.*, 2001). The adaptation response involving the CheV was observed using a *cheV* truncated mutant that was not able to return to the prestimulus state, a characteristic of microbe adaptation (Karatan *et al.*, 2001). *B. subtilis* also has a FliY phosphatase protein known to act on CheY~P and unlike *H. pylori* has a CheY~P binding sequence (Szurmant *et al.*, 2003).

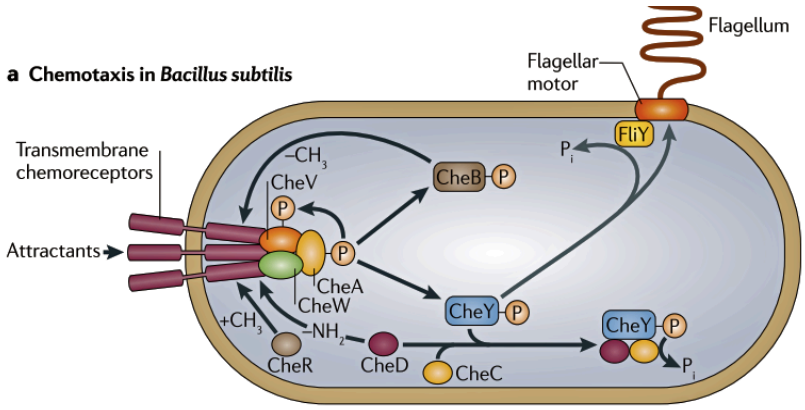

Figure 1.4 (Porter, Wadhams and Armitage, 2011)**: *B. subtilis* chemotaxis system.** Upon binding of an attractant to the chemoreceptors, CheA is autophosphorylated and donates its phosphoryl group to CheY; CheY~P binds to FliM resulting in swimming by anticlockwise flagellar rotation and CheY~P dephosphorylation occurs by FliY; CheW and CheV function to link the chemoreceptor and CheA kinase. CheC—CheD and CheR—CheB systems function in adaptation. This figure was obtained from Porter et al. 2011.

The chemotaxis system is thus a critical conserved system found in various motile microbes with slight alterations between different bacterial species as noted in Table 1.

Table 1.1. Chemotaxis system comparisons. Some data was obtained from Porter et al. 2011.

	E. coli	***H. pylori***	***B. subtilis***	***C. jejuni***
Phylum	Proteobacteria	Proteobacteria	Firmicutes	Proteobacteria
Class	Gammaproteobacteria	Epsilonproteobacteria	Bacilli	Epsilonproteobacteria
Stimuli detected	Periplasmic concentration of stimuli; Oxygen	Periplasmic and cytomplasmic concentration of stimuli	External concentration of stimuli; Oxygen	Periplasmic concentration of stimuli
Chemoreceptors present	5	4 (3 integral and 1 soluble)	10	10 (7 integral membrane and 3 soluble)
Chemoreceptor types	Transmembrane	Transmembrane & cytoplasmic	Transmembrane & cytoplasmic	Transmembrane and cytoplasmic
Flagella	4-6, peritrichous	6-8, polar	4-9, peritrichous	Single, bipolar
Rotation direction	Bidirectional	Bidirectional	Bidirectional	Bidirectional
CheY~P rotation effect	counterclockwise → clockwise (tumbling/direction changes)	counterclockwise→ clockwise (tumbling/direction changes)	Clockwise → anticlockwise	counterclockwise→ clockwise (tumbling/direction changes)
Default flagella rotation	Counterclockwise	Counterclockwise	Clockwise	Counterclockwise
Signaling cluster locations	Cell poles	Cell poles (unpublished)	Cell poles	Cell poles(Briegel *et al.*, 2009)
Signal termination mechanisms	CheZ phosphatase for CheY-P	CheZ & possibly FliY phosphatases for CheY-P	No CheZ, CheC & FliY phosphatases for CheY-P	CheZ & FliY phosphatases for CheY-P dephosphorylation
CheVs present	none	3 CheVs	1	1
CheV function	N/A	-All 3 CheVs important for chemotaxis--exact function not known	-CheW-like coupling protein -Mediates adaptation	-*cheV* mutants have a chemotaxis defect like *chew* mutant

		-*cheV1* mutants have most severe chemotaxis phenotype -*cheV2* & *cheV3* show slight effects -*cheV1* and *cheV2* mutants show smooth swimming behavior -*cheV3* mutants have opposite hyperswitching behavior	to attractants	so maybe plays a rold as an alternate coupling protein
Adaptation proteins	-CheR and CheB methylation adaptation system	-No methylation adaptation system	-CheR and CheB methylation adaptation system -CheV -CheC, CheD	-CheR and CheB methylation adaptation system
Other unique chemotaxis proteins		-ChePep -FliY	-CheC, CheD	-FliY

1.4 Experimental methods for investigating the chemotaxis protein interactions and localization

The chemotaxis system has been investigated thoroughly in bacteria using various methods often including motility assays, protein-protein interaction methods, and localization assays (Miller, Russel, Matthew and Alexander, 2009).

1.4.1 Protein-protein interaction

Protein-protein interaction methods are a valuable tool to better understand the possible function of chemotaxis proteins whose exact function has yet to be elucidated.

Two-hybrid system: Two-hybrid screening is a method to test the various proteins that a protein physically interacts with in a cell. In this system, yeast and bacteria (generally *E. coli*) have been used as popular model organisms for studying protein interactions, each model has its own advantages and disadvantages discussed below.

Bacterial two-hybrid system: The bacterial adenylate cyclase two-hybrid (BACTH) system was developed in 1998 and relies on reconstituting the activity of adenylate cyclase in *E. coli* (Karimova *et al.*, 1998). This system allows you to study the interaction among both membrane and cytoplasmic proteins and is thus very useful. The method is based on using the adenylate cyclase toxin of *Bordetella pertussis* because of its unique properties in *E. coli*. Adenylate cyclase is an enzyme that synthesizes cyclic adenosine 3', 5'-monophosphate (cAMP). cAMP forms a complex with the catabolite activator protein (CAP); the cAMP/CAP complex is responsible for regulating the transcription of many genes such as *lactose* gene activation. The simple detection of such activated genes controlled by the cAMP/CAP forms the basis of this system in *E. coli*.

The adenylate cyclase toxin of *B. pertussis* is a large protein with a catalytic domain that contains 2 sub-domains: a 25 kDa fragment and an 18 kDa fragment. The adenylate cyclase toxin becomes active when it binds calmodulin (only found

in eukaryotes) and the 18 kDa fragment contains the binding site for the calmodulin protein. The two sub-domains interact when calmodulin is present to synthesize cAMP. It is this close interaction between the 25 kDa catalytic fragment and the 18 kDa fragment resulting in cAMP production that forms the basis of the BACTH system. Proteins of interest are fused to the T25 and T18 fragments to test for their interaction; protein-protein interaction is detected when proteins fused to the two sub-domains interact in a bacterial strain whose endogenous adenylate cyclase enzyme has been deleted (*cya*- strain) resulting in cAMP production.

This method is experimentally typically done in an *E. coli cya*- strain that has been transformed with T25 and T18 plasmids. The T25 and T18 plasmids contain the proteins of interest fused to the individual fragments and positive interaction between both plasmids is detected in the transformed *E. coli* strain using the appropriate assay (i.e. blue colonies on LB/X-gal plates or red color on lactose/maltose MacConkey plates).

BACTH compatible vectors with antibiotic resistance are designed with the proteins of interest fused at to their N-terminal or C-terminal based on their characteristics to the T25 and T18 fragments. The fused proteins are obtained by inserting the gene of interest in a multiple cloning site contained in both the T25 and T18 fragments. The multiple cloning sites of the fragments contain various restriction enzyme cutting sites allowing for digestion of the fragment plasmids with appropriate enzymes that are also used to digest the genes of interest. After digestion of the plasmids and genes of interest, the gene of interest is ligated to the

plasmid creating fusion proteins within the plasmids. The T25 fragment is contained in the plasmid PKT25 or PKNT25; the T18 fragment is contained in the PUT18 or PUT18C plasmid. The plasmid pairs differ in the location of the multiple cloning site in the T25 or T18 fragments allowing for the fusion at either the N or C-terminal of the protein fragments.

The recombinant plasmids are under the transcriptional control of a lac promoter. These hybrid plasmids are then transformed in *E. coli* strains DHM1 and BTH101 which are both *cya*- strains commonly used in BACTH. A common positive control measure used is performed with T25-zip and T18-zip plasmids; a common negative control is done with empty T25 and T18 plasmids against each protein of interest. The protein of interest, commonly termed the "bait" is for example fused with the T18 domain and other protein interacting candidates, termed the "prey" are constructed as a genomic library to test for bait-prey interaction. Interaction is then detected using reporter genes that are transcribed upon cAMP/CAP complex binding to their respective promoters.

After detection of interaction on reporter assays, analysis and confirmation of the specific protein-protein interactions can be done using various ways including: redoing the BACTH using the fully cloned protein of interest instead of the commonly used protein fragment, co-purification analysis, and doing a yeast-two hybrid (Battesti and Bouveret, 2012).

In comparison to other hybrid screening systems, BACTH is highly beneficial because of its ability to detect membrane protein interactions as

previously shown in membrane protein studies(White, Kitich and Gober, 2010). This is due to the product of the BACTH protein interaction being cAMP, a diffusible molecule so protein interaction is detected and can occur anywhere in the cell(Battesti and Bouveret, 2012). The BACTH is thus a good useful system for investigating the interaction of chemotaxis proteins such as CheV proteins with membrane proteins. Another advantage of the system is that it uses *E. coli* as the host, a very efficient transformation model. Drawbacks of the BACTH include the possible detection of false positives due to "sticky protein" formation as well as the possibility of getting no interaction due to the nature of protein fusion to the T25 and T18 fragments causing incorrect protein folding or instability (Battesti and Bouveret, 2012).

Yeast two-hybrid system: The yeast two-hybrid system is very similar in theory to the BACTH discussed above. The yeast two hybrid system has also been previously used to successfully investigate the protein-protein interaction of a *C. jejuni* chemoreceptor Tlp1 (Hartley-tassell *et al.*, 2010). In brief, a protein of interest (termed the "bait') is fused to the DNA binding domain (DNA-BD) and other interacting protein candidates are fused to the activation domain (AD). Fusion proteins are created by cloning the gene of interest into the multiple cloning site of either the AD or DNA-BD domains within the appropriate plasmids. The multiple cloning sites of the domains contain unique restriction enzyme cutting sites similar to those found in the T25 and T18 fragments of the BACTH system allowing for in-

frame cloning of genes of interest into the appropriate plasmids containing complementary domains.

The interaction of the bait protein with another protein brings the DBD and AD close together in yeast. This results in the reconstitution of a transcription factor, typically the yeast GAL transcription factor that can bind to the upstream activating sequence of GAL to activate transcription of a reporter gene such as lacZ or HIS3. The reporter gene can by easily assayed similarly to the methods used to assay the transcription of various reporter genes in the BACTH system.

A possible benefit of this system over the BACTH is for studying eukaryotic proteins that are post-translationally modified which the *E. coli* system cannot do. Another advantage of the yeast two hybrid system is that it is an *in vivo* assay unlike other protein-protein interaction methods such as co-immunoprecipitation. One complication of the yeast two hybrid system is false positives due to the false activation of reporter genes. Both two hybrid systems, bacterial and yeast, may also be insufficient due to the possibility of changing protein stability because of the creation of fusions.

Co-immunoprecipitation

Another widely-used method for the investigation of protein-protein interactions is co-immunoprecipitation. This method has been previously used in *H. pylori* and is a valuable assay to study all the possible protein interactions a single protein may have as well as being an additional method to confirm the results of a

two-hybrid screens (Voland *et al.*, 2003). Co-immunoprecipitation essentially works by co-precipitating out a protein complex of interacting proteins potentially bound to the protein of interest (the "bait") being studied. This procedure is done by designing an antibody targeted against the protein of interest (the antigen) which immunoprecipitates out of a sample while also co-precipitating other interacting proteins (Fig.5) (Motif, 2008). Antibody binding beads are then added to the sample to capture the protein complex which is eluted out by a series of washes. The precipitated protein complex is then analyzed by running an SDS-PAGE and Western blot.

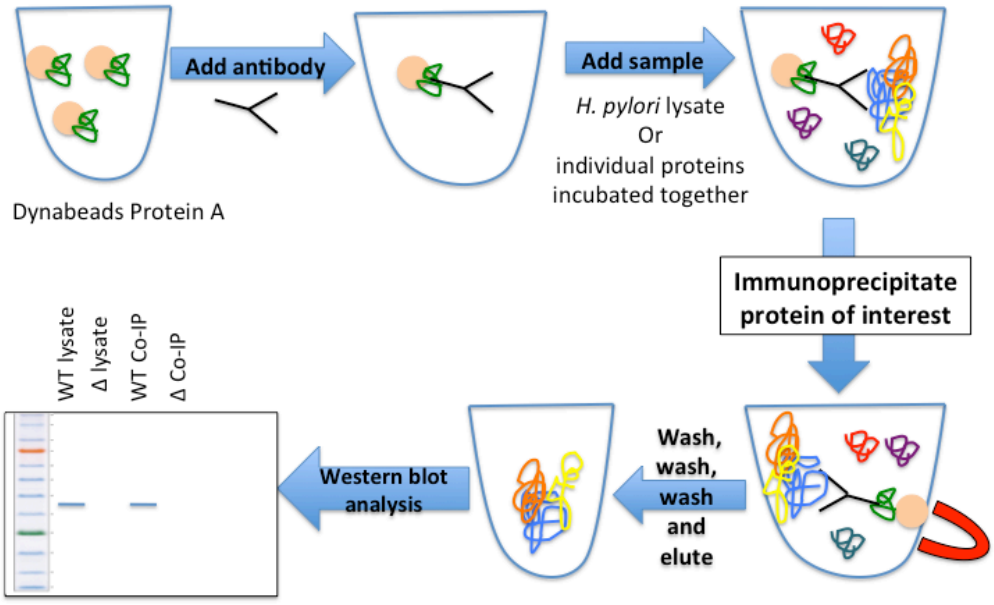

Figure 1.5: Co-Immunoprecipitation procedure. In brief, an antibody designed to target the protein of interest is used to precipitate out the protein of interest. This also results in precipitation of all interacting proteins with the protein of interest. The precipitated products are analyzed using a Western blot to determine the various interacting proteins.

An advantage of using co-immunoprecipitation to study protein-protein interactions is that the protein structures are usually not disrupted as seen in the two-hybrid assays due to protein fusion constructions. The proteins studied are also post-translationally modified and the conditions under which co-immunoprecipitation is done are generally non-denaturing and very close to the cell's physiologic state. Some caveats of the co-immunoprecipitation method include the significance of designing a correct antibody against the protein of interest. Also, it is sometimes difficult to detect low-affinity protein interactions using this method.

1.4.2 Protein localization

Immunofluorescence has proved to be a valuable method for investigating the localization of chemotaxis proteins within bacterial cells. Clustering of chemotaxis proteins has been studied extensively in chemotactic microbes that have shown to have various localization of their chemotaxis proteins classified as polar, lateral, and/or diffused (Piñas *et al.*, 2016).

This technique is generally done in multiple steps that with the goal of eventually being able to view the localization of the protein of interest using fluorescence microscopy. Cells are first fixed on microscope slides coated with poly-L-lysine. Fixation is done to preserve cell integrity and is achieved using a fixative, typically periodate-lysine paraformaldehyde (PLP) which works by cross-linking proteins. The specimen is then washed and blocking buffer is added to inhibit any non-specific binding of antibodies. Primary antibody designed to target

the protein of interest is then added as well as a primary antibody targeting the specific microbe that is being investigated. These two primary antibodies must have different animal sources such as rabbit and chicken. The specimen is then incubated and washed again with blocking buffer. After these steps, secondary antibodies with a conjugated fluorescent tag are added. The secondary antibodies are designed for detecting the primary antibodies added initially and are also made in another animal source such as goat. The specimen is then washed and ready for visualization under a fluorescent microscope (Fig. 6).

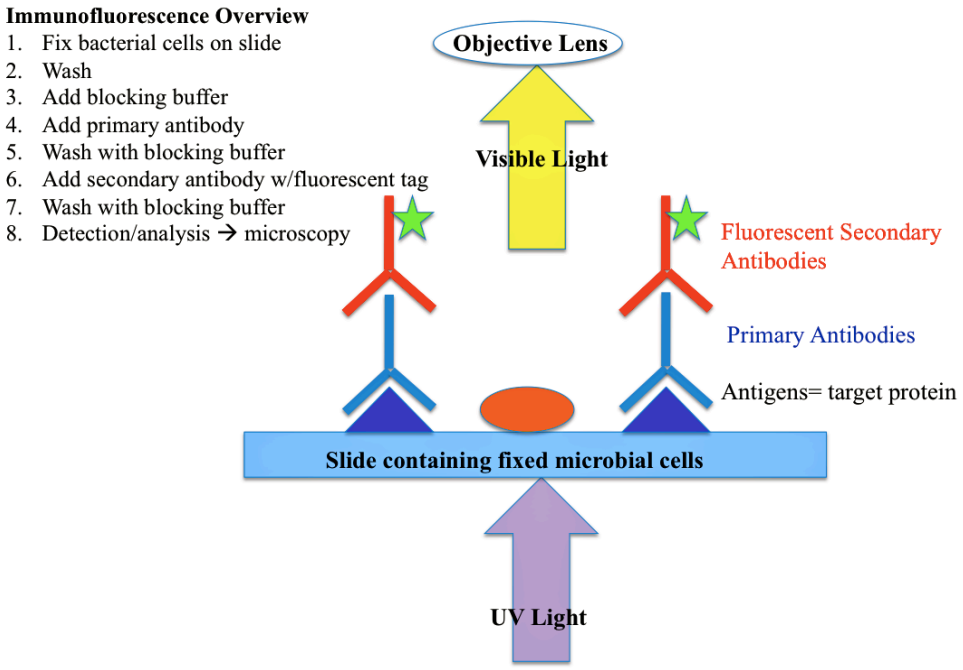

Figure 1.6: Immunofluorescence General Procedure.

Immunofluorescence is thus a very important technique that has advanced the understanding of the spatial distribution of chemotaxis proteins through many

localization studies. For example, chemoreceptors have been shown to cluster near cell poles in *E. coli*(Sourjik, 2004) (Kentner *et al.*, 2006) and ChePep has been shown to localize at flagella poles of *H. pylori* (Howitt and Lee, 2011).

Thus, several experimental methods have evolved to investigate the chemotaxis system of microbes. Protein-protein interaction methods to investigate unknown protein partners include two-hybrid assays and co-immunoprecipitation—each with its relative advantages and disadvantages. Localization of chemotaxis proteins within cells is also important for helping to determine the function of chemoreceptors that sense environmental signals. Using immunofluorescence, CheV proteins have been shown to localize as polar, later, and diffuse.

1.5 Summary

Although the chemotaxis signal transduction system has been extensively studied in *E. coli*, there is still much to be learned about this system in *H. pylori*.

In this thesis, I investigated the function of proteins involved in the chemotaxis system of *H. pylori*. I report findings on the characterization of the coupling proteins CheV1 and CheW through protein-protein interaction experiments *in vitro* and *in vivo*. Ultimately, I found that the coupling proteins work together to create chemotaxis cluster formation and localize chemotaxis complexes to cell poles to ensure proper chemotaxis signaling. The stoichiometry of the chemotaxis proteins in *H. pylori* was also investigated, and revealed a universal CheW-CheA kinase ratio. Additionally, the interactions between proteins within the chemotaxis

chemoreceptor-CheA complex revealed to be critical for protecting coupling proteins and the CheA kinase from proteolytic cleavage. Finally, CheV1 was demonstrated to be an essential coupling protein and *cheV1* mutants were shown to accumulate mutant suppressors. My analyses of the coupling proteins and stoichiometry of the chemotaxis system of *H. pylori* provide novel knowledge on the role of having multiple coupling proteins in a single chemotaxis system.

1.5.1 Summary points

- *H. pylori* is a gram negative bacterium that infects over half of the world's population and causes multiple diseases ranging from gastritis to stomach cancer.
- In order to fully successfully colonize and infect the gastric niche, *H. pylori* relies on chemotaxis to swim across the stomach pH gradient to reach epithelial cells.
- Chemotaxis is used by various bacteria and is the ability to swim toward or away from various nutrient/chemical gradients.
- In *E. coli,* the bacterial chemotaxis system includes multiple transmembrane chemoreceptors, the CheW coupling protein, CheA histidine kinase, and the CheY response regulator.
- The motility behavior of bacteria, whether swimming or tumbling is influenced by CheY phosphorylation status.
- Typically, when a negative stimulant binds to a chemoreceptor, CheA autophosphorylates itself and passes the phosphoryl group to CheY.

Phosphorylated CheY (CheY~P) results in cell tumbling by Che Y~P binding the flagella motor proteins, FliM and FliN, and changes the rotation of flagella from counterclockwise to clockwise rotation.

- When a positive stimulant binds to a chemoreceptor, CheA kinase activity is inhibited resulting in counterclockwise flagellar rotation and leading to smooth swimming activity.
- Some bacterial cells have an adaptation system which refers to bacteria's ability to chemotactically respond to various distinct environmental cues.
- In the *E. coli* chemotaxis system, the adaptation response is maintained by the methylesterase CheB protein and the methyltransferase CheR protein.
- Common deviations observed in microbial chemotaxis systems include: the presence of alternative coupling proteins known as CheVs, differences in proteins involved in adaptation, various CheY~P phosphatase proteins, and other accessory chemotaxis proteins.
- The chemotaxis signal transduction pathway of *H. pylori* is different from that found in *E. coli* in a few ways, including the presence of three CheV coupling proteins in *H. pylori*, the absence of the adaptation proteins CheB and CheR, the presence of an atypical CheZ phosphatase, and a protein of unknown function called ChePep.
- *H. pylori* has three CheV proteins that all have different degrees of affecting the chemotactic system and may play a role in adaptation.

- A *cheV1* mutant was found to have a severe chemotaxis effect as reflected through a severe decrease in its motility rate compared to *cheV2* and *cheV3* mutants; *cheV2* and *cheV3* mutants have a slight chemotaxis effect.
- *cheV1* and *cheV2* mutants are smooth swimming behavior biased and a *cheV3* mutant is hyperswitching behavior biased.
- Protein-protein interaction methods are a valuable tool to better understand the possible function of chemotaxis proteins and include two hybrid assays and co-immunoprecipitation.
- Immunofluorescence is a valuable method for investigating the localization and clustering of chemotaxis proteins within bacterial cells.

CHAPTER 2

Cooperation of two distinct coupling proteins creates network connections between chemosensory complexes

Abstract

Coupling or scaffold proteins provide critical connections in signal transduction pathways between input receptors and output kinases, and also build higher order connections that allow signal amplification. CheW coupling proteins are used in bacterial chemotaxis to connect chemoreceptors to the CheA kinase and build multi-protein chemosensory arrays. Many bacterial chemotaxis signaling systems however possess more than one coupling protein, but the benefits these confer over better-studied single coupling protein systems are not known. *Helicobacter pylori* uses two distinct coupling proteins: CheW, and CheV1, a fusion of a CheW and a phosphorylatable REC domain. In this study, we analyzed the function of these multiple coupling proteins. We report that CheV1 and CheW have largely redundant protein-protein interactome, and ability to activate CheA's kinase activity. They are not redundant, however, for formation of the higher order chemoreceptor supercluster, with each being required for this activity. CheW and CheV1 each interacted with CheA and each other, independent of the chemoreceptors, in vitro and in vivo. Our data suggests that some microbes have divided the supercluster formation function between multiple coupling proteins, and

furthermore that proper formation of a polar chemoreceptor supercluster is essential for normal chemotaxis.

Significance Statement:

Signal transduction systems are important pathways that all organisms use to sense and respond to their environments. Chemotaxis is controlled by a signal transductionsystem that allows bacteria to coordinate their movement in response to their environment. This response requires proper assembly and localization of large multiprotein chemotaxis complexes, which are built by interactions between coupling proteins. The significance of having multiple types of coupling proteins in a single signal transduction system, however, is poorly understood. Here, we show that multiple coupling proteins allow bacteria to build super protein interaction networks and localize them to cell poles, a role that is required for optimal chemotaxis.

2.1 Introduction

Coupling or scaffold proteins provide critical connections between input receptors and output kinases in many types of signal transduction pathways (Bhattacharyya *et al.*, 2006; Shaw and Filbert, 2009; Piñas *et al.*, 2016). These connections confer multiple advantages such as cooperativity, signaling complex assembly, and proper localization of proteins (Shaw and Filbert, 2009). Indeed, many cellular signaling systems utilize multiple coupling proteins to fine tune these advantages, a process that has been well studied in eukaryotic systems (Shaw and

Filbert, 2009; Zeke *et al.*, 2009; Good, Zalatan and Lim, 2011). Bacterial chemotaxis is an example of a prokaryotic system that relies on coupling proteins of the CheW family to connect chemoreceptors to the CheA kinase. Many bacterial chemotaxis systems possess multiple coupling proteins (Wadhams and Armitage, 2004; Alexander *et al.*, 2010), but the advantages of having more than one for these systems is not well understood.

The core bacterial chemotaxis sensory unit is composed of chemoreceptor, CheW family coupling protein, and the CheA output kinase (Wadhams and Armitage, 2004). The coupling protein allows the chemoreceptors to control the CheA kinase and promotes connections between core units (Wadhams and Armitage, 2004; Liu *et al.*, 2012; Piñas *et al.*, 2016). Chemotaxis coupling proteins have two basic architectures, CheW or CheV. CheW is a single domain protein with two defined subdomains, and CheV proteins are hybrids that add a C-terminal response regulator-like domain (Rec) to an N-terminal CheW domain (Pittman, Goodwin and Kelly, 2001; Piñas *et al.*, 2016).

Chemotaxis core sensory units exist in the cell as large multi-protein complexes at the cell poles (Maddock and Shapiro, 1993; Briegel *et al.*, 2009; Liu *et al.*, 2012). Connections that form these complexes have been elucidated in the single-coupling protein system of *E. coli*, and are driven by interactions between CheW and a subdomain of CheA called P5, which is a structural mimic of CheW. These connections are vital for complex formation, kinase control, and positive cooperativity that allow small signals to be greatly amplified (Porter, Wadhams and

Armitage, 2011). There are two documented types of CheW-CheA P5 interactions. Interactions at interface 1 occur between CheA P5 subdomain 1 and CheW subdomain 2, and lead to control of the CheA kinase activity (Liu *et al.*, 2012; Piñas *et al.*, 2016). Interactions at interface 2 occur between CheA P5 subdomain 2 and CheW subdomain 1, and lead to inter-complex connections that build the chemoreceptor arrays, and positive cooperativity. Thus coupling proteins participate in two types of CheA interactions that are vital for the function of the chemotaxis system.

While these types of CheW-CheA interactions have been elucidated in the single coupling protein *E. coli* system, it is not yet known how and whether these interactions differ in multi-coupling protein systems. To date, the best studied multi coupling protein system is that of *Bacillus subtilis*, a microbe that uses one CheV and one CheW to both perform receptor-kinase coupling in a functionally redundant manner (Rosario *et al.*, 1994; Karatan *et al.*, 2001). Recent evidence suggests that some coupling proteins display chemoreceptor specificity and differential ability to activate the CheA kinase (Hartley-tassell *et al.*, 2010; Ortega and Zhulin, 2016). Thus the prevailing model is that multiple coupling proteins are used to promote receptor-specific control of the CheA kinase, operating at the individual receptor-kinase unit.

The human pathogen *Helicobacter pylori* has a chemotaxis system with four chemoreceptors called Tlp's (TlpA, TlpB, TlpC, and TlpD), a CheA kinase, a CheY response regulator, and—relevant to this work-- multiple coupling proteins

(Lertsethtakarn, Draper and Ottemann, 2012; Keilberg and Ottemann, 2015). Two of the *H. pylori* coupling proteins—CheW and CheV1 are critical for wild-type chemotaxis, acting in a non-redundant manner. Mutants lacking *cheW* or *cheV1* appear unable to activate the CheA kinase as they swim without changing direction, and are either completely (*cheW*) or severely (*cheV1*) compromised in a soft agar chemotaxis assay (Pittman, Goodwin and Kelly, 2001; Lowenthal, Simon, *et al.*, 2009). *H. pylori* also possesses two other CheV-type coupling proteins, but these play only minor roles in chemotaxis (Pittman, Goodwin and Kelly, 2001) (Lowenthal, Simon, *et al.*, 2009). Because *H. pylori* CheW and CheV1 were both essential for chemotaxis in a non-redundant manner, we thought it ideal to dissect how these contribute to chemotaxis.

We initiated our work analyzing the protein interaction network of CheW and CheV1, as well as their ability to activate and control CheA's kinase function. We found that they had nearly identical abilities in these regards. However, when we examined their roles in assembly of the polar chemosensory super cluster, we found that both were required and fulfilled non-redundant roles in these interactions. Our data suggest that some microbes use multiple coupling proteins to build the polar chemoreceptor supercluster and thus suggest this aspect of chemotaxis may be fine tunable by modulating the levels or activities of these coupling proteins.

2.2 Results

2.2.1 CheW and CheV1 behave as canonical coupling proteins by forming direct interactions with CheA and chemoreceptors.

Our first goal was to characterize the protein-protein interaction network of the *H. pylori* CheV1 and CheW coupling proteins. We initially identified directly interacting proteins using the bacterial adenylate cyclase two-hybrid (BACTH) system (Karimova *et al.*, 1998). For this approach, CheV1 and CheW were fused to the N or C terminus of T25 fragments, and CheV1, CheW, CheA, CheV2, CheV3, and the chemoreceptors (TlpA, TlpB, and TlpD) were fused to the bait T18 fragments. We found that both CheV1 and CheW displayed interactions with themselves, the other coupling proteins, CheA, and at least one chemoreceptor (Fig. 1A, 1C). We found that only one fusion orientation—with the T25 fragment at the C-terminal end—was functional (Table S3). We thus focused on these fusions, and quantified all positive interactions using a β-galactosidase assay (Fig. 1). CheV1 and CheW both displayed typical coupling protein interactions with CheA and chemoreceptors. The interaction with CheA was quite strong, yielding β-galactosidase levels that were almost double that of the positive control (Fig. 1). Both proteins also interacted with the TlpA chemoreceptor, with CheV1 showing significant interactions additionally with TlpB and TlpD (Fig. 1). Both CheV1 and CheW were able to interact with one another and with themselves. Lastly, CheV1 interacted with CheV2 and CheV3.

The BACTH protein interactions were verified using co-immunoprecipitation with purified proteins. Consistent with the BACTH, both proteins interacted with CheA and *H. pylori's* cytoplasmic chemoreceptor, TlpD (Fig. 2A-2B). Because all *H. pylori* chemoreceptors have highly similar signaling regions that conserve residues that interact with coupling proteins (Fig. S1), this finding suggests that both CheW and CheV1 are able to interact with all chemoreceptors (Alexander *et al.*, 2010) (Ortega and Zhulin, 2016). Finally, we saw that both CheV1 and CheW interacted with each other (Fig. 2C). Thus the BACTH and co-immunoprecipitation results suggest that the protein interaction networks of both CheV1 and CheW are largely similar (Fig. 2D). Both interact directly with CheA, chemoreceptors, each other, and themselves. CheV1 may have several additional interactions with other coupling proteins as well, but these were not pursued (Fig. 2D).

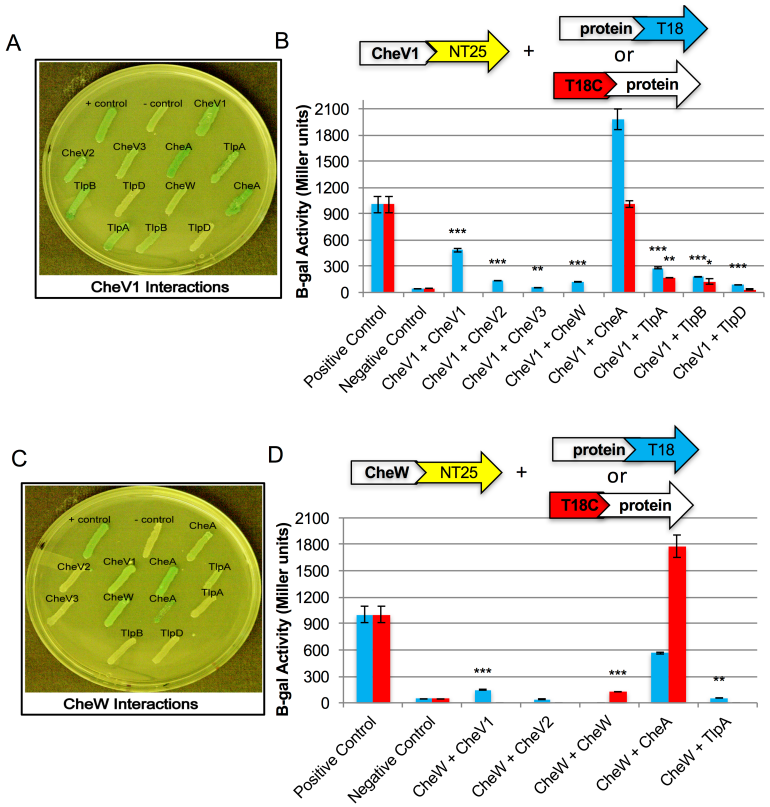

Fig. 2.1. BACTH analysis of CheV1 and CheW interactions. *H. pylori* proteins (A) CheV1 or (B) CheW were fused to the N- or C- termini of the T25 fragments and tested for their interaction with the chemotaxis proteins CheV1, CheV2, CheV3, CheW, CheA, TlpA, TlpB, or TlpD, fused to the N- or C- termini of the T18 fragments. The plasmid combinations were tested in the *E. coli cya*$^{-}$ strain BTH101. The positive (+) control contained pKT25-zip and pUT18C-zip while the negative (-) control utilized CheV1 or CheW fused to the T25 fragments co-transformed with empty T18 plasmids. (A) and (C). Representative LB X-gal and IPTG plates. Each transformation was repeated three independent times. (B) and (D). Measurement of β-galactosidase levels from the positive interactions. The mean values from three independent experiments and standard deviations are shown for each sample. The strains were each compared with a negative control using un-paired T-test to test statistical significance (***P < 0.0001, **P < 0.001, *P = 0.0127).

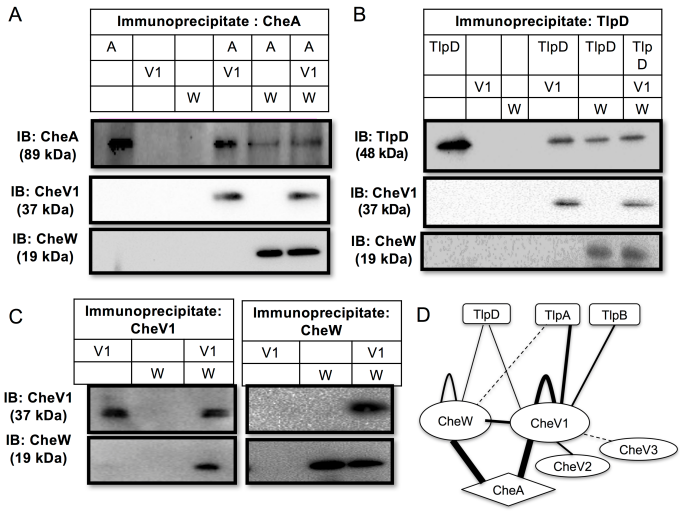

Fig. 2.2. Co-immunoprecipitation with purified proteins confirm that CheV1 and CheW interact with CheA, with TlpD, and with each other. (A-C). Mixtures of purified CheA (A), TlpD, CheV1 (V1) and/or CheW (W) were preincubated and the immunoprecipitated as indicated along the top, followed by detection of specific proteins as indicated at the left. Each gel is representative of three immunoprecipitations (n=3). (D) Model of the CheV1 and CheW protein interaction network identified by BACTH and co-immunoprecipitation. The thickness of the line denotes the strength of interaction based on beta-galactosidase quantification. Dashed lines indicate a weak interaction.

2.2.2 CheV1 retains receptor-CheA coupling activity that is marginally less than CheW in an in vitro kinase assay.

We next tested whether CheV1 and CheW could each allosterically function to activate CheA autophosphorylation and to couple CheA to a chemoreceptor. These studies were done using an *in vitro* CheA phosphorylation assay similar to previous studies (Jiménez-Pearson *et al.*, 2005; Lertsethtakarn and Ottemann, 2010). In this assay, purified CheA ± coupling protein and receptor are incubated *in vitro* with radioactive [γ^{-32} P] ATP, and the amount of phosphorylated CheA determined (Fig. 3A, Fig. 3D).

We first examined how addition of CheW or CheV1 to purified CheA protein would affect the rate and extent of CheA phosphorylation. We determined total CheA activity because the rate of CheA phosphorylation was not linear (Fig. 3B). CheV1 or CheW protein each significantly increased the CheA activity by 1.8- or 2.8-fold, respectively (Fig. 3C). These differences were not changed upon addition of a greater amount of CheW or CheV1 protein, suggesting the CheA was largely saturated. These results suggest that both CheV1 and CheW produce conformational changes in CheA that cause it to be more active, with CheW triggering greater activation.

We then examined CheV1 and CheW for their abilities to couple CheA to a chemoreceptor. In other systems, CheA becomes substantially more active when coupled to chemoreceptor (Li *et al.*, 2011; Greenswag *et al.*, 2015). We thus incubated purified TlpD and CheA with either CheV1 or CheW. CheA phosphorylation was significantly increased with the addition of the chemoreceptor TlpD alone by 2-fold (Fig. 3F). The addition of CheV1 or CheW to the chemoreceptor-TlpD reaction significantly increased CheA phosphorylation by 3-fold or 4.8-fold respectively compared to CheA alone (Fig. 3G). Although both coupling proteins significantly increased CheA phosphorylation, CheW was marginally better able to activate CheA than CheV1 (*P* value= 0.0186). Overall, these data suggest that both CheV1 and CheW can connect chemoreceptors to CheA and lead to its activation, with CheW having a greater activity in this respect.

We then determined how a combination of both CheV1 and CheW coupling

proteins would affect CheA phosphorylation. Addition of both CheV1 and CheW resulted in CheA activation that was in between that of CheV1 and CheW (Fig. 3). This outcome was true whether there was chemoreceptor or not. This finding suggests that both proteins act independently on CheA, but do not appear to synergize.

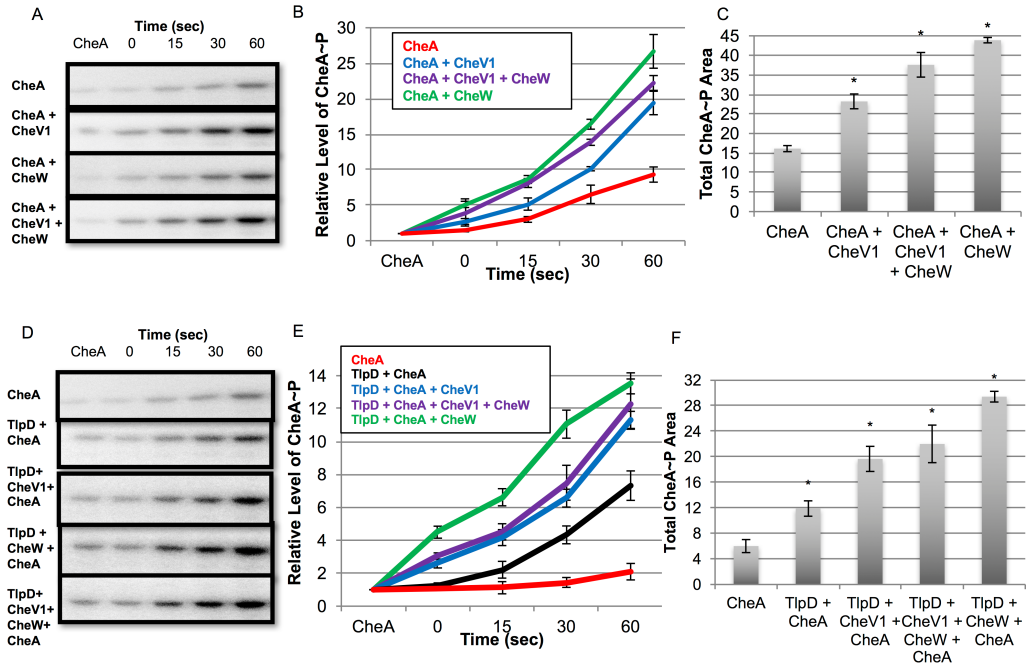

Fig. 2.3. CheV1 and CheW activate CheA phosphorylation on their own and with the addition of the chemoreceptor TlpD. Equimolar mixtures of purified proteins (2 μM of each) were incubated with [γ-^{32}P]-ATP. The reactions were stopped at the indicated times by mixing with 2x SDS sample buffer. (A) and (D): Phosphorylated CheA was detected using SDS-PAGE. (A) CheA and coupling proteins, CheV1 and CheW, and (D) TlpD addition. (B & E): The level of phosphorylated CheA was compared to phosphorylated CheA at time 0. The intensity of the bands representing CheA phosphorylation was determined using ImageJ software and plotted over sixty seconds. (C & F) The area under the respective curves was calculated by finding the definite integral. Error bars represent the standard deviation of three independent experiments (n=3). Asterisk (*) represents a *P* value < 0.001 determined by an unpaired T-test for all compared to CheA only.

2.2.3 CheV1 and CheW independently promote CheA-chemoreceptor interactions in vivo.

Our results above showed that CheV1 and CheW have overlapping interaction networks and both activate CheA, although to somewhat different levels. Given their similarities, one would predict that either could function in chemotaxis, but this is not the case (Pittman, Goodwin and Kelly, 2001; Lowenthal, Simon, *et al.*, 2009). We therefore hypothesized that CheV1 and CheW have *in vivo* activities in addition to protein-protein interactions and kinase activation. We thus sought to gain more insight into these putative *in vivo* roles. Our first step was to analyze the CheW and CheV1's roles in promoting the formation of the chemoreceptor-CheA complex. Chemoreceptors are transmembrane proteins, and retain CheA, which is normally-cytoplasmic, at the membrane via coupling protein interactions (Erbse and Falke, 2009; Piasta and Falke, 2015). We therefore measured the amount of CheA associated with the cell membrane as an indicator of overall complex formation. We isolated membrane and cytoplasmic fractions from multiple strains, using high-speed centrifugation and membrane washing as previously described (Erbse and Falke, 2009; Collins *et al.*, 2016). Equal amounts of total protein from each fraction were separated by SDS-PAGE, followed by western blotting (Fig. S2A). Control blots confirmed that the membrane and cytoplasmic fractions were substantially free of cross-contamination (Fig. S2B) (Collins *et al.*, 2016).

We then quantified and compared the amount of CheA found in the membrane relative to the cytoplasm of each strain (Fig. 4A). In wild type, there was

twice as much CheA in the membrane compared with the cytoplasm. In a mutant lacking all chemoreceptors, CheA was almost fully cytoplasmic, consistent with the idea that CheA membrane interactions occur via chemoreceptors. CheA at the membrane was partially decreased in strains lacking either *cheV1* or *cheW*, compared to wild type, and more substantially decreased when both proteins were lacking (Fig. 4B). These findings suggest that CheV1 and CheW each promote CheA interactions with the chemoreceptor complex *in vivo*. Furthermore, our data shows they function in an additive way, suggesting each acts in a way that is independent of the other.

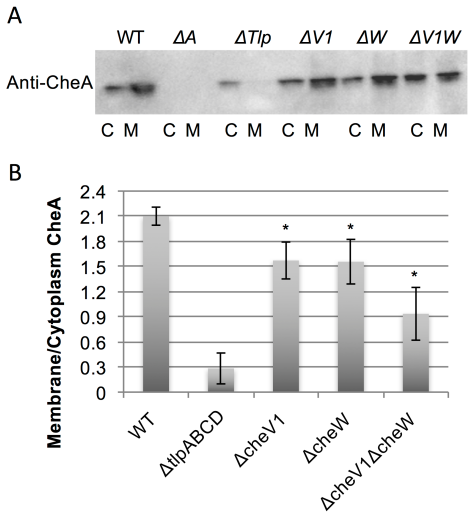

Fig. 2.4. CheV1 and CheW are necessary to retain CheA at the cell membrane. (A) Western blots from cytoplasmic "C" and membrane "M" fractions of various strains probed with anti-CheA. (B) Quantification of the amount of CheA found in membrane fractions relative to CheA amount found in cytoplasmic fractions. Each image is representative of three independent cultures (n=3). The intensity of the bands was quantified using ImageJ software. Asterisk (*) represents a *P* value < 0.01 determined by an unpaired Students T-test for strains compared to WT. Error bars represent the standard deviation. *Δtlp*= strain lacking all chemoreceptors, *ΔA= ΔcheA, ΔV1= ΔcheV1, ΔW= ΔcheW,* and *ΔV1W= ΔcheV1 ΔcheW*.

2.2.4 CheV1 and CheW alter each other's interaction with CheA and chemoreceptors *in vivo*.

The membrane fractionation results suggested that CheV1 and CheW each promote CheA-chemoreceptor interactions *in vivo*. We next confirmed these interactions, and examined what proteins were critical for forming them. To accomplish this goal, CheA, CheV1, or CheW were immunoprecipitated from whole cell lysates and then examined for the presence of the other proteins.

In wild-type cells, all three proteins interacted with each other, with each being able to immunoprecipitate the other two (Fig. 5B-D). Similar results were obtained in mutants lacking all chemoreceptors (Fig. 5B). This outcome suggested that CheA forms complexes with each coupling protein independent of chemoreceptors.

We also found evidence that CheV1 and CheW interacted with each other in wild-type *H. pylori* and in mutants lacking CheA or all chemoreceptors. These experiments were somewhat challenging, as the expression of CheW in the Δ*cheA* background was substantially lessened (5C & 5D). These experiments are consistent with the idea that CheA, CheW, and CheV1 all form independent interactions.

We next examined whether the interactions of CheV1 or CheW with CheA were dependent on the other coupling protein. A strain lacking CheW resulted in less CheV1 immunoprecipitated with CheA as compared to the wild-type strain (Fig. 5B). A strain lacking CheV1 also showed reduced levels of CheW pulled down from CheA immunoprecipitation, as compared to wild type (Fig. 5B).

Deletion of either *cheV1* or *cheW* did not affect the expression of the other (Fig. 5A), consistent with the fact that both are in separate operons and under distinct transcriptional control (Alexander *et al.*, 2010). Taken together, these results and the CheA membrane association experiments suggest that CheV1, CheW, and CheA all interact *in vivo* in a chemoreceptor independent manner. Furthermore, CheV1 and CheW interact with each other and enhance the interaction of the other with CheA.

Given the similarities in the interactions between CheV1 and CheW, we revisited whether addition of each protein would affect the interaction of the other with purified CheA protein in this same assy. We mixed CheA or chemoreceptor with a combination of CheW and CheV1. These samples were then immunoprecipitated with anti-CheA or anti-chemoreceptor antibodies, and then compared using western blotting to samples that had only CheW or CheV1. Using this approach, we found that neither CheW nor CheV1 changed the amount of the other pulled down *in vitro* (Fig. 2A-B). These results may suggest that CheW and CheV1 may have distinct and independent binding interactions. Ultimately the combination of our *in vivo* and *in vitro* interaction experiments suggest that both work together to enhance complex binding in a chemoreceptor-coupling protein (CheW and CheV1)-CheA manner in which both also possibly have distinct binding sites.

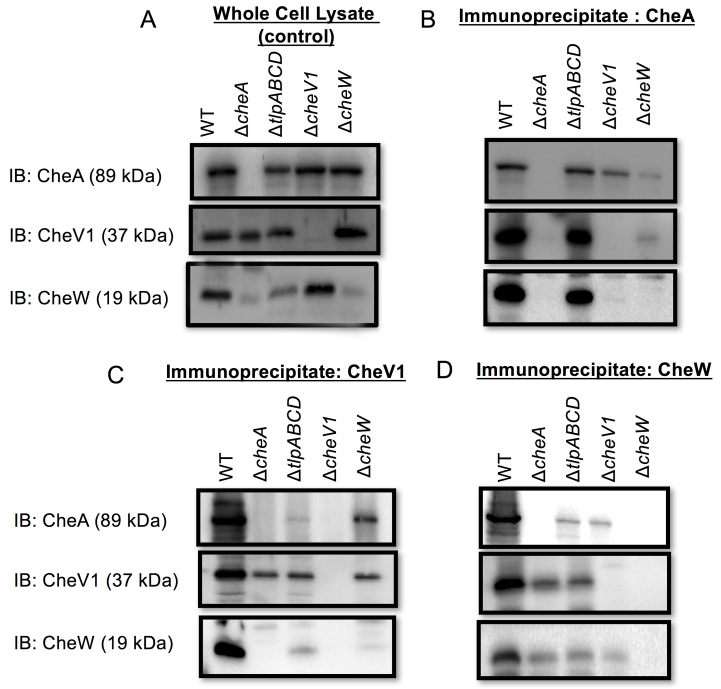

Fig. 2.5. **CheV1 and CheW interact between themselves and with CheA in whole cell lysates.** (A) CheV1 and (B) CheW were detected by immunoblotting (IB) from whole-cell protein extracts of wild-type, *ΔcheA*, *ΔcheV1, ΔcheW*, and *ΔcheV1cheW H. pylori* strains. Identical amounts of whole cell extracts were immunoprecipitated (IP) using anti-CheV1, anti-CheW, and anti-CheA antibodies. Ten microliters of precipitates were probed for the presence of proteins by immunoblotting (IB) using the respective antibody. Each gel is representative of three immunoprecipitations (n=3).

2.2.5 Loss of CheV1, CheW, or both abrogates chemoreceptor-CheA complex formation at cell poles.

The above experiments showed that CheW and CheV1 interact directly and with CheA. CheW is known to interact with another CheW-like domain in the form of CheA's P5 domain (Piñas *et al.*, 2016). These interactions build the multi-protein chemoreceptor-CheA arrays at the cell pole and promote signal amplification (Kentner and Sourjik, 2006; Sourjik and Armitage, 2010). Given that CheV1 has a

CheW domain, we thus explored the role of CheW and CheV1 in the building of the *H. pylori* chemoreceptor array. We employed immunofluorescence on whole cells, with all proteins expressed from the native loci in native forms. The polar chemotaxis complex was detected using anti-CheA, anti-chemoreceptors (Tlps), or anti-CheW. All antibodies detected a discrete locus at one or both cell poles in the wild-type strain, as reported previously (Fig. 6A) (Lertsethtakarn *et al.*, 2015; Behrens *et al.*, 2016; Collins *et al.*, 2016). Mutants lacking the chemoreceptors lost polar localization of the other complex members, consistent with the idea that these proteins are critical to build the chemotaxis arrays (Fig. 6C), as reported previously (Lertsethtakarn *et al.*, 2015; Collins *et al.*, 2016). ,*cheA*, *cheV1,* or *cheW* mutants also were unable to build a polar signaling complex (Fig. 6D-F). In other words, none of these proteins was redundant with any other. These results suggest that polar chemosensory array creation requires two coupling proteins, CheV1, and CheW, in addition to CheA.

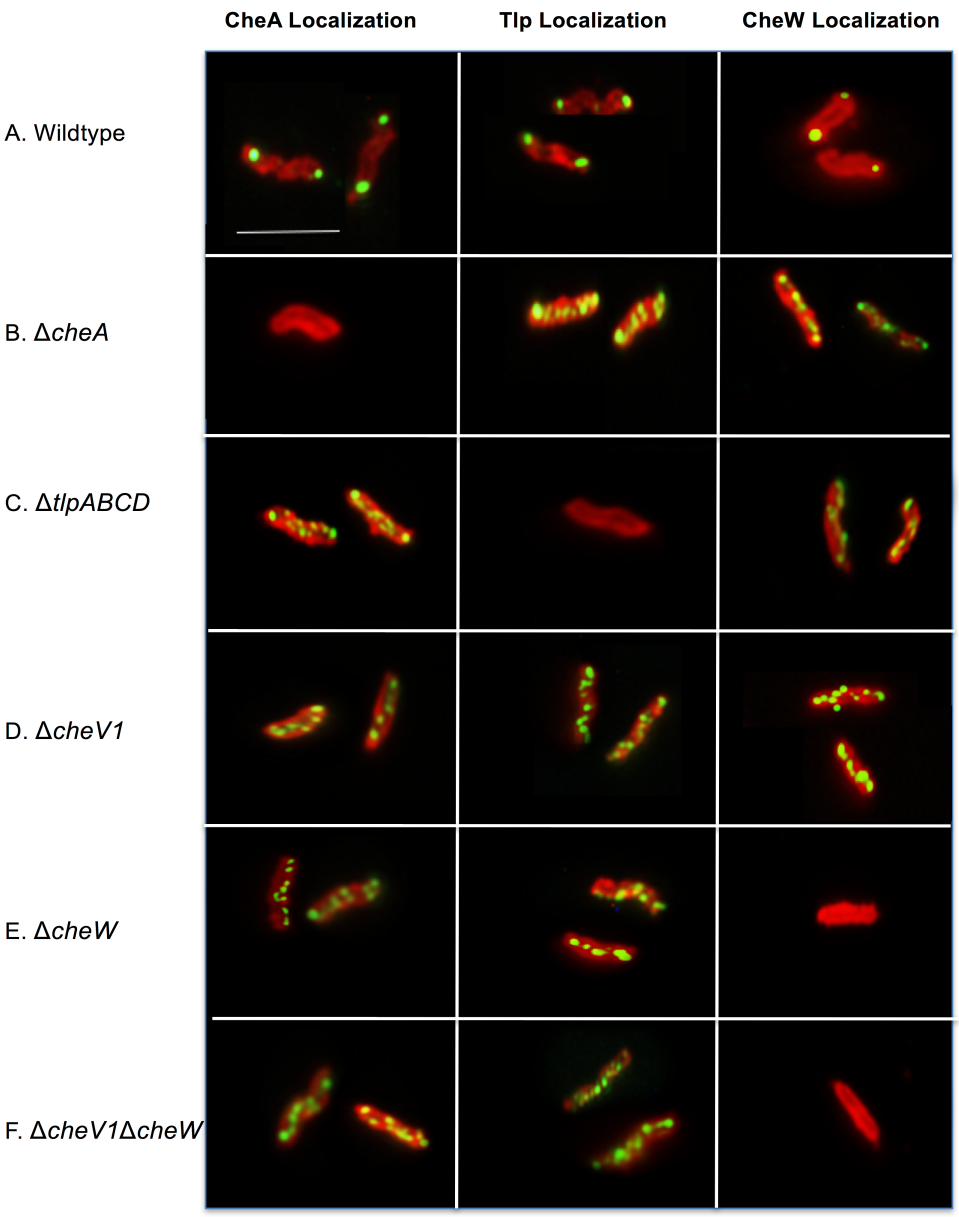

Fig. 2.6. *cheV1* and *cheW* mutants are defective in localizing CheA and chemoreceptors to polar chemosensory clusters. CheA, the chemoreceptors (Tlp), and CheW were visualized in *H. pylori* G27 and its isogenic mutants using immunofluorescence. All proteins were expressed from their native loci. Antibodies against CheA, TlpABCD, and CheW (Green) were used to determine localization in (A) wild type (B) Δ*cheA* (C) Δ*tlpABCD* (D) Δ*cheV1* (E) Δ*cheW* and (F) Δ*cheV1*Δ*cheW*. *H. pylori* were visualized with anti-*H. pylori* antibodies and red secondary antibodies. Scale bar= 4um.

2.3 Discussion

Coupling proteins are key components of many types of signal transduction systems, providing functions beyond simply holding proteins together. Here, we analyzed the roles of two different coupling proteins, a CheW and a CheV, in a single chemotaxis system. Altogether, our results suggest that some microbes employ two coupling proteins to build a robust chemosensory complex.

The results presented here show that CheW and CheV1 are both required to create the functional polar chemosensory array. Mutants that lack either CheW, CheV1, or both have chemotaxis proteins that appear in punctate, non-polar structures by immunofluorescence (Fig. 6), and also do not retain CheA at the membrane (Fig. 4). Because both *cheW* and *cheV1* mutants are non-chemotactic, we surmise that these non-polar chemotaxis units are not functional. This finding sheds light on why *cheV1* and *cheW* mutants are non-chemotactic, while both proteins are capable of typical coupling protein functions as we show here. Large chemosensory arrays are critical for chemotaxis because they allow the high positive cooperativity (Hill coefficients of 15-20) required for signal amplification. This property underlies the high sensitivity and ability to amplify the chemotaxis system's response to ligands (Liu *et al.*, 2012; Parkinson, J. S., Hazelbauer, G. L. & Falke, 2015; Piñas *et al.*, 2016). Indeed, isolated core chemoreceptor-CheW-CheA signaling complexes are able to regulate CheA, but with little positive cooperativity (Li and Hazelbauer, 2014). These studies suggest that *cheW* and *cheV1* mutant

arrays are defective because they lack the positive cooperativity necessary for wild-type chemotaxis.

We envision several mechanisms that might underlie the ability of CheV1 or CheW to form functional polar chemosensory arrays. Recent work has shown that in *E. coli*, which does not contain CheV, CheW interacts with other CheW and CheA molecules to form large chemosensory arrays that are critical for cooperativity of signal response (Liu *et al.*, 2012; Piñas *et al.*, 2016). Piñas and colleagues defined two CheW-CheA interaction faces: interface 1, which promotes CheW-CheA interactions required for kinase control, and interface 2, which creates the interactions that connect chemosensory arrays (Piñas *et al.*, 2016). Our work suggests that some microbes have altered CheW such that the array forming function is split between two coupling proteins. Indeed, the residues that form interface 2 are conserved amongst enteric CheW, but not amongst CheW as a whole (Alexander *et al.*, 2010; Ortega and Zhulin, 2016). Other support comes from models, that suggested receptors lacking CheA and having only CheW—so called CheW-only linkers—create high cooperativity in signal sensing (Eismann and Endres, 2015). In *Borrelia burgdorferi* two distinct CheW proteins are necessary for chemotaxis and formation of the chemosensory arrays (Zhang *et al.*, 2012). These two CheW, like CheV1 and CheW in *H. pylori*, are under distinct transcriptional control (Fraser, Casjens and Huang, 1997; Tomb *et al.*, 1997; Alexander *et al.*, 2010; Zhang *et al.*, 2012). We speculate that bacteria that utilize

two coupling proteins may thus modulate the expression of each in order to alter the cooperativity behavior of the chemoreceptor-CheA cluster array.

We report here that CheV1 and CheW possess nearly identical key coupling protein interactions. Both activate CheA and couple it to a chemoreceptor. CheW, however, had a greater ability to activate CheA than CheV1. This observation is consistent with the data presented by Ortega and Zhulin, that CheV proteins limit CheA kinase output and thus can function with chemoreceptors that have a high intrinsic ability to activate CheA (Ortega and Zhulin, 2016). These authors proposed that this limitation is due to CheV acting as a phosphate sink, a protein that can be phosphorylated by CheA to direct phosphates away from other targets (Ortega and Zhulin, 2016). We did not detect phosphorylated CheV1 in our CheA kinase assay, a finding also reported by others, so do not have direct support for this aspect of the model (Jiménez-Pearson *et al.*, 2005) (Lertsethtakarn and Ottemann, 2010). Another possibility, consistent with our data, is that CheV1 itself is less able to activate CheA, via aspects of its structure. Our results may reflect the nature of the chemoreceptor-CheA complex as demonstrated in *B. subtilis* where CheV increased CheA kinase activity depending on the methylation nature of chemoreceptors which is reflective of ligand binding (Walukiewicz *et al.*, 2014). CheV was also able to decrease CheA activity in *B. subtilis* when its coupling domain was mutated leaving only its receiver domain active; this suggests an important interplay between CheV's domains influencing its ultimate function (Karatan *et al.*, 2001). The idea that coupling proteins have different abilities to enhance or inhibit signal

transduction is also seen in eukaryotic scaffold systems (Locasale, Shaw and Chakraborty, 2007). We suggest that while both CheV1 and CheW appear to have similar functions, CheW may play a more critical role for CheA kinase activation than CheV1.

CheV1 may function to connect the chemoreceptor complex to additional proteins and may be able to interact with more proteins than CheW, including CheV2 and CheV3. It's also possible that CheV1 or CheW have additional interactions beyond chemotaxis proteins, similar to the ParP protein from *Vibrio parahaemolyticus,* which is also involved in chemotaxis (Ringgaard *et al.*, 2014). ParP, like CheV1, is a hybrid protein with a CheW-like domain. Like CheV1, ParP mutants have decreased soft agar migration and are more smooth swimming than wild type (Ringgaard *et al.*, 2014) (Lowenthal, Simon, *et al.*, 2009) (Pittman, Goodwin and Kelly, 2001). ParP interacts with CheA, and with a membrane protein called ParC, which in turn stabilizes chemotaxis complexes at the cell pole by preventing CheA dissociation (Ringgaard *et al.*, 2014). A common theme is the use of the CheW domain as connection point for protein-protein interactions either between arrays or with other proteins.

Cryo-electron tomography have also revealed the existence of CheW rings symbolic of CheW-CheW interactions in *E. coli* chemoreceptor array structures revealing the importance of such interactions for chemosensory signaling (Cassidy *et al.*, 2015). We suggest a similar chemotaxis array in *H. pylori* in which CheW-CheV1 rings form the core of the complex. In this model, we hypothesize that

CheW forms stronger interactions with CheA because the CheW domain of CheV1 may be slightly inhibited by the REC domain fused at its C terminus. Thus, we suggest that CheV1 plays important roles in interacting with CheW and the chemoreceptors to build super arrays. We hypothesize that CheW maintains its universal function in *H. pylori* as *E. coli* and other organisms but that in *H. pylori* both CheV1 and CheW are important to build arrays.

In sum, our work suggests that division between two coupling proteins in a signaling complex may provide several advantages to bacteria similar to the advantages conferred by scaffolding proteins in mammalian cell signaling. The combination of two coupling proteins results in proper formation of the chemoreceptor-CheA chemotaxis complex and large polar arrays, localization to the cell membrane of the complex components, and finally stimulating CheA kinase activity leading to optimal chemotaxis in *H. pylori*. Our results thus highlight the important functions of multiple coupling proteins in signal transduction systems in helping organisms efficiently respond to dynamic environments by rewiring key interactions among signal transduction proteins.

2.4 Materials and Methods

2.4.1 Bacterial strains and growth conditions.

All *H. pylori* and *E. coli* strains used in this study are listed in Table S1. *H. pylori* was grown on Columbia horse blood agar (5% defibrinated horse blood, 50 μg/ml cycloheximide, 10 μg/ml vancomycin, 5 μg/ml 130 cefsulodin, 2.5 Units/ml

polymyxin B, and 0.2% (w/v) β-cyclodextrin) at 37°C in microaerobic conditions (5-10% O_2, 10% CO_2, and 80-85% N_2. For liquid cultures, *H. pylori* was grown in Brucella broth with 10% heat-inactivated fetal bovine serum (BB10) under the same conditions stated above. Antibiotic concentrations used for mutant selection were: 15 μg/ml kanamycin or 13 μg/ml chloramphenicol. *E. coli* was grown on LB media with 100 μg/ml ampicillin or 60 μg/ml kanamycin.

2.4.2 Construction of bacterial two-hybrid plasmids and bacterial two-hybrid analysis.

Genomic DNA from *H. pylori* strain mG27 was extracted using the Wizard genomic DNA kit (Promega). The full-length *tlpD, cheW, cheV1, cheV2, cheV3,* and *cheA* genes were amplified from this genomic DNA using the primers listed in Table S2 using Phusion DNA polymerase with the following thermocycler conditions: 98ºC for 5 minutes, 98ºC for 10 seconds, 55ºC for 30 seconds, 72ºC for 2.5 minutes, repeat 39 times, 72ºC for 10 minutes. Cytoplasmic signaling domains of *tlpA* (nucleotide #988-2028, amino acid # 330-675) and *tlpB* (nucleotide #718-1695, amino acid #240-565) genes were amplified as above. PCR products of all genes were digested with the appropriate restriction enzyme (Table S2). BACTH plasmids pKT25, pKNT25, pUT18, and pUT18C were also digested using the appropriate restriction enzymes. Digested plasmids were phosphatase treated using TSAP phosphatase following the manufacturer's suggested protocol (Promega). PCR products and plasmids were gel purified using the illustra GFX PCR DNA and gel band purification kit (GE Healthcare). The purified digested PCR gene products

and plasmids were ligated and used to transform *E. coli* DH5a to appropriate antibiotic resistance. Colony PCR screening was used to determine which colonies contained correct plasmids. All cloned plasmids were verified by sequencing and contained no errors.

Recombinant BACTH plasmids at 40 ng each were co-transformed into competent *E. coli* BTH101 cells (Table S2). For positive controls, pKT25-zip and pUT18C-zip were co-transformed in BTH101. These plasmids express leucine zipper motifs that results in a strong dimer interaction (Karimova *et al.*, 1998). For negative controls, empty BACTH plasmids were co-transformed with each other and with each recombinant plasmid. Transformed cells were plated on LB plates containing 100 µg/ml ampicillin, 30 µg/ml kanamycin, 40 µg/ml X-gal, 0.5 mM IPTG and incubated at 30ºC for 40-48 hours using the positive and negative controls as reference for recording colony colors.

2.4.3 β-galactosidase assay.

The efficiency of BACTH interactions between plasmids was quantified using a β-galactosidase assay as described previously (Karimova et al. 1998). Transformants were grown in LB broth with 0.5 mM IPTG, 100 µg/ml ampicillin, and 30 µg/ml at 30ºC overnight. Liquid cultures were then diluted 1:100 in LB broth, and grown again until OD_{600} was 0.3-0.7. The OD_{600} was recorded, and 100 µl of each culture was mixed with 0.9 ml of cold Z buffer (0.06 M $Na_2HPO_4.7H_2O$, 0.04 M $NaH_2PO_4.H_2O$, 0.01 M KCl, 0.001 M $MgSO_4.7H_2O$, 0.056 M 2-mercaptoethanol, pH 7.0). 100 µl of chloroform followed by 50 µl of 0.1% SDS were added, followed

by vortexing to permeabilize the cells. The samples were placed at 30ºC for 5 minutes with the tops off. 0.2 ml of ONPG substrate solution (4 mg/ml ortho-Nitrophenyl-β-galactoside (ONPG) in 0.1 M phosphate buffer, pH 7.0) was added to the sample and the color observed until the sample turned yellow. At this point, the reaction was stopped by adding 0.5 ml 1 M Na_2CO_3 and the time recorded. The OD_{420} of the samples was measured. Miller units (β-galactosidase activity) were calculated using the following formula: 1,000 x (OD_{420} / (time (mins) x volume of culture used x OD_{600}) (Miller, 1972).

2.4.4 Protein purification.

TlpD, CheV1, CheW, and CheA were purified as previously described (Draper, Karplus and Ottemann, 2011) (Lertsethtakarn and Ottemann, 2010) (Collins *et al.*, 2016). In brief, all fusion plasmids were expressed in *E. coli* BL21 at 37ºC and induced with 0.5 mM IPTG. The glutathione *S*-transferase (GST) fusion expression plasmids (TlpD, CheV1, and CheW) were applied to a GST Prep column for purification (GE Healthcare). GST tags were cleaved using Precission protease. His-tagged CheA was applied to a His Prep column (GE Healthcare). All purified proteins were dialyzed in storage buffer (50 mM HEPES, pH 7.6, 50 mM KCl, 20% glycerol) and stored in -80^{o} C. Protein concentrations were determined by measuring absorption at 280 nm on a nanodrop and using the coextinction coefficient of each protein based on its amino acid composition.

2.4.5 Whole cell lysate preparation.

H. pylori whole cell extracts for use in co-immunoprecipitation were prepared by resuspending *H. pylori* cell pellets grown from liquid cultures in BB10 to an OD_{600} of 1 in B-PER reagent (ThermoFisher Scientific) and half a tablet of protease inhibitor (Roche) or 0.5 mM phenylmethylsulfonyl fluoride (PMSF) (Gold Biotechnology).

2.4.6 Co-immunoprecipitation.

Co-immunoprecepitations were performed using Dynabeads Protein A for Immunoprecipitation following the manufacturer's suggested protocol (ThermoFisher Scientific). In brief, antibodies (10 µl of anti-CheA (Lertsethtakarn *et al.*, 2015), 40 anti-CheV1 (Lertsethtakarn *et al.*, 2015), 10 anti-TlpD (Williams *et al.*, 2007), or 40 anti-CheW (Collins *et al.*, 2016)) diluted in a total of 200 µl washing buffer (phosphate buffered saline, 0.02% tween, pH 7.4) were first bound to Dynabeads by incubating with rotation at room temperature for 25 minutes followed by removal of supernatant from the beads using a magnetic rack. Dynabeads were crosslinked to antibodies using bis(sulfosuccinimidyl)suberate (BS3) following the manufacturer's instructions (ThermoFisher Scientific). Either purified protein mixtures or whole cell lysate was used in these experiments as the antigen, and mixed with the antibody-beads for 30-60 minutes at room temperature in phosphate buffered saline containing 0.5 mM of PMSF. For purified protein, mixtures containing 100 µM of each protein were pre-incubated together before adding beads for 30-60 minutes at room temperature in phosphate buffered saline containing 0.5 mM of PMSF. For whole cell lysate, 1000 µl at OD_{600} 1.6-1.8 was

added to the Dynabeads-antibody complex and gently resuspended by pipetting. The protein-antibody complexes were washed three times using washing buffer from above and then eluted with 50 mM glycine, pH 2.8. Samples were mixed with Laemmli sample buffer (60mM Tris-HCl pH 6.8, 2% SDS, 5% glycerol, 1% β-mercaptoethanol, 0.02% bromophenol blue) and stored at -20°C. Before running on an SDS-PAGE gel, samples were heated for 10 minutes at 95°C.

2.4.7 Immunoblotting.

Samples were separated on 12% SDS-PAGE gels. SDS-PAGE gels were then either stained using Coomassie Brilliant Blue R-250 Dye (ThermoFisher Scientific) or used for immunoblotting. For immunoblotting, gels were soaked in transfer buffer (48 mM Tris-base, 39 mM glycine, 1.3 mM SDS, 20% methanol) for 25 minutes and then transferred to a Immuno-blot polyvinylidene diflouride (PDVF) membrane (Biorad) by semi-dry transfer for 45 minutes at 12 V. The membrane was blocked for 1 to 2 hours with blocking buffer (phosphate buffered saline with 1% milk plus 0.2% Tween-20) at room temperature. Primary antibody was added and incubated for 16 hours at 4^{o} C using the following antibody dilutions: 1:1500 for anti-TlpA22, 1:60 for CheV1, 1:150 for CheW, 1:1000 for CheA. After incubation, the membranes were washed and HRP-conjugated secondary antibodies (Santa Cruz Biotech) added at 1:1500. For anti-TlpA22, anti-CheV1, and anti-CheA goat anti-rabbit IgG was used, and for anti-CheW, goat anti-guinea pig was used. After incubation, the membranes were washed and treated with 250 mM luminol, 90 mM p-coumaric acid, and 3% hydrogen peroxide in 1M Tris-HCl pH 8.5 for one minute.

Blots were then visualized using a Phosphoimager (Biorad).

2.4.8 Cellular fractionation.

Bacteria were grown as above in BB10 and collected at an OD of 1-1.5 by centrifugation and stored at -20^{o} C. Bacterial pellets were resuspended in lysis buffer (50 mM Tris-HCl pH 7, 10% glycerol, 1 mM 4-(2-aminoethyl) benzenesulfonyl fluoride hydrochloride (AEBSF), and 10 mM dithiothreitol (DTT)). Cells were further lysed by sonication in 30 second bursts for 3-5 minutes while kept on ice. Unlysed cells were removed by centrifugation at 4,000 g, 4^{o}C. 15 minutes. The supernatant was then pelleted using an ultracentrifuge at 240,000 g for 30 minutes at 4^{o}C (Beckman TLA 100.3). The supernatant was collected and considered to be the "cytoplasmic" fraction. The remaining pellet was rinsed three times with high salt buffer (2 M KCl in lysis buffer). The pellet was resuspended in high salt buffer using light sonication (20 Amp in 30 second bursts). The resuspended pellet was spun again at 240,000 g for 20 minutes at 4^{o}C. The pellet was then washed and resuspended in high salt buffer as above, followed by centrifugation at 240,000 g as above for 20 minutes at 4^{o}C. The pellet was then washed three times with lysis buffer and resuspended in lysis buffer by light sonication. The final resuspended pellet was spun for 240,000 g for 20 minutes. The final pellet was resuspended in a small volume of lysis buffer. Total protein concentration from cytoplasmic and membrane fractions were quantified by measuring absorption at 280 nm and analyzed using Coomassie Blue staining of SDS-PAGE gels as described above.

2.4.9 Phosphorylation assay.

In vitro phosphorylation assays were performed using purified proteins as described previously (Lertsethtakarn and Ottemann, 2010). In brief, 2 µM each of CheA, CheV1, and CheW were incubated in a final volume of 30 µl reaction buffer (20 mM $MgCl_2$, 50 mM KCl, 50 mM Tris-HCl pH 7.5) for 30-45 minutes at room temperature. A radioactive ATP mixture (11uM [γ-^{32}P]-ATP (Perkin- Elmer LAS) and 2mM unlabeled ATP) was used to start the reactions, by adding to a final concentration of 0.2 mM. The reactions were stopped at the indicated times by mixing with 2x Laemmli sample buffer. CheA collected right after adding radioactive ATP (time 0) was used as a reference control for all reactions. The reactions were electrophoresed on a 12% SDS-PAGE gel. Gels were dried and exposed to a phosphoimager cassette (Biorad) overnight. Autoradiography images were obtained by scanning the cassette on a Personal Molecular Imager (Biorad). The intensity of the CheA bands was determined using ImageJ software and plotted. The area under the curve was determined by calculating definite integrals (Area between each point= $(x_2 - x_1)$ [$f(x_2) + f(x_1) / 2$]).

2.4.10 Image analysis.

Western blots and phosphorylation assay images were analyzed using Image Lab Software (Biorad) or ImageJ Software (NIH) (Schneider, Rasband and Eliceiri, 2012).

2.4.11 Immunofluorescence.

Bacterial cultures were grown to an OD_{600} of 0.5 in BB10, and concentrated using centrifugation to OD_{600} of 1. Cells were prepared and stained as described in Lertsethtakarn 2015. Briefly, 50 µl of each culture was placed on poly-L-lysine coated slides, and fixed with PLP (75mM $NaPO_4$, pH 7.4, 2.5 mM NaCl, 2% paraformaldehyde). Cells were then washed, blocked (3% BSA, 0.1% Triton X-100 in PBS) and then primary antibodies added in 3% BSA, 1% saponin, 0.1% triton X-100, and 0.02% Na azide in PBS. All protein antibodies were preabsorbed as previously described and used at the following dilutions: 1:200 anti-CheA (Lertsethtakarn *et al.*, 2015), 1:200 anti-Tlps (Williams *et al.*, 2007),1:50 anti-CheW (Collins *et al.*, 2016), or 1:500 chicken anti-*H. pylori* (AgriSera AB). After incubation, the cells were washed and fluorescent secondary antibodies that recognize each of the primary protein and *H. pylori* antibodies were incubated with the cells. Goat anti-rabbit Alexa Fluor 594 (1:300 dilution), goat anti-guinea pig Alexa Fluor 594 (1:300 dilution), or goat anti-chicken 238 Alexa fluor 488 (1:500 dilution) (Abcam) were used as secondary antibodies. After incubation, the cells were washed four times with blocking buffer and aspirated off. Finally, a drop of mounting media was placed on the bacteria before covering with a cover slip to prevent photobleaching (Vectashield). The cells were then visualized using a Nikon Eclipse E600 fluorescent microscope; the Texas Red filter was used for the Alexa Fluor 594 channel and the GFP filter for the Alexa fluor 488 channel. Images were merged and analyzed using Adobe Photoshop C2.

2.5 Acknowledgements

We would like to thank Susan Williams and Eli Davis (UC Santa Cruz) for creating the *cheV1 cheW* double mutant; James Gober (UCLA) for the kind gift of the BACTH plasmids; Fitnat Yildiz (UCSC) for comments on the manuscript; Sandy Parkinson and German Piñas (U. Utah) for providing many thoughtful and useful comments on the work. The described project was supported by National Institutes of Health National Institute of Allergy and Infectious Disease (NIAID) grants number RO1AI116946 (to K.M.O.). The funders had no role in study design, data collection and interpretation, or the decision to submit the work for publication.

CHAPTER 3

Chemotaxis complex stoichiometry in *Helicobacter pylori* reveals a universal CheW to CheA kinase ratio

Abstract

Chemotaxis requires assembly of a very large multiprotein complex consisting of multiple types of chemoreceptors connected to a CheA kinase through coupling proteins. Different bacterial species have distinct components, and how the stoichiometry of these chemotaxis complex proteins varies is not fully understood. Here we determined the concentration of the chemoreceptors, four coupling proteins, and CheA kinase in the chemotactic gastric pathogen *Helicobacter pylori*. The coupling proteins, consisting of CheW and three CheV proteins, made up the majority of the chemotaxis proteins at 50%, followed by the chemoreceptors at 40%. CheA made up 10% of the total chemotaxis complex proteins. The concentration per cell of the chemoreceptors, coupling proteins, and CheA were significantly higher than that found in *Escherichia coli* and *Bacillus subtilis*. Strikingly, we found that the ratio of chemoreceptors and CheW to the CheA dimer was almost identical between species: 3.3 chemoreceptor and 1.8 CheW to 1 each CheA dimer. We also determined the chemotaxis protein stoichiometry in strains lacking either of the two main coupling proteins, CheW or CheV1. Loss of either *cheW* and *cheV1* did not affect the amounts of most chemotaxis proteins except for CheA. Strains lacking *cheW* had low amounts of CheA protein, despite having the same *cheA* transcript expression as wild type. A similar result was seen in a mutant

lacking all chemoreceptors, suggesting that CheA was degraded when the complex components were missing. In support of this idea, CheA amounts could be restored in a *cheW* mutant and a receptorless mutant upon addition of a protease inhibitor. This suggests that the binding of the chemoreceptors, CheW, and CheA helps to protect the proteins from proteolytic cleavage. These results ultimately suggest that there is a universal ratio of CheW to CheA and a highly conserved chemoreceptor ratio to CheA. This analysis also indicates that interactions between the main proteins in the chemotaxis complex not only are important for efficient signaling but also protect each other from proteolysis.

Importance:

In *Helicobacter pylori,* there are multiple chemotaxis coupling and coupling-like proteins—1 CheW and 3 CheV proteins. Coupling proteins link chemoreceptors to the CheA kinase forming a chemotaxis complex at cell poles. The chemoreceptor-CheA kinase complex represents the core unit of a chemoreceptor complex. The concentration and ratio of the core components of this complex in *Helicobacter pylori* is unknown. We found that *H. pylori* contains high concentrations of the chemotaxis proteins compared to *E. coli* and *B. subtilis. H. pylori* also maintains the trimer of dimers to 1.8 CheW to 1 CheA kinase dimer in both wildtype and mutants lacking each coupling-like protein. We also found that the core protein units of the chemotaxis proteins relay on the interactions within the chemotaxis complex to protect each other from proteolytic cleavage.

3.1 Introduction

Chemotaxis is the ability of bacteria to respond to their dynamic environments effectively and efficiently. The chemoreceptor-coupling protein-CheA kinase complex is at the core of robust chemotaxis signaling (Wadhams and Armitage, 2004) (Typas and Sourjik, 2015). In the chemotaxis signaling system, chemoreceptors sense various environmental ligands and transmit that response to a histidine kinase, CheA, through coupling proteins. Coupling proteins are crucial components that physically link chemoreceptors to the CheA kinase forming the chemotaxis chemoreceptor-CheA signaling complex.

The chemotaxis signal transduction system of the stomach pathogen, *Helicobacter pylori,* is important for its colonization stomach (Terry *et al.*, 2005). *H. pylori* has four chemoreceptors. TlpA and TlpB are transmembrane chemoreceptors and TlpD is a soluble chemoreceptor. TlpA senses arginine and bicarbonate (Cerda *et al.*, 2011). TlpB senses pH, urea, and the quorum-sensing molecule autoinducer-2 (Croxen *et al.*, 2006) (Huang *et al.*, 2015) (Rader *et al.*, 2011) . TlpD senses oxidative stress (Collins *et al.*, 2016) (Behrens *et al.*, 2016).

Chemotactic organisms have only a CheW or CheV coupling protein, or both (Alexander *et al.*, 2010). The chemotaxis signal transduction system of the stomach pathogen, *Helicobacter pylori,* is unusual compared to that found in other chemotactic microbes by the presence of multiple coupling proteins. *H. pylori* has a CheW protein in addition to three CheV proteins, CheV1, CheV2, and CheV3 whose exact function is not quite known (Pittman, Goodwin and Kelly, 2001)

(Alexander *et al.*, 2010). CheV is a hybrid protein made up of a CheW-like domain and a phosphorylatable response regulator (REC) domain (Alexander *et al.*, 2010).

Bacteria are non-chemotactic without the CheW coupling protein linking chemotaxis components because information cannot be signaled between the chemoreceptor and kinase (Boukhvalova, Dahlquist and Stewart, 2002). *H. pylori*'s coupling proteins—CheW and three CheVs (CheV1, CheV2, CheV3)—all affect the chemotactic system to different degrees. Previous data has shown that *cheV1* mutants have sever chemotaxis defects whereas *cheV2* and *cheV3* have modest chemotaxis defects (Pittman, Goodwin and Kelly, 2001) (Lowenthal, Simon, *et al.*, 2009).

The stoichiometry of the chemoreceptor-coupling protein-CheA proteins is not known in *H. pylori*. In *E. coli*, which only contains only a CheW protein, the ratio of chemoreceptor-CheW-CheA is 3 receptor dimers to 1.6 CheW to 1 CheA dimer (Li and Hazelbauer, 2004). The same 1.6 CheW-1 CheA dimer ratio is conserved in *Bacillus subtilis* which also contain one additional CheV coupling protein (Karatan *et al.*, 2001) (Cannistraro *et al.*, 2011).

Using quantitative immunoblotting, we determined the concentration and ratio of the chemotaxis proteins that make up the chemoreceptor-CheA complex. We also determined the stoichiometry of these proteins in mutant strains lacking the main coupling proteins CheV1 and CheW.

3.2 Results

3.2.1 Quantification of the chemoreceptor-coupling protein-CheA kinase complex members in *H. pylori*

We first determined the protein concentration of various chemotaxis proteins at a cellular level in *H. pylori*, using quantitative immunoblotting. *H. pylori* requires rich media with serum for optimal growth, motility, and chemotaxis (Sanders, Andermann and Ottemann, 2013). We therefore examined the concentration of each protein per cell in *H. pylori* grown under these standard laboratory conditions, with cells at mid-late exponential phase. To be able to calculate the number of molecules per cell, we determined the number of cells per volume in *H. pylori* G27 corresponding to an optical density (OD) of 1 at 600 nm by two different methods: counting colony forming units on agar plates and counting bacteria through microscopy. We found that an OD of 1 in *H. pylori* G27 is equal to 1.78×10^8 cells per milliliter (Fig. S1).

At least three independent *H. pylori* cultures were used to determine the average concentration of each chemotaxis protein, by comparison to a standard curve composed of purified protein standards. The concentration of purified proteins in the standards were determined using three independent methods: Bradford assay, SDS-PAGE gels with known bovine serum albumin standards, and NanoDrop A280 measurements, and we used the average of all three measurements. Overall, we observed that cultures grown to mid-late exponential phase were fairly consistent in terms of both chemotaxis and housekeeping protein amounts (Fig. S2).

We first quantified the chemoreceptors. *H. pylori* encodes up to four chemoreceptors although *H. pylori* G27, like many *H. pylori* strains, expresses only three functional chemoreceptors (Tlps), TlpA, TlpB, and TlpD due to a frameshift in *tlpC* (Baltrus *et al.*, 2009) (Collins *et al.*, 2016). Purified TlpD was used to determine the concentration of all three chemoreceptors because it is a soluble protein (Fig. 1A). Chemoreceptors have very similar signaling domains, and so an antibody that recognizes all of the chemoreceptors by virtue of recognizing this domain was used (Williams *et al.*, 2007). We determined that the soluble chemoreceptor, TlpD was found at 30,145 ± 4800 copies/cell. TlpD made up the majority of all chemoreceptors in *H. pylori* and was almost double the amount of the membrane chemoreceptors with TlpA having 15,281 ± 2020 and TlpB having 16,413 ± 1,763 molecules per cell (Fig. 1A). In total, there were approximately 60,000 chemoreceptors per *H. pylori* cell.

We next focused on the signal transduction molecules CheA and the coupling proteins. We determined that there were 18,573 ± 1,547 CheA molecules per cell (Fig. 1B). Coupling proteins are important proteins that physically link chemoreceptors to the CheA kinase.

H. pylori possesses three CheV proteins CheV1, CheV2, and CheV3, in addition to the common CheW coupling protein (Pittman, Goodwin and Kelly, 2001). We quantified all the coupling proteins (Fig. 1C-G). We found that CheV1 made up the majority of all the coupling proteins at around 38,333 ± 3,917 CheV1 molecules per cell (Fig. 1E). CheW and CheV3 were similar in quantity at about

16,921 ± 749 CheW and 20,508 ± 725 molecules of each per cell (Fig. 1C, 1F). Finally, CheV2 made up the least amount of all coupling proteins at around 3211 ± 170 CheV2 molecules per cell (Fig. 1D). Ultimately, there was a total of approximately 80,000 coupling proteins per *H. pylori* cell (Fig. 1E).

Overall, our data suggest that *H.pylori* has significantly higher concentrations of chemoreceptors, coupling proteins, and CheA kinase in comparison to those measured for the orthologous proteins in *B. subtilis* and *E. coli* (Fig. 2) (Cannistraro *et al.*, 2011) (Li and Hazelbauer, 2004). Of the total chemotaxis proteins in *H. pylori*, coupling proteins (CheW, CheV1, CheV2, CheV3) comprise 50%, chemoreceptors make up 40%, and CheA makes up 10% (Fig. 2). In *B. subtilis,* chemoreceptors comprise a greater percent of the total, at 83%, while coupling proteins (CheW, CheV1) make up 13%, and CheA makes up 4% of chemotaxis complex proteins (Cannistraro *et al.*, 2011) (Fig. 2). In *E. coli*, chemoreceptors make up 52%, coupling proteins (CheW) make up 24%, and CheA makes up 24% (Fig. 2) (Li and Hazelbauer, 2004).

Another way to examine this data is to evaluate the ratio of the proteins within a system, using the CheA dimer as the common comparator. In *H. pylori*, we determined that there were 3.3 chemoreceptor dimers to 1 CheA dimer, a ratio that was similar to that seen in *E. coli* (Fig. 3) (Li and Hazelbauer, 2004). Interestingly, *H. pylori* had 1.8 CheW to 1 CheA dimer which is highly similar to the 1.6 ratio of CheW to CheA in both *B. subtilis* and *E. coli* (Fig. 3) (Cannistraro *et al.*, 2011) (Li

and Hazelbauer, 2004). For the other *H. pylori* coupling proteins, there were 4.1 CheV1, 0.3 CheV2, and 2.2 CheV3 per CheA dimer (Fig. 3).

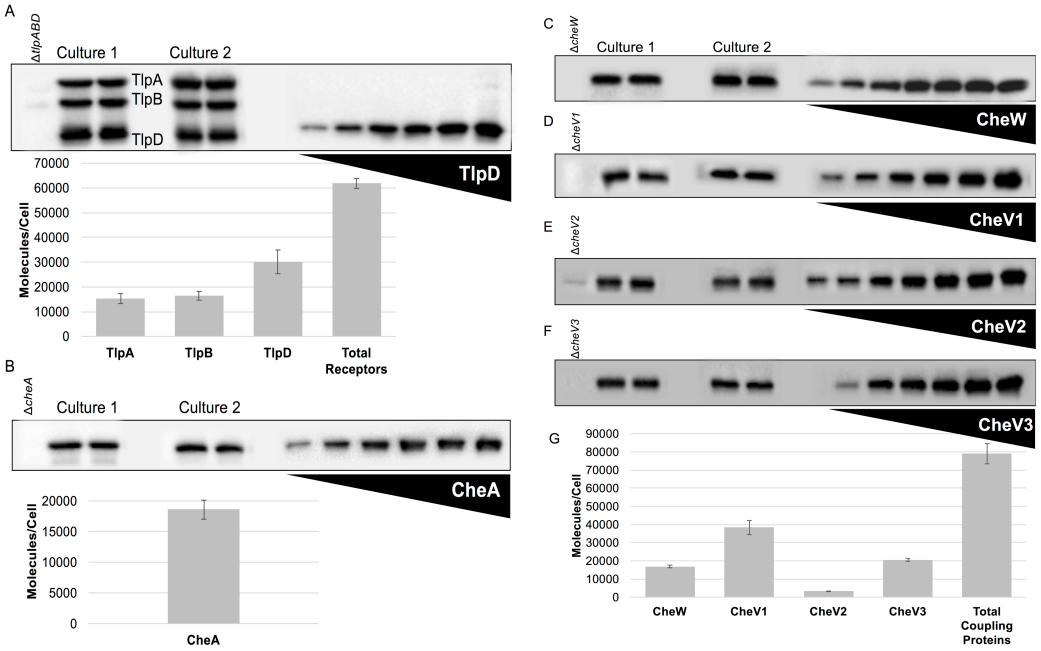

Figure 3.1. Quantitative immunoblots of the chemoreceptors, CheA kinase and coupling proteins from wild-type *H. pylori*. Immunoblots were used to quantify the cellular concentration of the the chemotaxis proteins from wild-type *H. pylori* G27. All cultures' whole cell lysates were made from liquid cultures grown to an OD_{600} 0.8-1 and all equalized to an OD_{600} of 0.7. Equal amounts of cell lysates were loaded per culture including a null mutant strain for each protein. (A) Anti-GST-Tlp-A22 was used to detect all chemoreceptors (TlpA, TlpB, and TlpD) from *H. pylori* G27. (B) Anti-CheA was used to detect CheA. (C) Anti-CheW was used to detect CheW. (D) Anti-CheV1 was used to detect CheV1 (E) Anti-CheV2 was used to detect CheV2 and (F) Anti-CheV3 was used to detect CheV3. The concentration of each protein was determined using purified protein standards. Purified TlpD standards were used to determine the concentration of all chemoreceptors. Bar graphs represent the number of protein molecules per cell calculated from the average concentration of each protein from 3 independent cultures. Error bars represent data from 3 independent cultures ran in duplicate (n=6).

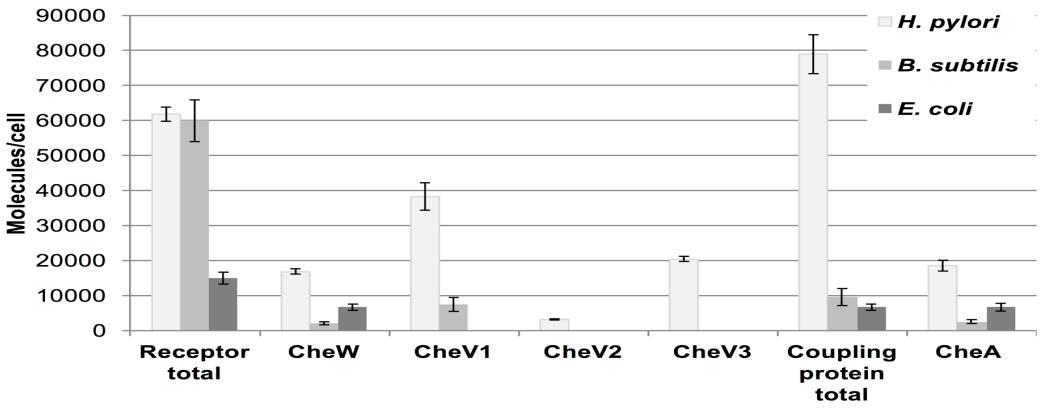

	H. pylori			*B. subtilis*			*E. coli*		
Receptor total	61838	±	2020	59960	±	5960	15000	±	1700
CheW	16921	±	749	2100	±	430	6700	±	890
CheV1	38333	±	3917	7500	±	2000			
CheV2	3211	±	170						
CheV3	20508	±	725						
Coupling protein total	78973	±	5560	9600	±	2430	6700	±	890
CheA	18573	±	1547	2600	±	560	6700	±	1100

Figure 3.2. Concentration of chemotaxis proteins in *H. pylori* in comparison to *B. subtilis* and *E. coli* (Cannistraro et al. 2011) (Li and Hazelbauer 2004). Bar graph and table show the concentrations of the chemotaxis proteins in number of protein molecules per cell from *H. pylori*, *B. subtilis* (data obtained from Cannistraro *et al.* 2011) and *E. coli* (data obtained from Li *et al.* 2004). For *E. coli*, we used the numbers obtained for *E. coli* RP437, a standard strain, grown in rich media because it most closely resembles the media used for *H. pylori* (Li and Hazelbauer, 2004). Error bars represent data from 3 independent cultures ran in duplicate (n=6).

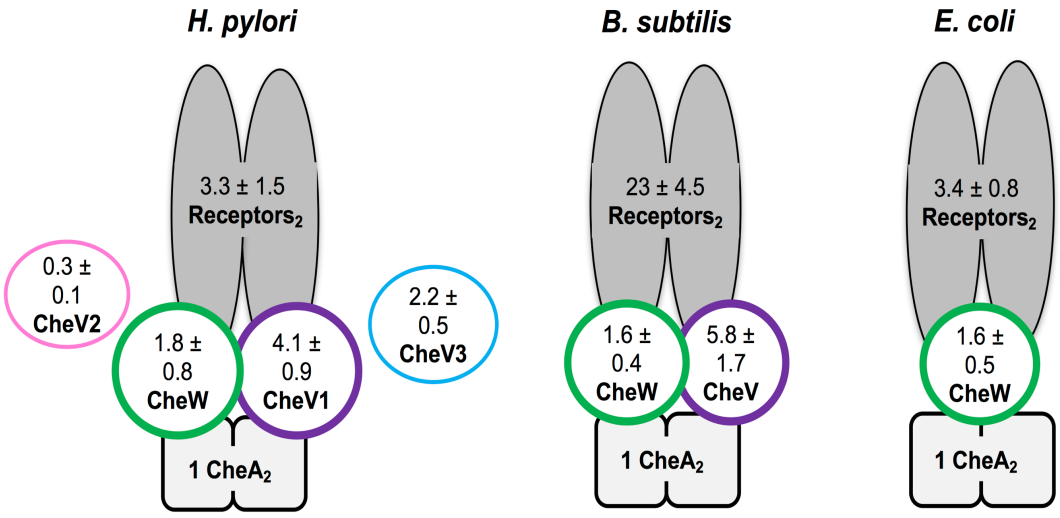

Fig. 3.3. Schematic diagram of chemotaxis signaling complex of *H. pylori*, *B. subtilis*, and *E. coli*. Cellular ratios of total chemoreceptors and coupling proteins to one CheA dimer are shown for *H. pylori, B. subtilis* (Cannistraro et al. 2011), and *E. coli* (Li and Hazelbauer 2004). Values for the ratios determined from cellular stoichiometry are shown. Chemoreceptors are represented as dimers.

3.2.2 Coupling proteins do not change amounts in *cheV1* and *cheW* mutants

The *H. pylori* system possesses multiple coupling proteins. We next examined whether the relative expression of one coupling protein could affect the other, with a focus on the two main coupling proteins CheW and CheV1. The *H. pylori* system possesses multiple coupling proteins. We next examined whether the relative expression of one coupling protein could affect the other, with a focus on the two main coupling proteins. Quantitative immunoblots were performed to determine the concentration of the coupling proteins and chemoreceptors in mutant *H. pylori* lacking the main coupling proteins CheW or CheV1 (Fig. 4). Mutant *H. pylori* strains lacking *cheW* or *cheV1* had similar amounts of coupling proteins as wild type (Fig. 4A-E). Overall, these data suggest that loss of *cheW* or *cheV1* does not affect the amount of the other.

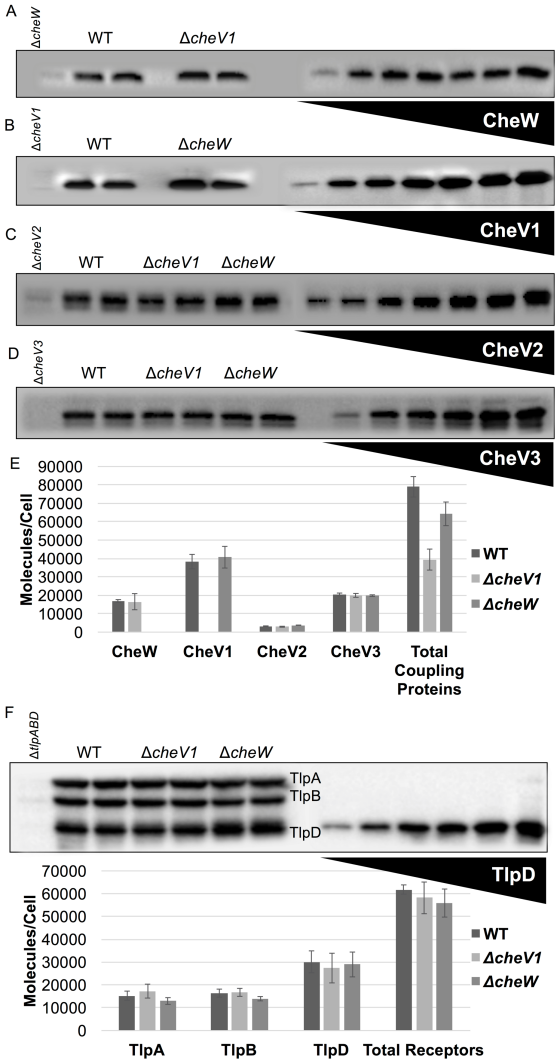

Figure 3.4. Concentration of the coupling proteins and chemoreceptors in *cheV1* and *cheW* mutant strains. Immunoblots were used to quantify the cellular concentration of the coupling proteins: (A) CheW, (B) CheV1, (C) CheV2, and (D) CheV3 and the chemoreceptors (TlpA, TlpB, and TlpD) in Δ*cheV1*, Δ*cheW,* and wild-type (WT) *H. pylori* G27 strains. All cultures were grown as described earlier. The concentration of each protein was determined using purified protein standards as described. The bar graph (E, F) represents the number of protein molecules per cell calculated from the average concentration of each protein from 3 independent cultures. Error bars represent data from 3 independent cultures ran in duplicate (n=6).

3.2.3 CheA is degraded in mutants lacking *cheW* or the chemoreceptors

We next examined how loss of the two key coupling proteins would affect CheA kinase and chemoreceptors quantities (Fig. 5A). While both *cheW* and *cheV1* mutant strains had similar amounts of chemoreceptors as wild type (Fig. 4F), they diverged with regard to CheA amounts. *cheV1* mutants had similar CheA amounts as wild type, while *cheW* mutants, in contrast, had approximately 50% the amount of CheA protein found in wild type (Fig. 5A).

cheA and *cheW* are found in the same operon in *H. pylori* (Tomb *et al.*, 1997). We thus wondered if the lowered CheA in a *cheW* mutant was due to being in the same operon. Using quantitative real-time PCR, we saw no difference in *cheA* expression in *cheV1 or cheW* mutants in comparison to wildtype (Fig. 5D).

Another possibility is that there was less CheA as a result of disrupting chemoreceptor-CheW-CheA core complex interactions. We therefore to investigated the amount of CheA in a receptorless mutant, lacking all chemoreceptors. We determined that a receptorless mutant had approximately 40% the amount of CheA found in wildtype (Fig. 5B). As observed in the *cheW* mutant, there was no decrease in *cheA* transcript, suggesting the loss of CheA occurred post-transcriptionally.

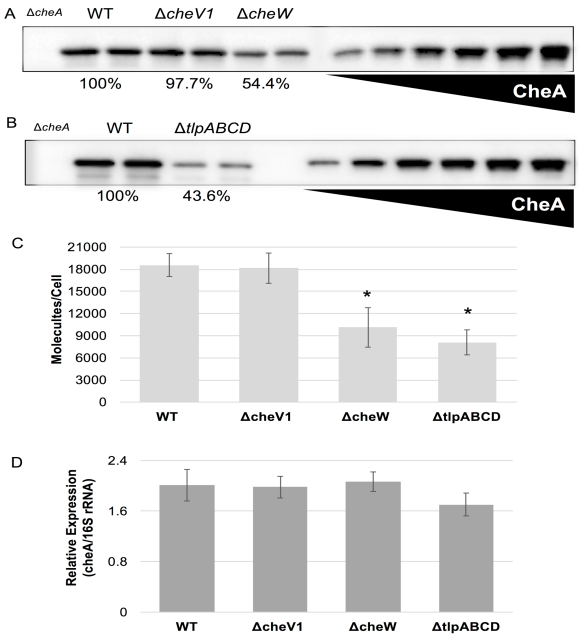

Figure 3.5. CheA concentrations and *cheA* expression in mutant strains. Immunoblots were used to quantify the cellular concentration of the CheA kinase in (A) Δ*cheV1*, Δ*cheW,* (B) Δ*tlpABCD H. pylori* G27 strains. All cultures were grown as described earlier. The concentration of each protein was determined using purified CheA protein standards. (C) Bar graph represents the number of protein molecules per cell calculated from the average concentration of each protein from 3 independent cultures. Error bars represent data from 3 independent cultures ran in duplicate (n=6). (D) *cheA* transcript expression was determined from each strain using qRT-PCR and normalized to 16S rRNA gene expression. RNA was extracted from liquid cells grown to an OD_{600} 0.8-1. Error bars represent data from 3 independent cultures.

3.2.4 CheW is similarly decreased without chemoreceptors or CheA

Our data above suggest that the amount of CheA is lessened when not in a complex with normal CheW and chemoreceptors. We next determined whether the reciprocal effects were true: whether CheW amounts would be changed in receptorless mutants. Indeed, we discovered that *cheA* mutants made approximately 10% of wild type CheW protein levels (Fig. 6A). Receptorless mutants made approximately 30% of wildtype CheW protein levels (Fig. 6A). Because CheV1 is

also a coupling protein, we also determined its amount in a receptorless mutant and found that it was only very slightly decreased in comparison to wildtype (Fig. 6B).

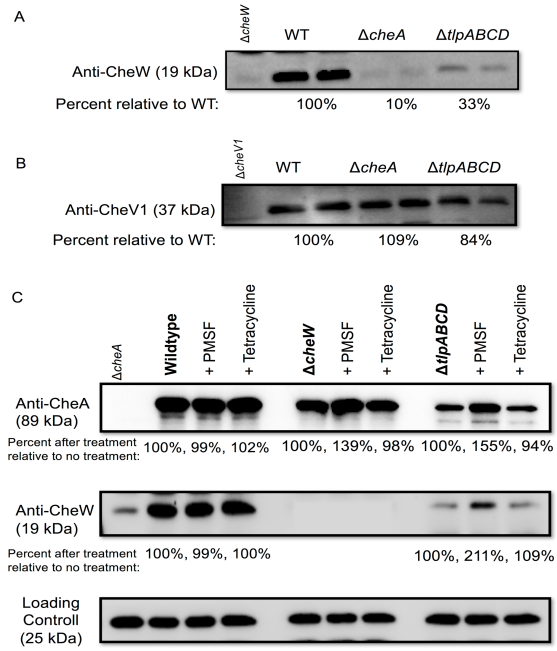

Figure 3.6. Effect of translational inhibition and protease inhibitors on CheA and CheW concentrations. Immunoblots were used to compare the cellular concentration of (A) CheW and (B) CheV1 in Δ*cheA* and Δ*tlpABCD* mutant *H. pylori* G27 strains in comparison to wildtype. Equal amounts of cells were loaded. Percentages under the (A) CheW and (B) CheV1 immunoblots indicate the percent of each protein in the mutant strains relative to wildtype. (C) Immunoblots of wildtype and mutant strains without (-) and with (+) tetracycline or PMSF treatment. Percentages under blots indicate the amount of protein after treatment in comparison to no treatment. The loading control represents an unspecfic23 kDa protein detected by anti-CheW.

3.2.5 CheA and CheW are more prone to proteolytic cleavage when not bound to each other or the chemoreceptors

To examine the mechanism for the decreased levels of CheA and CheW seen above, we analyzed whether this result was translational or post-translational.

We grew wild-type cells and mutant cells to exponential phase and then split the culture into three cultures, one with no treatment, one with the addition of tetracycline, and one with the addition of phenylmethylsulfonyl fluoride (PMSF). Tetracycline is an antibiotic that inhibits tRNA binding to mRNA and has been previously used in *H. pylori* to inhibit translation (Pereira and Hoover, 2005). PMSF is a serine protease inhibitor and has been previously used to inhibit proteolytic cleavage in various bacteria including the chemotactic bacterium *Myxococcus* (Konovalova, Löbach and Søgaard-Andersen, 2012). Upon addition of tetracycline or PMSF, we let the cells grow for another 2 hours before harvesting the cells and doing quantitative immunoblotting as described.

The amount of CheA and CheW in wildtype cells was unaffected with the addition of tetracycline or PMSF (Fig. 6C). Tetracycline treatments did not affect CheA or CheW levels in any of the mutant strains (Fig. 6C). Addition of PMSF increased CheA amounts in a *cheW* mutant by approximately 40% and by approximately 55% in a receptorless mutant (Fig. 6C). CheW protein amounts were also increased by over 100% in a receptorless mutant (Fig. 6C). Neither PMSF nor tetracycline changed CheW protein levels in a *cheA* mutant (data not shown).

3.3 Discussion

H. pylori has a high concentration of chemotaxis proteins

TlpD, a soluble chemoreceptor is the most abundant chemoreceptor in *H. pylori* (Fig. 1A). TlpD senses oxidative stress in *H. pylori* and is present in all *H.*

pylori strains despite the variation of other chemoreceptors (Collins *et al.*, 2016) (Behrens *et al.*, 2016). TlpD mutants also have the most significant animal colonization defects in comparison to mutants lacking other chemoreceptors (Rolig *et al.*, 2012) (Behrens *et al.*, 2016). This is similar to *B. subtilis*, where the receptor HemAT which senses oxygen was the most abundant (Cannistraro *et al.*, 2011). The total amount of chemoreceptors in *H. pylori* is very similar to *B. subtilis,* both have a total of around 60,000 chemoreceptors per cell (Cannistraro *et al.*, 2011).

It is not surprising that there were similar amounts of CheA, CheW, and CheV3 per cell considering that the genes for these proteins are all located on a single operon in *H. pylori* (Baltrus *et al.*, 2009).

It is interesting that *H. pylori* has significantly higher concentrations of all the chemotaxis proteins compared to the concentrations found in *B. subtilis* and *E. coli* (Li and Hazelbauer, 2004) (Cannistraro *et al.*, 2011). It is noted though that there were also significantly higher concentrations in *B. subtilis* in comparison to *E. coli* chemotaxis concentrations (Cannistraro *et al.*, 2011). There were even differences in concentrations between *E. coli* strains RP437 and *E. coli* OW1 grown in both minimal media (Li and Hazelbauer, 2004). This differences may be attributed to variations in chemotaxis protein expression.

In *E. coli,* chemotaxis genes are under the control of the sigma-28 factor (Soutourina and Bertin, 2003). In *B. subtilis,* chemotaxis genes are under control of the sigma-D factor (Fredrick and Helmann, 1994) (Mirel *et al.*, 2000). Little is known about the regulation of the chemotaxis genes in *H. pylori* although it is

thought that sigma-28 and the housekeeping sigma factor may be controlling the chemotaxis proteins (Sharma *et al.*, 2010).

H. pylori, *B. subtilis,* and *E. coli* inhabit different niches and vary in size and flagellar arrangement. *H. pylori* has 3-5 unipolar flagella. *B. subtilis* and *E. coli* both have peritrichous flagella all over their surface. Despite these significant concentration differences the ratio between chemotaxis proteins remained conserved.

***H. pylori* maintains a trimer of chemoreceptor dimers to CheA kinase ratio**

There are about 3 chemoreceptor dimers per CheA dimer. There are also 1 coupling protein per chemoreceptor dimer in *H. pylori* considering it has so many coupling proteins (Fig. 1). The ratio presented here is also supported by recent cryo-electron images that saw hexagonal units indicative of a trimer of dimer ratio in *H. pylori* (Qin *et al.*, 2016).

***H. pylori* has a conserved 1.8 CheW per CheA dimer**

The CheW to CheA dimer ratio is always conserved between different bacterial strains (*B, subtilis* and *E. coli)* (Fig. 3). The CheW to CheA dimer ratio is even conserved in *H. pylori* mutants lacking the key coupling protein CheV1.

The ratio of proteins to a CheA dimer is consistent between strains: 3.3 receptor dimers to 1 CheA dimer (like *E.* coli) and 1.8 CheW to 1 CheA dimer (like both *Bacilllus* and *E. coli*) (Fig. 3). *H. pylori* also has a similar CheV1 to CheA ratio as *B. subtilis* (Fig. 3) (Cannistraro *et al.*, 2011).

We conclude that CheV1, CheV2, and CheV3 do not affect CheA in the same manner that the coupling protein CheW does.

Loss of the main coupling proteins does not change the stoichiometry of the other coupling proteins

The concentration of chemoreceptors and coupling proteins did not change in strains lacking *cheW* or *cheV1* compared to wildtype (Fig. 4). We determined that loss of the main coupling proteins, CheW or CheV1, did not change the concentration of the other coupling proteins CheV2 or CheV3 (Fig. 4). Loss of CheW did not change CheV1 and loss of CheV1 did not change the amount of CheW (Fig. 4). This may explain why both CheV1 and CheW are essential for chemotaxis and neither can make up for the other. The ratio of CheW to CheA also remained conserved in *cheV1* mutants again suggesting and confirming that universal ratio of CheW to CheA (Fig. 4).

CheV1 and CheW are non-redundant coupling proteins in *H. pylori*. Our results from the soft agar assay suggest that CheV1 is just as important as CheW and other core chemotaxis proteins for chemotactic migration. Essentially, without CheV1, bacteria are non-chemotactic. These results conflict with previous studies that showed only a partial chemotaxis defect in *cheV1* mutants (Pittman, Goodwin and Kelly, 2001) (Lowenthal, Simon, *et al.*, 2009). This discrepancy may be due to previous studies that analyzed bacterial migration at later time points (7-8 days) as opposed to our earlier time points. We speculate that mutations occur at these later

time points, as demonstrated previously for suppressors of chemotaxis null mutants (Terry, Go and Ottemann, 2006).

CheA is degraded in mutants lacking *cheW* or the chemoreceptors

The finding that there is significantly less CheA in mutants lacking chemoreceptors or the coupling protein CheW suggest that core complex proteins relay on complex formation and interactions to protect each other from proteolytic cleavage. This is also the case with very little CheW amounts found in receptorless mutants and *cheA* mutants. CheW appears to be at the heart of the complex protecting itself from degradation of coupling chemoreceptors to the CheA kinase. In *E. coli*, *cheA* mutants that weaken or inhibit CheA's interaction with CheW resulted in low levels of CheA suggesting in vivo degradation (Zhao and Parkinson, 2006).

3.4 Materials and Methods

3.4.1 Bacterial strains and growth conditions

All *H. pylori* strains used in this study are listed in Table S1. *H. pylori* was grown on Columbia horse blood agar (5% defibrinated horse blood, 50 μg/ml cycloheximide, 10 μg/ml vancomycin, 5 μg/ml 130 cefsulodin, 2.5 Units/ml polymyxin B, and 0.2% (w/v) β-cyclodextrin) at 37^{o}C in microaerobic conditions (5-10% O_2, 10% CO_2, and 80-85% N_2. For liquid cultures, *H. pylori* was grown in brucella broth with 10% heat-inactivated fetal bovine serum (BB10) under the same conditions stated above. Antibiotic concentrations used for mutant selection were:

15 µg/ml Kanamycin or 13 µg/ml chloramphenicol. *E. coli* was grown on LB media with 100 µg/ml ampicillin or 60 µg/ml kanamycin.

3.4.2 Determination of optical density for *H. pylori* G27 cells per milliliter

The OD_{600} of representing *H. pylori* cells/ml was determined using two independent methods. First, colony forming units were counted from *H. pylori* G27 grown in liquid culture and plated on blood agar at various dilutions. Second, *H. pylori* was counted from a liquid culture using microscopy.

3.4.3 Whole cell lysate preparation

Whole cell lysates were prepared from *H. pylori* liquid cultures that were all grown to mid/late log phase (OD_{600} 0.8-1) in BB10. Cell pellets were resuspended in ice cold phosphate buffered saline with 0.5 mM phenylmethylsulfonyl fluoride (PMSF) (Gold Biotechnology). Cell lysates were mixed with Laemmli sample buffer (60mM Tris-HCl pH 6.8, 2% SDS, 5% glycerol, 1% β-mercaptoethanol, 0.02% bromophenol blue) to a final OD_{600} of 0.7 and heated at 95°C for 10 minutes. Aliquots were stored at -80°C.

3.4.4 Protein purification

TlpD, CheA, CheW, CheV1, CheV2, and CheV3 were purified as previously described (Draper, Karplus and Ottemann, 2011) (Lertsethtakarn and Ottemann, 2010) (Collins *et al.*, 2016). In brief, all fusion plasmids were expressed in *E. coli* BL21 at 37ºC and induced with 0.5 mM IPTG. The glutathione *S*-transferase (GST) fusion expression plasmids (TlpD, CheW, CheV1, CheV2, and CheV3) were

applied to a GST Prep column for purification (GE Healthcare). GST tags were cleaved using Precission protease. His-tagged CheA was applied to a His Prep column (GE Healthcare). All purified proteins were dialyzed in storage buffer (50 mM HEPES, pH 7.6, 50 mM KCl, 20% glycerol) and stored in -80^{o} C.

3.4.5 Protein quantification

Purified proteins were quantified using a Bradford assay. Proteins were also quantified using an independent method in which the concentration of purified proteins were calculated by running on a Coomassie stained SDS-PAGE gel and comparing to bovine serum albumin (BSA) protein standards. We also measured protein absorption at 280 nm on a nanodrop using the coextinction coefficient of each protein based on its amino acid composition. Following quantification, purified proteins were mixed with Laemmli sample buffer and heated at 95°C for 10 minutes. Aliquots at concentrations 50-150 ng/µl were stored at -80°C.

3.4.6 Immunoblotting

Whole cell lysate samples and purified proteins were ran on 10-12% SDS-PAGE gels. Whole cell lysate at OD_{600} of 0.7 (7,000,000 cells/lane) were ran for all immunoblots other than anti-CheA blots in which less whole cell lysate at OD_{600} of 0.7 was ran (6,360,000 cells/lane). The following protein standard ranges were loaded:1-50 ng TlpD, 4.5-27 ng CheA, 0.5-6 ng CheW, 1-30 ng CheV1, 0.5-4 ng CheV2, and 1-20 ng CheV3. Gels were then soaked in transfer buffer (48 mM Tris-base, 39 mM glycine, 1.3 mM SDS, 20% methanol) for 25 minutes and then

transferred to a Immuno-blot polyvinylidene diflouride (PDVF) membrane (Biorad) by semi-dry transfer for 50 minutes at 12 V. The membrane was blocked for 1 to 2 hours with blocking buffer (phosphate buffered saline with 1-2% milk plus 0.2% Tween-20) at room temperature. Primary antibody was added and incubated for 16 hours at 4^{o} C using the following antibody dilutions: 1:1500 for anti-TlpA22, 1:1000 for CheA. 1:150 for CheW, 1:60 for CheV1 and CheV2, and 1:30 for CheV3. After incubation, the membranes were washed and HRP-conjugated secondary antibodies (Santa Cruz Biotech) added at 1:1500. For anti-TlpA22, anti-CheV1, anti-CheV2, anti-CheV3, and anti-CheA goat anti-rabbit IgG was used, and for anti-CheW, goat anti-guinea pig was used. After incubation, the membranes were washed and treated with 250 mM luminol, 90 mM p-coumaric acid, and 3% hydrogen peroxide in 1M Tris-HCl pH 8.5 for one minute. Blots were then visualized using a Phosphoimager (Biorad).

3.4.7 Quantification analysis

Protein concentrations from each whole cell lysate were calculated from the standards of purified proteins based on a standard curve using Image Lab Software (Biorad). Protein concentrations of each whole cell lysate were then used to determine the total number of protein molecules per cell based on the number of cells per lane in each immunoblot.

3.4.8 RNA preparation, cDNA synthesis, and quantitative real-time PCR

RNA was isolated from G27 wild type and mutant *H. pylori* strains using TRIzol (Invitrogen) extraction method in combination with RNeasy columns (Qiagen) as described previously (Sause, Castillo and Ottemann, 2012). cDNA synthesis was carried out using the Tetro cDNA synthesis kit (Bioline) following the manufacturer's instructions and incubated using a thermocycler with the following conditions: 10 minutes at 25ºC, 30 minutes at 45ºC, 5 minutes at 85ºC. Generated cDNA was used in quantitative real-time PCR using the Sensifast SYBR No-ROX Kit (Bioline) following the manufacturer's instructions using a CFX Connect™ Real-Time PCR cycler (Biorad) using the following cycling conditions: 95ºC for 3 minutes, followed by 40 cycles of 95ºC for 5 seconds, 55ºC for 10 seconds, and 72ºC for 20 seconds. Transcripts from 16S rRNA were used for normalization of *cheA* expression in all strains. 16S rRNA was amplified using a forward primer (5'-GGAGGATGAAGGTT TTAGGATTG) and a reverse primer (5'-TCGTTTAGGGCGTGGACT). *cheA* was amplified using a forward primer (5'-ATGGTAAGGGATTTGAGCCG) and a reverse primer (5'-CGGTTTCAGGTT TGTTAAGCC). All reactions were performed from 2-3 independent cultures ran in experimental triplicates.

3.4.9 Determination of protein amounts effected by tetracycline and protease inhibitor addition

Liquid *H. pylori* cultures were grown in BB10 to mid/late log phase (OD_{600} 0.7-0.8). The culture was split and the following were added to each: 30 μg/ml tetracycline, 2

mM phenylmethylsulfonyl fluoride (PMSF), 2 mM 4-benzenesulfonyl fluoride hydrochloride (AEBSF), 5mM ethylenediaminetetraacetate disodium salt (EDTA), and protease inhibitor EDTA-free cocktail tablet (Thermo Scientific Pierce) at 2x concentration. The cultures were further incubated for 3 hours shaking in a microaerophilic incubator as described in growth conditions. Cell pellets were obtained and resuspended in ice cold PBS to contain 1.78 X 10^8 cells/ml. Cells were then prepared for immunoblotting as described.

3.5 Acknowledgments

I would like to thank Jashwin Sagoo for his great contribution in helping with immunoblotting and protein quantification.

CHAPTER 4

CheV1 mutants are non-chemotactic and readily accumulate suppressor mutants to regain chemotaxis in *Helicobacter pylori*

4.1 Introduction

Chemotaxis is a system that helps bacteria coordinate their motility towards beneficial environments and away from harmful ones. *Helicobacter pylori* contains a chemotaxis system with chemoreceptors that sense the environment, coupling proteins that physically link chemoreceptors to a histidine kinase CheA, and a response regulator CheY that influences motor rotation. *H. pylori* is unique to other chemotactic bacteria, in that it contains multiple coupling proteins—1 CheW in addition to 3 CheV proteins—CheV1, CheV2, and CheV3 (Pittman, Goodwin and Kelly, 2001). CheW is an essential coupling protein, yet little is known about the exact function of the CheV proteins. Previous data has shown that all three CheV proteins play a role in chemotaxis with varying degrees. CheV1 appears to have the most significant chemotaxis defects. *cheV1* mutants have a smooth-swimming bias similar to a *cheW* mutant in a fixed-time diffusion assay (Lowenthal, Simon, *et al.*, 2009). In a soft agar assay, *cheV1* mutants have severely decreased chemotaxis abilities in comparison to wildtype whereas *cheW* mutants are completely non-chemotactic (Pittman, Goodwin and Kelly, 2001) (Lowenthal, Simon, *et al.*, 2009).

Previous work from our lab has shown that CheV1 and CheW have nearly identical protein interaction networks and coupling abilities (S.A. and K.M.O.,

unpublished). We were struck, however, by previous reports that these two proteins do not equally promote *H. pylori* chemotaxis: *cheW* mutants are completely non-chemotactic, suggesting that CheV1 cannot function on its own, while *cheV1* mutants have a small amount of chemotaxis ability, suggesting that CheW can partially function on its own (Pittman, Goodwin and Kelly, 2001) (Lowenthal, Simon, *et al.*, 2009). We noticed, however, that the previous chemotaxis soft agar assays were all done with relatively long incubation times, when genetic chemotaxis-able suppressors could arise, as seen previously (Terry, Go and Ottemann, 2006). The goal of this study was to reassess the phenotypes of a *cheV1* mutant and *cheV1 cheW* double mutant in a soft agar assay.

4.2 Results

4.2.1 *cheV1* mutants are non-chemotactic

We thus assessed the phenotypes of Δ*cheV1* and Δ*cheW* mutants at early assay time points. We compared them to wildtype and multiple *H. pylori* chemotaxis mutants including mutants lacking both *cheV1* and cheW, as well as mutants lacking the coupling-like proteins CheV2 and CheV3. All strains are listed in Table 4.1. Mutants lacking various chemotaxis proteins were inoculated into soft agar and compared to a well-characterized non-chemotactic mutant lacking *cheA* (Fig. 1A). After 4-5 days of incubation, the wild type had an average diameter of 16 mm. The *cheA* mutant was non-chemotactic, with an average diameter of ~3 mm (Fig. 1B). As reported before, Δ*cheW* behaved as a non-chemotactic strain with a

similar diameter of 3.5 mm. Δ*cheV1* mutants, unexpectedly, had similarly small diameters, measuring 4 mm. *cheV2* and *cheV3* mutants both displayed near wild-type diameters, as previously shown (Pittman, Goodwin and Kelly, 2001) (Lowenthal, Simon, *et al.*, 2009) (Fig. 1C, 1D). These results confirm that strains lacking CheV1 or CheW have severe and nearly equal migration defects. Longer incubations for 6-7 days, in contrast, resulted in *cheV1* mutants but not *cheW* mutants gaining significant migration ability, consistent with previous reports (Fig. 1E) (Pittman, Goodwin and Kelly, 2001) (Lowenthal, Simon, *et al.*, 2009). These data thus suggest that both couplling proteins are needed for wild type chemotaxis when assessed at early time points.

Table 4.1. Bacterial strains and plasmids

Strain/plasmid	**Description/genotype**	**Origin/reference**
H. pylori G27		(Censini *et al.*, 1996)/ Nina Salama
H. pylori G27 Δ*cheA*	*ΔcheA::cat*	(Lertsethtakarn *et al.*, 2015)
H. pylori MG27 Δ*tlpABCD*	*ΔtlpC::aphA3*	(Lertsethtakarn *et al.*, 2015)
H. pylori G27 Δ*cheW*	*ΔcheW::aphA3*	(Terry *et al.*, 2005)
H. pylori G27 Δ*cheV1*	*ΔcheV1::cat*	(Lertsethtakarn *et al.*, 2015)
H. pylori G27 Δ*cheV2*	*ΔcheV2::cat*	(Lertsethtakarn *et al.*, 2015)
H. pylori G27 Δ*cheV3*	*ΔcheV3::cat*	(Lertsethtakarn *et al.*, 2015)
H. pylori G27 Δ*cheV1cheW*	*ΔcheW::aphA3* *ΔcheV1::cat*	This work

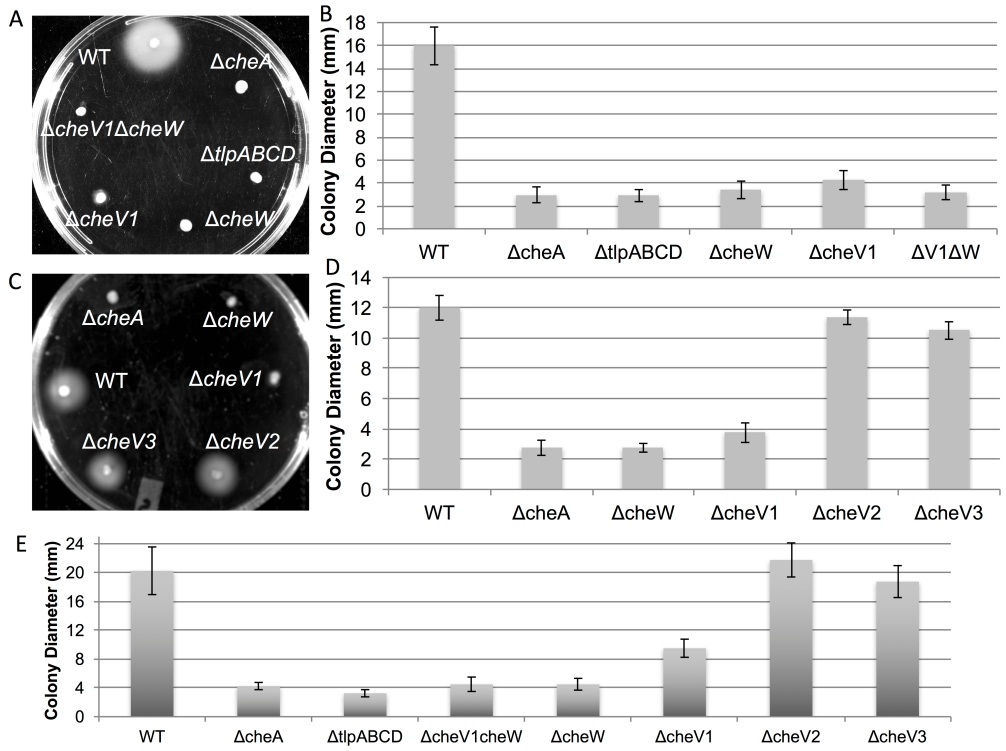

Fig. 4.1. Chemotaxis mutants have severe soft agar defects. Chemotaxis abilities were determined using a soft agar assay of wild-type G27 and its isogenic mutant strains. Bacteria were inoculated from blood plates with a pipette tip into 0.3% Brucella broth-FBS soft agar plates and incubated for at 37°C under microaerobic conditions. (A) (C) Soft agar plate showing expanded colony phenotypes of wild type and mutant strains incubated for 4-5 days. (B) (D) Quantification of colony diameters in soft agar plates of plates from panel (A) and (C). (E) Quantification of colony diameters for plates incubated for 6-7 days. Data are shown as a mean and error bars represent standard deviation (n= 14 for all strains).

4.2.2 *cheV1* mutants accumulate chemotaxis suppressor mutations

We then focused on further examining *cheV* mutants over a longer period of time (4-10 days) on soft agar plates (Fig. 2A). We found that the cheV1 mutant displayed a non-chemotactic phenotype for 5-6 days of incubation. *cheV1* mutants had similar diameters to the non-chemotactic mutants *cheW* and *cheV1cheW* which all had an average diameter of approximately 3 mm after 5-6 days of incubation (Fig. 2B). After 9 days of incubation, the average diameter of the *cheV1* mutant had

tripled to 9 mm whereas the *cheW* and *cheV1cheW* mutants maintained a small diamtere of 5 mm (Fig. 2B). This is reflective of previous published data which states that a *cheV1* mutant has a severe chemotaxis defect rather than being completely non-chemotactic similar to a *cheW* mutant (Pittman, Goodwin and Kelly, 2001). This outcome suggested that either cheV1 mutants had a slow ability to induce soft agar migration or were accumulating genetic suppressors. We also noticed that not every cheV1 experiment results in rapid soft agar colony expansion, suggesting there was variation in the outcome.

We next determined whether the ability of the cheV1 mutants to migrate in the soft agar was a stable inherited phenotype. We collected bacteria from the outer edge of the cheV1 soft agar colony, colony purified the bacteria, and retested them in soft agar. To further investigate this finding, we inoculated the outer bacterial colonies of all strains around the edges of the chemotaxis halo from 5 days of incubation on to new soft agar plates as previously described and incubated for 4-10 days (Fig. 2C) (Terry, Go and Ottemann, 2006). We found that as early as 5 days of incubation, the *cheV1* mutant was much better than the non-chemotactic mutants with an average diameter of 9 mm in comparison to 3 mm diameter of *cheW* mutants (Fig. 2D). The *cheV1* mutant had an average diameter of 15 mm after 9 days of incubation whereas the *cheW* mutant remained at 3 mm after 9 days of incubation (Fig. 2D).

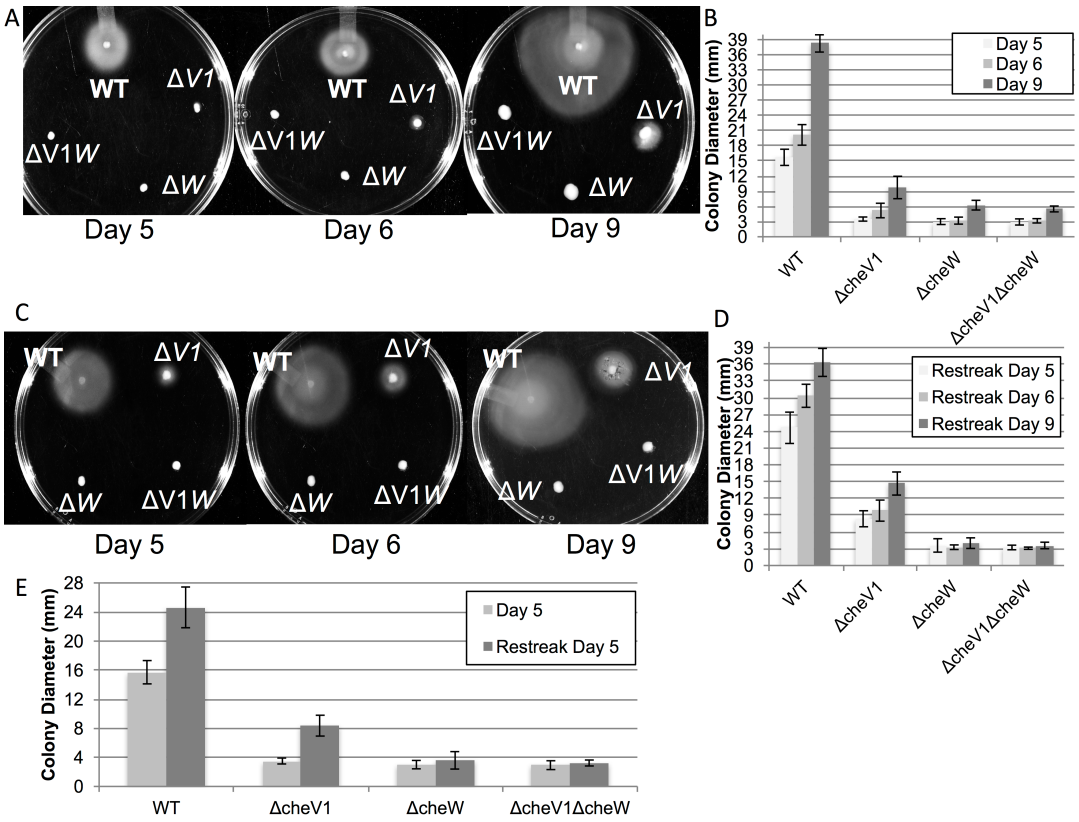

Fig. 4.2. Chemotaxis assay over various time points. Chemotaxis abilities were determined in soft agar as described earlier. (A) Bacteria were inoculated from blood plates with a pipette tip into 0.3% Brucella broth-FBS soft agar plates and incubated for 5-9 days. (B) Quantification of colony diameters in soft agar plates. (C) Bacteria were inoculated from the edges of the bacterial growth halo ("restreak") from soft agar plates with a pipette tip into 0.3% Brucella broth-FBS soft agar plates and incubated for 5-9 days. (D) Quantification of colony diameters in soft agar plates. (E) Comparison of colony diameters after 5 days incubation between soft agar plates with bacteria streaked from blood plates and soft agar plates restreaked from the edges of the bacterial grown halo from soft agar plates. Data are shown as a mean and error bars represent standard deviation (n= 12-15 for all strains).

4.2.3 *cheV1* revert mutants are almost as chemotactic as wildtype

Seeing that the restreaked *cheV1* mutant had restored chemotactic abilities, we wanted to investigate this further by redoing a soft agar assay using frozen bacterial strains. We did this by inoculating outer colonies from the *cheV1*

chemotaxis halo on the soft agar plates in Fig. 2 to blood plates and let them grow under standard conditions on the blood plates in a microaerophiic incubator for 48 hours. We inoculated 11 different spots on the outer halo of the *v1* mutant to restreak on blood plates and called them revert colonies 1-11. After growth on blood plates, we collected the cells and stored them at -80 ^{o}C with all other bacterial strains. After a few days, we passaged cells stored at -80 ^{o}C onto blood plates for 48 hours. After growth, we again did a soft agar assay on wild-type *H. pylori*, a non-chemotactic strain missing all chemoreceptors, the original *cheV1* mutant, and the 11 colonies from the *cheV1* mutant outer halo (Fig. 3A). The soft agar plates were incubated for 4-10 days and the diameter of all colonies measured. We discovered that the original *cheV1* mutant remained non-chemotactic for up to 6 days of incubation with an average diameter of 3 mm similar to the receptorless non-chemotactic mutant (Fig. 3B). By 8 days, the *cheV1* mutant had an average colony diameter of 6 mm (Fig. 3B). As early as day 4, the wildtype had an average colony diameter of 6 mm, double that of the *cheV1* mutant (Fig. 3B). Surprisingly 4 out of the 11 revert *cheV1* mutants also had diameters just as big as wildtype by 4 days of incubation and continued to expand colony diameter over time (Fig. 3B). All of the 11 *cheV1* revert mutants had bigger colony diameters than the original *cheV1* mutant yet 4 the 4 colonies described had the biggest colonies (Fig. 3B).

4.2.4 Recovering *cheV1* Che+ revertants

To explore this further, we extracted DNA from these 4 *cheV1* revert mutants called colony 5, 6, 8, and 11 and did whole genome sequencing in addition to sequencing the original *cheV1* mutant.

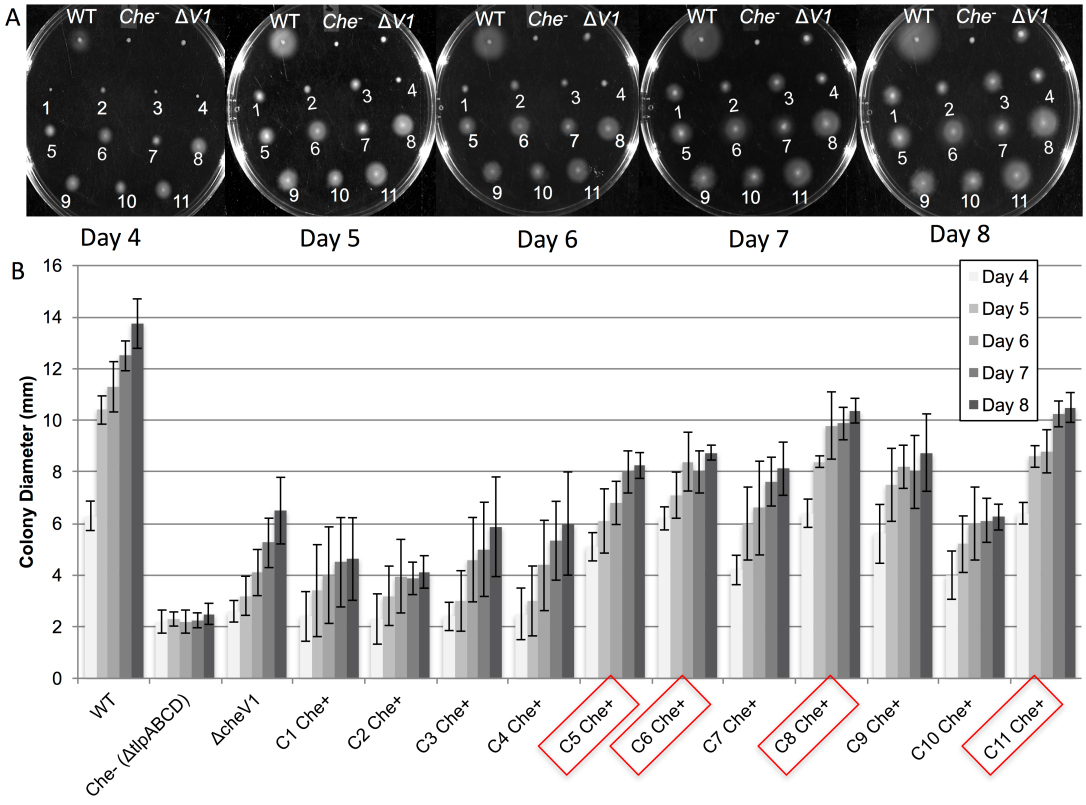

Fig. 4.3. Chemotaxis assay of *cheV1* mutants. Chemotaxis abilities were determined in soft agar as described earlier. *cheV1* mutants that gained the ability to do chemotaxis after 5-6 days were collected. A total of 11 colonies were collected (C1-C11) by poking a pipette tip on the outer edges of the bacterial growth halo of *cheV1* mutants as well as wildtype and a non-chemotactic strain (che$^-$ = *tlpABCD* mutant) grown on soft agar plates for 5-6 days. The bacteria on the pipette tip were streaked on blood plates and grown as described. (A) Bacteria were inoculated from these blood plates with a pipette tip into 0.3% Brucella broth-FBS soft agar plates and incubated for 4-8 days. (B) Quantification of colony diameters in soft agar plates. Red boxes represent colonies sent for genome sequencing—C5, C6, C8, and C9. Data are shown as a mean and error bars represent standard deviation (n= 9-12 for all strains).

4.2.5 *cheV1* Che+ revertant mutants' genome sequences

Analysis of the 4 *cheV1* revert mutants resulted in many polymorphisims in the mutants in comparison to the original *cheV1* mutant and the wild-type G27 genome. We first check if there were any changes to the sequences in the chemotaxis genes: all chemoreceptors (*tlpA, tlpB, tlpC*, and *tlpD*), the coupling proteins (*cheW, cheV1, cheV2, cheV3*), the histidine kinase *cheA*, the response regulator *cheY*, and the phosphatase *cheZ.* We found no polymorphisms in any of these genes or regions closeby within 500 base pairs.

Surprisingly all revert *cheV1* mutants had a conserved polymorphism in comparison to the wildtype G27 genome. The polymorphism occurred in a hypothetical protein HPG27_RSO1025. This protein is 302 base pairs in length and is located between base pairs 204,020-204,321 in the wildtype G27 genome. In the mutants, there was a "G" base pair insertion at position 204,167. This variant had a frequency of 92.2% resulting in a tandem repeat insertion where the wildtype genome had 6 Gs and the mutants had 7 Gs resulting in a frameshift mutation. The variant P value was 1.1e-200. The base pair sequences are shown below:

H. pylori G27 genome 204,020-204,321 base pairs:

ATGAAAAAGGTGATTTTTTTATTTTTAGTGGTGTTGGGGGGTTAAAGTCG
CAAAGCAGTTATTGCAGCGATTTTTGCGAAGGCACGCCAGATAGCCGTA
TCCCTCCTATGGGGTTTCATTTCAGTTTTGTGCATTCAGTGAAATATTACT
TGCAAGATCCACAAGAACGCGATCACAAGCTTAAAAAATGCCATGAAG

CCTTTGATTCGACCCTTAAGGTTAATTTTATTACGAAGTCTTTTAAAAAG

GATTGCAAGCATGCGCAAATGGCTTTAGAGCAAGCTCAAAAAGGAACTC

CATAA

Translation to DNA base pairs to amino acids:

MKKVIFLFLVVLGG*SRKAVIAAIFAKARQIAVSLLWGFISVLCIQ*NITCKIH

KNAITSLKNAMKPLIRPLRLILLRSLLKRIASMRKWL*SKLKKELH

*represents Stop codon

Revert *cheV1* mutants' genome 204,020-204,321 base pairs:

ATGAAAAAGGTGATTTTTTTATTTTTAGTGGTGTTGGGGGGGGTTAAAGTC

GCAAAGCAGTTATTGCAGCGATTTTTGCGAAGGCACGCCAGATAGCCGT

ATCCCTCCTATGGGGTTTCATTTCAGTTTTGTGCATTCAGTGAAATATTA

CTTGCAAGATCCACAAGAACGCGATCACAAGCTTAAAAAATGCCATGAA

GCCTTTGATTCGACCCTTAAGGTTAATTTTATTACGAAGTCTTTTAAAAA

GGATTGCAAGCATGCGCAAATGGCTTTAGAGCAAGCTCAAAAAGGAAC

TCCATAA

Translation to DNA base pairs to amino acids:

MKKVIFLFLVVLGGLKSQSSYCSDFCEGTPDSRIPPMGFHFSFVHSVKYYLQ

DPQERDHKLKKCHEAFDSTLKVNFITKSFKKDCKHAQMALEQAQKGTP*

*represents Stop codon

We translated this DNA sequence with the mutation and compared it to the original sequence. We found that in wildtype, there are multiple stop codons in the protein translation whereas the revert mutants resulted in a frameshift mutation that resulted in restoration of a full open reading frame (Fig. 4). PHYRE protein search of deemed the protein sequence a protease with minimal sequence identity.

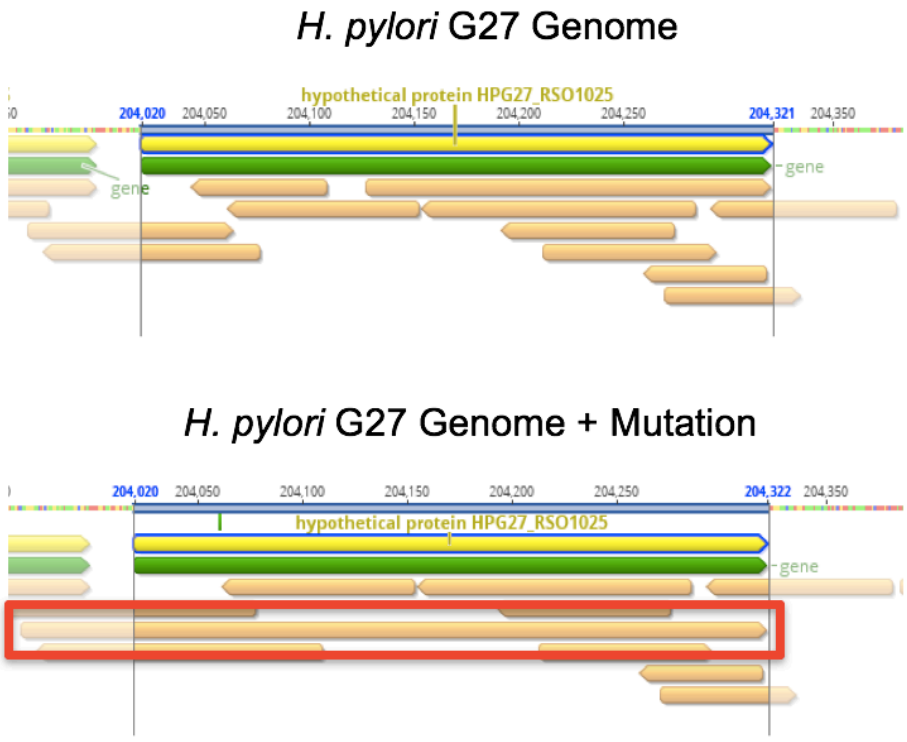

Fig. 4.4 Restoring open reading frame coding sequence in revert mutant sequences. The top panel indicates a gene in green and all open reading frames in orange from the wildtype G27 *H. pylori* genome for hypothetical protein HPG27_RS01025. The bottom panel shows the same region with the mutation of the revert mutants. The red box indicates an open reading frame covering the hypothetical gene area.

4.3 Discussion

The data here supports our previous findings that CheV1 is an essential chemotaxis protein. We had previously discovered that CheV1 shared a highly similar interaction network similar to CheW, an essential chemotaxis coupling protein. Both CheV1 and CheW were shown to increase CheA kinase activity and localize chemotaxis proteins to cell poles.

Previously published data had shown that *cheV1* mutants result in severe chemotaxis soft agar defects but are not completely non-chemotactic like *cheW* mutants (Pittman, Goodwin and Kelly, 2001) (Lowenthal, Simon, *et al.*, 2009). We saw that it took until after day 5 for the original *cheV1* mutant to start gaining ability to be chemotactic, before that it is just as non-chemotactic as the chemoreceptor mutant (Fig 1). For some of the *cheV1* revert mutant colonies that were selected from the CheV1 mutant outer colonies that were preserved and restreaked, it took as little as 4 days to be chemotactic (Fig. 2). Some of the *cheV1* revert mutants become as chemotactic as the wild-type strain even after only 4 days of incubation (Fig. 3).

The isolated *cheV1* revert mutants that gained chemotactic ability in soft agar assays did not show any sequence mutations in any of the chemotaxis genes indicating that the suppressor mutation of a non-chemotactic strain is not due to changes in known chemotaxis genes. It seems that the revert mutants restored an open reading frame of a hypothetical protein, HPG27_RS01025, that is not made in wildtype and does not have similarity to other proteins.

The results here do indeed support that CheV1 is an essential chemotaxis protein and that *H. pylori* are non-chemotactic without CheV1. These results are similar to previous findings that *cheW* mutants gained suppressor mutations in the CheZ phosphatase protein (Terry, Go and Ottemann, 2006). Future experiments should investigate the localization of the chemotaxis complex proteins in the *cheV1* Che+ suppressors as well as the swimming behavior. It would also be interesting to look at the function of the hypothetical protein, HPG27_RS01025 discovered in *cheV1* mutants by mutating it in wildtype and non-chemotactic strains to see if there are any phenotypic chemotaxis changes.

4.4 Materials and Methods

4.4.1 Bacterial strains and growth conditions.

All *H. pylori* and *E. coli* strains used in this study are listed in Table 1. *H. pylori* was grown on Columbia horse blood agar (5% defibrinated horse blood, 50 μg/ml cycloheximide, 10 μg/ml vancomycin, 5 μg/ml 130 cefsulodin, 2.5 Units/ml polymyxin B, and 0.2% (w/v) β-cyclodextrin) at 37^{o}C in microaerobic conditions (5-10% O_2, 10% CO_2, and 80-85% N_2. For liquid cultures, *H. pylori* was grown in Brucella broth with 10% heat-inactivated fetal bovine serum (BB10) under the same conditions stated above. Antibiotic concentrations used for mutant selection were: 15 μg/ml kanamycin or 13 μg/ml chloramphenicol. *E. coli* was grown on LB media with 100 μg/ml ampicillin or 60 μg/ml kanamycin.

4.4.2 Chemotaxis migration assay.

Soft agar plates were used to examine chemotaxis of various strains. Soft agar plates consisted of 0.3% agar in brucella broth with 2.5% FBS. Plates were dried at room temperature for 3 days prior to use. Bacterial strains were stab inoculated in the agar using pipette tips. Soft agar plates were incubated at 37^{o}C for 4-5 days under microaerobic conditions described above for H. pylori strain growth. The diameter of the bacterial colony was measured using a ruler.

4.4.3 Isolation of chemotaxis positive mutants from *cheV1* mutants.

A pipette tip was used to poke outer colonies of *H. pylori* wildtype and mutant strains on soft agar plates after 4-5 days of growth. The pipette tip either inoculated in new soft agar plates or was restreaked on blood agar plates that were incubated for 48 hours until *H. pylori* growth was observed. Strains were frozen in BB10 liquid media with glycerol in -80^{o}C.

4.4.4 Genome sequencing & sequence analysis.

Genomic DNA was isolated from all the original *H. pylori* G27 *cheV1* mutant and 4 revert mutants. Genomic DNA was sent for whole genome sequencing at UC Davis using a Miseq sequencer. Genome sequences were analyzed using FastQC for quality trimming and Geneious version 9.1.5. The sequences were mapped to the *H. pylori* G27 genome.

4.5 Acknowledgments

I would like to thank Dr. Jenny Draper for teaching me how to analyze genome sequences. We would like to thank Susan Williams and Eli Davis (UC Santa Cruz) for creating the *cheV1 cheW* double mutant.

CHAPTER 5

Conclusions and future directions

Two-component pathways are important signal transduction pathways in bacteria and are generally made up of a sensory histidine kinase and a response regulator. Chemotaxis is one of the most extensively studied signal transduction pathways and is a sensory pathway that bacteria use to help them survive in their respective environments. Much has been learned about the structure and function of signal transduction pathways from studying chemotaxis in *E. coli* which contains a histidine kinase, CheA, and a response regulator that together drive the bacterium's chemotactic response. Deviations from this simple chemotaxis system have been observed in other bacteria such as *H. pylori* that has a hybrid histidine kinase protein, CheA, and additional coupling proteins, CheW and 3 CheV proteins, that contain a response regulator. Understanding the biochemical mechanism of signaling in chemotaxis is important to advancing knowledge on this critical ubiquitous sensory pathway.

The findings of this thesis present information on the function of the coupling proteins CheV1 and CheW, the cellular stoichiometry of the chemotaxis proteins, and *cheV1* suppressor mutants in *H. pylori*. CheV1 and CheW are both important coupling proteins that provide stabilization to the chemotaxis complex and localize the complex to cell poles. In *H. pylori,* the concentration and ratio of the chemotaxis proteins provide knowledge on the chemotaxis complex suggesting a trimer of chemoreceptor dimers to CheA ratio and a conserved CheW to CheA

ratio. The ratio of the CheV2 and CheV3 proteins to CheA kinase is also analyzed. It is also demonstrated that *cheV1* mutants rapidly accumulate suppressor mutations that regain chemotaxis ability. The studies here provide support that CheV1 is an essential chemotaxis protein and that chemotaxis systems benefit from multiple coupling proteins in various ways. There remains, however, multiple questions to build on the results discovered here.

5.1 CheV1 and CheW coupling proteins

The findings of Chapter 2 suggest that indeed multiple types of coupling proteins are necessary to promote critical connections within the chemotaxis complex between chemoreceptors and the CheA kinase. Both proteins are also important for localizing the chemotaxis complex to cell poles.

For future studies investigating the reasons why *H. pylori* has multiple CheV proteins, it would be helpful to explore the hybrid domains of the CheV protein. CheVs are hybrid proteins made up of an N-terminal CheW-like domain and a C-terminal phosphoryltable response regulator (REC) domain. It has been demonstrated that all three CheV proteins result in a decrease of phosphorylated CheA at much lower efficiency than CheY (Jiménez-Pearson *et al.*, 2005). Mutants containing each domain individually may provide mechanistic information in protein interaction studies as well as phosphorylation assays. There is not much known about what role of the REC domain in the CheV proteins and thus a phosphorylated mutant would provide much interesting interaction studies. Another

important future experiment would be to look at the interaction of the membrane chemoreceptors TlpA and TlpB with CheW and all three CheV proteins in an immunoprecipitation assay using purified proteins. We showed here that the soluble chemoreceptor TlpD does interact with CheV1 and CheW yet were not able to look at the membrane receptors and further investigate their interaction with the other CheV proteins.

5.2 Chemotaxis stoichiometry

The findings of Chapter 3 suggest that there is a conserved trimer of chemoreceptor dimers ratio to CheA kinase and a universal CheW to CheA kinase ratio. The most interesting finding is that the chemotaxis complex proteins rely on each other for protein stabilization suggesting the importance of complex formation. This study was limited because it only focused on one strain of *H. pylori* grown in relatively rich media (BB10) despite finding a conserved ratio of chemotaxis proteins. It might be important to see how various conditions might affect the chemotaxis protein stoichiometry such as acid (repellant) or nutrient (attractant) addition. It is plausible that the 3 CheV proteins are used as couplers depending on environmental conditions encountered by *H. pylori*. It has been seen that in *C. jejuni,* the aspartate chemoreceptor prefers CheV over the CheW coupling protein (Korolik, 2010). It is noted that there was a difference in chemotaxis protein stoichiometry between *E. coli* strains grown in minimal and rich media (Li and Hazelbauer, 2004).

The finding that mutant *H. pylori* missing core chemotaxis proteins result in proteolytic cleavage of other chemotaxis proteins suggests that there may be protein regulation on the chemotaxis system or that proteins are degraded if they are not properly assembled. Future studies should focus on investigating the regulation of the chemotaxis proteins in *H. pylori* (Yamaoka, 2008).

5.3 *cheV1* suppressor mutants

The findings of Chapter 4 indicate that CheV1 is indeed an essential chemotaxis protein and that *H. pylori* cannot migrate in soft agar plates without CheV1. It seems that revert mutants that regain chemotaxis over time have regained a protein that is otherwise not translated as a full-length protein. The main question is: what is the function of this hypothetical protein. Future studies could focus on mutating the gene for this protein similar to the mutation that the *cheV1* suppressor mutants have and looking for chemotaxis phenotypes. It is possible that this protein may be important for chemotaxis just like the discovery of CheZ in *cheW* suppressor mutants (Terry, Go and Ottemann, 2006).

5.4 Conclusion

Many open questions remain in terms of the chemotaxis system of *H. pylori* and other microbes. *H. pylori* is a gram-negative bacterium that causes multiple diseases ranging from gastritis to peptic ulcers to stomach cancer. It depends on chemotaxis to colonize and infect and survive in the human stomach. Many pathogenic microbes rely on chemotaxis to survive in their relative environments so

that they can swim toward favorable chemical gradients and away from unfavorable environments. The chemotaxis pathway has been well-studied in *E. coli* and the system generally includes a chemoreceptor to sense environmental stimulants, a coupling protein that physically couples the chemoreceptor to a histidine kinase which goes to act on the response regulator. The response regulator affects the flagellar motility resulting in swimming or tumbling activity. Deviations from the *E. coli* system exist in other microbes mainly in having alternative CheV coupling proteins, differences in their adaptation response, and phosphatase proteins. *C. jejuni*, *B. subtilis, Salmonella,* and other bacteria have been shown to have a CheV protein. *H. pylori* illustrates a unique chemotaxis system by having 3 CheV proteins that are all involved in chemotaxis. Despite having various experimental methods for studying the chemotaxis system of microbes, there remains to be many unanswered questions.

5.4.1 Open questions

- What role does the phosphorylation status of CheV proteins play in *Epsilonproteobacteria*?
- What is the function of CheV2 and CheV3 *H. pylori* chemotaxis?
- Do the CheV proteins of *H. pylori* aid in chemotactic adaptation?
- Do the CheV proteins prefer interactions with specific chemoreceptors?
- Does the concentration of the chemotaxis proteins change when *H. pylori* encounters different environmental conditions?
- What is the function of the restored protein in *cheV1* suppressor mutants?

APPENDIX 1

This appendix provides supplemental information to Chapter 2.

```
TlpD    GQDIESLYEKMQNATSLADSLNQRSNEITQVISLIDDIAEQTNLLALNAAIEAARAGEHGRGFAVV
TlpA    SKTIENITTSIQGVSSQSEAMIEQGQDIKSIVEIIRDIADQTNLLALNAAIEAARAGEHGRGFAVV
TlpB    ----------EELSSKVEQLSRNADDVKSILDIINDIADQTNLLALNAAIEAARAGEHGRGFAVV
TlpC    TQSLEEITNIITTIDSKSQEMISQGEDIKSVVDMIRDIADQTNLLALNAAIEAARAGEHGRGFAVV

                 *  : :  ..:::..::.:* ***:*************************

TlpD    ADEVRKLAEKTQKATKEIAVVVKSMQQEANDIQTNTHDINSIVGSIKGDVEELKS---TVKNNM--
TlpA    ADEVRKLAERTQKSLSEIEANINILVQSISDTSESIKNQVKEVEEINASIEALRS---VIEGNL--
TlpB    ADEVRNLAGRTQKSLAEINSTIMVIVQEINAVSSQMNLNSQKMERLSDMSKSVQETYEKMSSNLSS
TlpC    ADEVRKLAERTQKSLSEIEANINILVQSIADNAESIKMQNKGVENIHNSINALQQ---DVQDNL--

*****:** :***:  **   :  : *.     . :   . :  :    : ::.    :..*:
```

Figure S2.1. Alignment of the signaling domain of *H. pylori* chemoreceptors. Alignment of the signaling domain of the *H. pylori* chemoreceptors, TlpD (HPG27_559), TlpA (HPG27_91), TlpB (HPG27_95), and TlpC (HELPY_0078) was done using T-Coffee Software Version 11. Red highlighting corresponds to good alignment and yellow highlighting corresponds to average alignment.

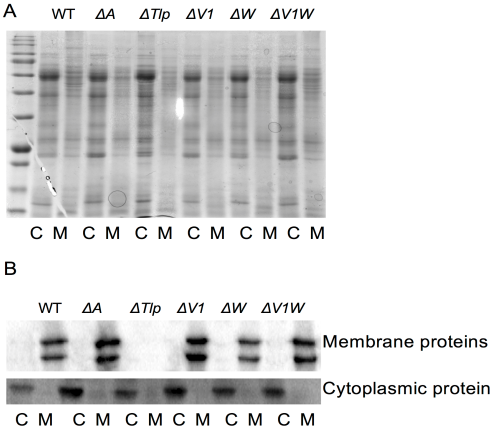

Fig. S2.2. Cellular Membrane Fractionation (A) Coomassie Blue stained SDS-PAGE gel with equal amounts of cytoplasmic "C" and membrane "M" cellular fractions (25 µg protein/lane) of various *H. pylori* strains. (B) Western blot controls from cytoplasmic "C" and membrane "M" fractions of various strains shown from the SDS-PAGE gel. The top panel "Membrane proteins" was probed with anti-TlpA22 which detects the membrane chemoreceptors TlpA and TlpB. The bottom panel "Cytoplasmic protein" was probed with anti-CheV1 which detects a cytoplasmic protein and has been previously used as a cytoplasmic control [14].

Δtlp= strain lacking all chemoreceptors, *ΔA= ΔcheA, ΔV1= ΔcheV1, ΔW= ΔcheW,* and *ΔV1W= ΔcheV1 ΔcheW*.

Table S2.1. Bacterial strains and plasmids

Strain/plasmid	Purpose	Description/genotype	Origin/reference
H. pylori mG27	BACTH	PCR template; Mouse adapted G27	(Castillo *et al.*, 2008)
H. pylori G27	Soft-Agar Co-ip		(Censini *et al.*, 1996)/ Nina Salama
H. pylori G27 Δ*cheV1*	Soft-Agar Co-ip	*ΔcheV1::cat*	(Lertsethtakarn *et al.*, 2015)
H. pylori G27 Δ*cheW*	Soft-Agar Co-ip	*ΔcheW::aphA3*	(Terry *et al.*, 2005)
H. pylori G27 Δ*cheV1cheW*	Soft-Agar Co-ip	*ΔcheW::aphA3 ΔcheV1::cat*	This work
H. pylori G27 Δ*cheV2*	Soft-Agar	*ΔcheV2::cat*	(Lertsethtakarn *et al.*, 2015)
H. pylori G27 Δ*cheV3*	Soft-Agar	*ΔcheV3::cat*	(Lertsethtakarn *et al.*, 2015)
H. pylori G27 Δ*cheA*	Soft-Agar Co-ip	*ΔcheA::cat*	(Lertsethtakarn *et al.*, 2015)
H. pylori mG27 Δ*tlpABCD*	Soft-Agar Co-ip	*ΔtlpC::aphA3*	(Lertsethtakarn *et al.*, 2015)
E. coli BL21 CheAY	Protein purification	pTrc-*cheAY*	(Jiménez-Pearson *et al.*, 2005)/ Dagmar Beir
E. coli BL21 TlpD	Protein purificatio	pGEX-6P-2-*tlpD*	(Draper, Karplus and Ottemann,

	n		2011)
E. coli BL21 CheW	Protein purification	pGEX-6P-2-*cheW*	(Collins *et al.*, 2016)
E. coli BL21 CheV1	Protein purification	pGEX-6P-2-*cheV1*	(Lertsethtakarn and Ottemann, 2010)
E. coli DH5 ✔	BACTH	Cloning strain; endA1 hsdR17 (rK-mK+) supE44 thi-1 recA1 gyrA (NalR) relA1 (lacIZYA-argF)U169 deoR (80dlac(lacZ)M15)	Invitrogen
E. coli BTH101	BACTH	Reporter strain for BACTH; *F-, gal E15, gal K16 mcrA1, mcrB1, ara D139, rpsL1(Strr), hsdR2, cya-99* (adenylate cyclase deficient) REC+	(Karimova *et al.*, 1998)
pKT25 (T25-X)	BACTH	BACTH plasmid encoding the T25 fragment allowing for in-frame protein fusion at the C terminal end of T25; Km^r	(Karimova *et al.*, 1998)/J. Gober
pUT18 (Y-T18)	BACTH	BACTH plasmid	(Karimova *et al.*,

		encoding the T18 fragment allowing for in-frame protein fusion at the N terminal end of T18; Ap^r	1998)/J. Gober
pKT25-zip (T25-zip)	BACTH	BACTH control plasmid with the yeast GCN4 leucine zipper fused to the T25 fragment at the C terminal end; Km^r	(Karimova *et al.*, 1998)/J. Gober
pUT18C-zip (T18-zip)	BACTH	BACTH control plasmid with the yeast GCN4 leucine zipper fused to the T18 fragment at the C terminal end; Ap^r	(Karimova *et al.*, 1998)/J. Gober
pKT25-*cheV1*	BACTH	Fusion, Km^r	This work
cheV1-pKNT25	BACTH	Fusion, Km^r	This work
pKT25-*cheW*	BACTH	Fusion, Km^r	This work
cheW-pKNT25	BACTH	Fusion, Km^r	This work
cheV1-pUT18	BACTH	Fusion, Ap^r	This work
pUT18C-*cheV1*	BACTH	Fusion, Ap^r	This work
cheV2-pUT18	BACTH	Fusion, Ap^r	This work
pUT18C-*cheV2*	BACTH	Fusion, Ap^r	This work
cheV3-pUT18	BACTH	Fusion, Ap^r	This work
pUT18C-*cheV3*	BACTH	Fusion, Ap^r	This work
cheW-pUT18	BACTH	Fusion, Ap^r	This work
pUT18C-*cheW*	BACTH	Fusion, Ap^r	This work

cheA-pUT18	BACTH	Fusion, Ap^r	This work
pUT18C-*cheA*	BACTH	Fusion, Ap^r	This work
tlpA-pUT18$_{aa330-675}$	BACTH	Fusion, Ap^r	This work
pUT18C-*tlpA*$_{aa330-675}$	BACTH	Fusion, Ap^r	This work
tlpB-pUT18 $_{aa240-565}$	BACTH	Fusion, Ap^r	This work
pUT18C-*tlpB* $_{aa240-565}$	BACTH	Fusion, Ap^r	This work
tlpD-pUT18	BACTH	Fusion, Ap^r	This work
pUT18C-*tlpD*	BACTH	Fusion, Ap^r	This work

Table S2.2. Primers used in this study

Primer	**Oligonucleotide sequence**	**Restriction site**
cheV1 pKT25 F	atatatCTGCAGaaATGGCTGATAGTTTAGCGGG	*PstI*
cheV1 pKT25 R	atatatGGATCCtcTGCTAATTCCAAAAATTGCTTAAC	*BamHI*
cheV1 pUT18 F	atatatCTGCAGaATGGCTGATAGTTTAGCGGG	*PstI*
cheV1 pUT18 R	atatatGGATCCtcTGCTAATTCCAAAAATTGCTTAAC	*BamHI*
cheV2 pUT18 F	atatatCTGCAGaGTGGTAAGAGATATTGACAAAACGA	*PstI*
cheV2 pUT18 R	atatatGGATCCtcTGAAAGCGTTTTTTTAAGCATTTCA	*BamHI*
cheV3 pUT18 F	atatatCTGCAGaATGGCAGAAAAAACAGCTAACG	*PstI*
cheV3 pUT18 R	atatatGGATCCtcCGCATTCTTGTCTAAAATCTTAGAAATT	*BamHI*

cheW pUT18 F	atatatCTGCAGaGTGAGCAATCAATTAA AAGATTTATTTGAAA	*PstI*
cheW pUT18 R	atatatGGATCCtcGAAGTCTTTTTTTAAG ATTTCTTCCACTC	*BamHI*
cheA pUT18 F	atatatGTCGACaATGGATGATTTGCAAG AAATAATG	*SalI*
cheA pUT18 R	atatatGGATCCtcCGATTCGCCTCCTTCTA ATTT	*BamHI*
*tlpA*pUT18 F (cytoplasmic signaling domain: nt #988-2028, aa #330-675)	atatatCTGCAGaCGTTTGGAAGTCGTTTC TAG	*PstI*
*tlpA*pUT18 R (cytoplasmic signaling domain: nt #988-2028, aa #330-675))	atatatTCTAGAgcAAACTGCTTTTTATTC ACAT	*XbaI*
tlpB pUT18 F (cytoplasmic signaling domain: nt #718-1695, aa #240-565)	atatatCTGCAGaGATGAACTGGTCCTTA AAAT	*PstI*
tlpB pUT18 R (cytoplasmic signaling domain: nt #718-1695, aa #240-565)	atatatGGATCCtcAGTTTTAAACAAATTC ACTT	*BamHI*
tlpD pUT18 F	atatatCTGCAGaATGTTTGGGAATAAGC AGTT	*PstI*
tlpD pUT18 R	atatatGGATCCtcTTCGCCTTTTTGAATTT TTTCA	*BamHI*

*Restriction sites are underlined; F= forward primer; R= reverse primer

Table S3. Bacterial Two-Hybrid Interactions. The chemotaxis proteins were fused to the N and C terminus of the adenylate cyclase T25 and T18 fragments.

	CheV1→T25	T25→CheV1	CheW→T25	T25→CheW
T18→CheA	+	-	+	-
CheA→T18	+	-	+	-
T18→TlpA	+	-	-	-
TlpA→T18	+	-	+/-	-
T18→TlpB	+	-	-	-
TlpB→T18	+	-	-	-
T18→TlpD	-	-	-	-
TlpD→T18	+/-	-	-	-
T18→CheW	+	-	+	-
CheW→T18	-	-	-	-
T18→CheV1	-	-	-	-
CheV1→T18	+	-	+	-
T18→CheV2	-	-	-	-
CheV2→T18	+	-	-	-
T18→CheV3	-	-	-	-
CheV3→T18	+/-	-	-	-

+ indicates protein pairs that showed blue colonies and thus indicate protein interaction, - indicates protein pairs that showed white colonies and thus no interaction, +/- indicates protein pairs that were hard to distinguish. The colors determined were confirmed independently on 3 different occasions.

APPENDIX 2

This appendix provides supplemental information to Chapter 3.

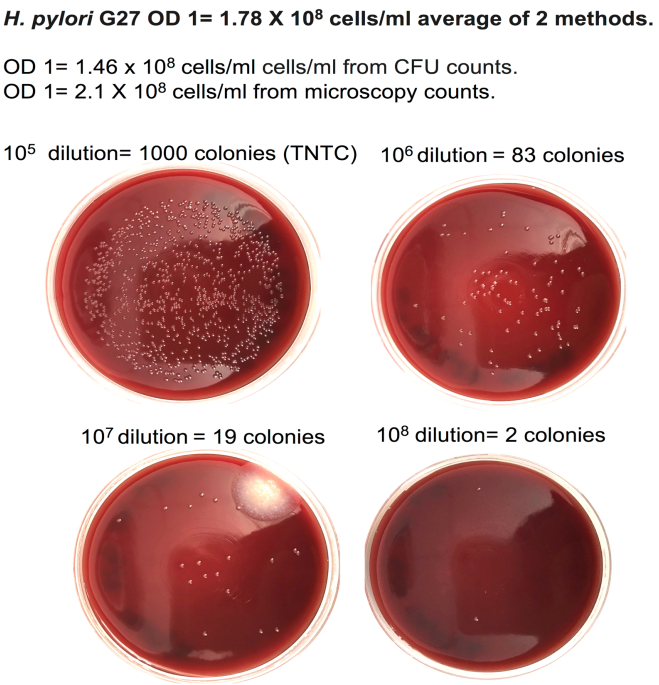

Figure S3.1. *H. pylori* cells were enumerated by microscopy and CFU counts. *H. pylori* liquid cultures were grown to an OD_{600} 0.2 and counted through microscopy. *H. pylori* liquid cultures were grown to various optical densities and plated on blood agar plates at various dilutions. Colony forming units (CFUs) were counted after 72 hours of growth as described.

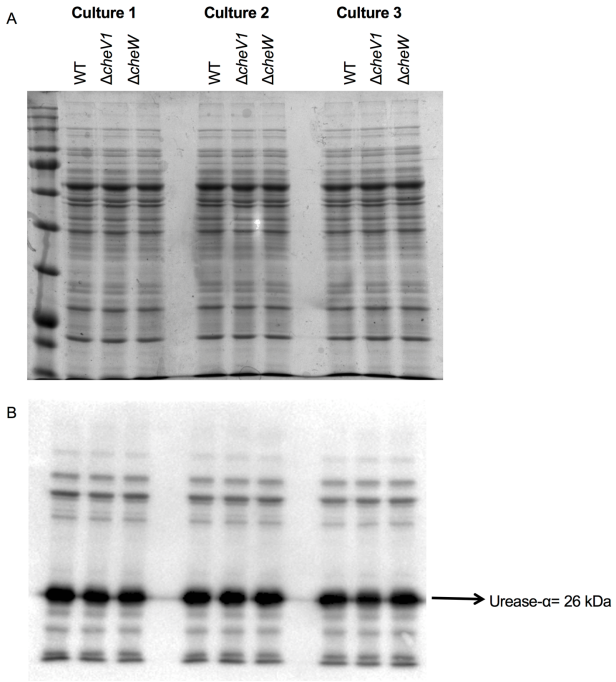

Figure S3.2. *H. pylori* cultures can be grown to yield constant protein amounts. *H. pylori* liquid cultures were grown to an OD_{600} 0.8-1 and all equalized to an OD_{600} of 0.7. Equal amounts of whole cell lysate from each culture was ran on a SDS-PAGE gel. (A) Commossie Blue stained SDS-PAGE gel with equal amount of cells (7.0×10^6 cells/well) of *H. pylori* G27 strains. (B) Urease-A western blot (3.5×10^6 cells/well) at 1:500 dilution anti-body.

Table S3.1. Bacterial strains and plasmids

Strain/plasmid	**Description/genotype**	**Origin/reference**
H. pylori G27		(Censini *et al.*, 1996)/ Nina Salama
H. pylori G27 Δ*cheA*	*ΔcheA::cat*	(Lertsethtakarn *et al.*, 2015)
H. pylori MG27 Δ*tlpABCD*	*ΔtlpC::aphA3*	(Lertsethtakarn *et al.*, 2015)
H. pylori G27 Δ*cheW*	*ΔcheW::aphA3*	(Terry *et al.*, 2005)
H. pylori G27 Δ*cheV1*	*ΔcheV1::cat*	(Lertsethtakarn *et al.*,

		2015)
H. pylori G27 Δ*cheV2*	*ΔcheV2::cat*	(Lertsethtakarn *et al.*, 2015)
H. pylori G27 Δ*cheV3*	*ΔcheV3::cat*	(Lertsethtakarn *et al.*, 2015)
E. coli BL21 CheAY	pTrc-*cheAY*	(Jiménez-Pearson *et al.*, 2005)/ Dagmar Beir
E. coli BL21 TlpD	pGEX-6P-2-*tlpD*	(Draper, Karplus and Ottemann, 2011)
E. coli BL21 CheW	pGEX-6P-2-*cheW*	(Collins *et al.*, 2016)
E. coli BL21 CheV1	pGEX-6P-2-*cheV1*	(Lertsethtakarn and Ottemann, 2010)
E. coli BL21 CheV2	pGEX-6P-2-*cheV2*	(Lertsethtakarn and Ottemann, 2010)
E. coli BL21 CheV3	pGEX-6P-2-*cheV3*	(Lertsethtakarn and Ottemann, 2010)

Table S3.2. Chemotaxis protein sizes

Protein	**Size (kDa)**
CheV1 (HPG27_18)	37
CheV2 (HPG27_576)	36
CheV3 (HPG27_1004)	36
CheW (HPG27_1006)	19
TlpA (HPG27_91)	75
TlpB (HPG27_95)	63
TlpD (HPG27_559)	48
CheA (HPG27_1005)	89

APPENDIX 3

This appendix provides supplemental information to Chapter 4.

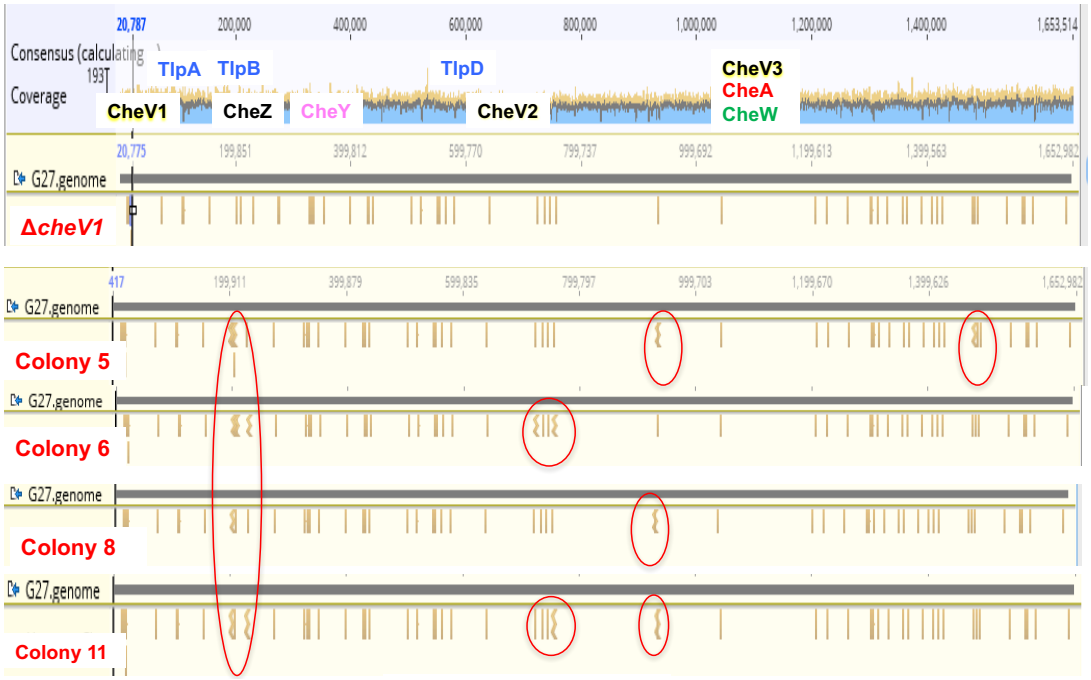

Figure S4.1. *cheV1* Che+ revertant sequences

References

Alexander, R. P., Lowenthal, A. C., Harshey, R. M. and Ottemann, K. M. (2010) 'CheV : CheW-like coupling proteins at the core of the chemotaxis signaling network', *Trends in microbiology*, 18(11), pp. 494–503. doi: 10.1016/j.tim.2010.07.004.

Baltrus, D. a, Amieva, M. R., Covacci, A., Lowe, T. M., Merrell, D. S., Ottemann, K. M., Stein, M., Salama, N. R. and Guillemin, K. (2009) 'The complete genome sequence of Helicobacter pylori strain G27.', *Journal of bacteriology*, 191(1), pp. 447–8. doi: 10.1128/JB.01416-08.

Battesti, A. and Bouveret, E. (2012) 'The bacterial two-hybrid system based on adenylate cyclase reconstitution in Escherichia coli', 58, pp. 325–334. doi: 10.1016/j.ymeth.2012.07.018.

Bauer, B. and Meyer, T. F. (2011) 'The Human Gastric Pathogen Helicobacter pylori and Its Association with Gastric Cancer and Ulcer Disease', *Ulcers*, 2011, pp. 1–23. doi: 10.1155/2011/340157.

Behrens, W., Schweinitzer, T., McMurry, J. L., Loewen, P. C., Buettner, F. F. R., Menz, S. and Josenhans, C. (2016) 'Localisation and protein-protein interactions of the Helicobacter pylori taxis sensor TlpD and their connection to metabolic functions', *Scientific Reports*. Nature Publishing Group, 6(April), p. 23582. doi: 10.1038/srep23582.

Bhattacharyya, R. P., Reményi, A., Yeh, B. J. and Lim, W. (2006) 'Domains, motifs, and scaffolds: the role of modular interactions in the evolution and wiring of cell signaling circuits.', *Annual review of biochemistry*, 75, pp. 655–680. doi: 10.1146/annurev.biochem.75.103004.142710.

Boukhvalova, M. S., Dahlquist, F. W. and Stewart, R. C. (2002) 'CheW binding interactions with CheA and Tar. Importance for chemotaxis signaling in Escherichia coli.', *The Journal of biological chemistry*, 277(25), pp. 22251–9. doi: 10.1074/jbc.M110908200.

Briegel, A., Ortega, D. R., Tocheva, E. I., Wuichet, K., Li, Z., Chen, S., Müller, A.,

Iancu, C. V, Murphy, G. E., Dobro, M. J., Zhulin, I. B. and Jensen, G. J. (2009) 'Universal architecture of bacterial chemoreceptor arrays.', *Proceedings of the National Academy of Sciences of the United States of America*, 106(40), pp. 17181–6. doi: 10.1073/pnas.0905181106.

Cannistraro, V. J., Glekas, G. D., Rao, C. V and Ordal, G. W. (2011) 'Cellular stoichiometry of the chemotaxis proteins in Bacillus subtilis.', *Journal of bacteriology*, 193(13), pp. 3220–7. doi: 10.1128/JB.01255-10.

Cassidy, C. K., Himes, B. A., Alvarez, F. J., Ma, J., Zhao, G., Perilla, J. R., Schulten, K. and Zhang, P. (2015) 'CryoEM and computer simulations reveal a novel kinase conformational switch in bacterial chemotaxis signaling', *eLife*, 4, pp. 1–20. doi: 10.7554/eLife.08419.

Castillo, A. R., Woodruff, A. J., Connolly, L. E., Sause, W. E. and Ottemann, K. M. (2008) 'Recombination-based in vivo expression technology identifies Helicobacter pylori genes important for host colonization.', *Infection and immunity*, 76(12), pp. 5632–44. doi: 10.1128/IAI.00627-08.

Censini, S., Lange, C., Xiang, Z., Crabtree, J. E., Ghiara, P., Borodovsky, M., Rappuoli, R. and Covacci, A. (1996) 'cag, a pathogenicity island of Helicobacter pylori, encodes type I-specific and disease-associated virulence factors (secretioninsertion sequenceinf lammationevolution)', *Genetics*, 93(December), pp. 14648–14653. doi: 10.1073/pnas.93.25.14648.

Cerda, O. A., Núñez-Villena, F., Soto, S. E., Ugalde, J. M., López-Solís, R. and Toledo, H. (2011) 'tlpA gene expression is required for arginine and bicarbonate chemotaxis in Helicobacter pylori', *Biological Research*, 44(3), pp. 277–282. doi: 10.4067/S0716-97602011000300009.

Clyne, M., Dolan, B. and Reeves, E. P. (2007) 'Bacterial factors that mediate colonization of the stomach and virulence of Helicobacter pylori.', *FEMS microbiology letters*, 268(2), pp. 135–43. doi: 10.1111/j.1574-6968.2007.00648.x.

Collins, K. D., Andermann, T. M., Draper, J., Sanders, L., Williams, S. M., Araghi, C. and Ottemann, K. M. (2016) *The* Helicobacter pylori *CZB cytoplasmic chemoreceptor TlpD forms an autonomous polar chemotaxis signaling complex that mediates a tactic response to oxidative stress*, *Journal of Bacteriology*. doi: 10.1128/JB.00071-16.

Cover, T. L. and Blaser, M. J. (2009) 'Helicobacter pylori in health and disease.', *Gastroenterology*. AGA Institute American Gastroenterological Association, 136(6), pp. 1863–73. doi: 10.1053/j.gastro.2009.01.073.

Croxen, M. A., Sisson, G., Melano, R. and Hoffman, P. S. (2006) 'The Helicobacter pylori chemotaxis receptor tlpB (HP0103) is required for pH taxis and for colonization of the gastric mucosa', *Journal of Bacteriology*, 188(7), pp. 2656–2665. doi: 10.1128/JB.188.7.2656-2665.2006.

Draper, J., Karplus, K. and Ottemann, K. M. (2011) 'Identification of a chemoreceptor zinc-binding domain common to cytoplasmic bacterial chemoreceptors.', *Journal of bacteriology*, 193(17), pp. 4338–45. doi: 10.1128/JB.05140-11.

Eismann, S. and Endres, R. G. (2015) 'Protein Connectivity in Chemotaxis Receptor Complexes', *PLoS Computational Biology*, 11(12), pp. 1–21. doi: 10.1371/journal.pcbi.1004650.

Erbse, A. H. and Falke, J. J. (2009) 'The core signaling proteins of bacterial chemotaxis assemble to form an ultrastable complex', *Biochemistry*, 48(29), pp. 6975–6987. doi: 10.1021/bi900641c.

Foynes, S., Dorrell, N., Ward, S. J., Stabler, R. a, McColm, a a, Rycroft, a N. and Wren, B. W. (2000) 'Helicobacter pylori possesses two CheY response regulators and a histidine kinase sensor, CheA, which are essential for chemotaxis and colonization of the gastric mucosa.', *Infection and immunity*, 68(4), pp. 2016–23.

Fraser, C., Casjens, S. and Huang, W. (1997) 'Genomic sequence of a Lyme disease spirochaete, Borrelia burgdorferi', *Nature*, 390(December), pp. 580–586. doi: doi:10.1038/37551.

Fredrick, K. L. and Helmann, J. D. (1994) 'Dual chemotaxis signaling pathways in Bacillus subtilis: a sigma D-dependent gene encodes a novel protein with both CheW and CheY homologous domains.', *Journal of bacteriology*, 176(9), pp. 2727–35.

Good, M. C., Zalatan, J. G. and Lim, W. A. (2011) 'Scaffold Proteins: Hubs for Controlling the Flow of Cellular Information', *Science*, 332(6030), pp. 680–686.

doi: 10.1126/science.1198701.

Greenswag, A. R., Li, X., Borbat, P. P., Samanta, D., Watts, K. J., Freed, J. H. and Crane, B. R. (2015) 'Preformed Soluble Chemoreceptor Trimers That Mimic Cellular Assembly States and Activate CheA Autophosphorylation', *Biochemistry*, 54(22), pp. 3454–3468. doi: 10.1021/bi501570n.

Hartley-tassell, L. E., Shewell, L. K., Day, C. J., Wilson, J. C., Sandhu, R., Ketley, J. M. and Korolik, V. (2010) 'Identification and characterization of the aspartate chemosensory receptor of Campylobacter jejuni', 75(January), pp. 710–730. doi: 10.1111/j.1365-2958.2009.07010.x.

Howitt, M. R. and Lee, J. Y. (2011) 'ChePep Controls Helicobacter pylori Infection of the Gastric Glands and Chemotaxis in the Epsilonproteobacteria'. doi: 10.1128/mBio.00098-11.Editor.

Huang, J. Y., Sweeney, E. G., Sigal, M., Zhang, H. C., Remington, S. J., Cantrell, M. A., Kuo, C. J., Guillemin, K. and Amieva, M. R. (2015) 'Chemodetection and destruction of host urea allows Helicobacter pylori to locate the epithelium', *Cell Host and Microbe*. Elsevier Inc., 18(2), pp. 147–156. doi: 10.1016/j.chom.2015.07.002.

Jiménez-Pearson, M.-A., Delany, I., Scarlato, V. and Beier, D. (2005) 'Phosphate flow in the chemotactic response system of Helicobacter pylori.', *Microbiology (Reading, England)*, 151(Pt 10), pp. 3299–311. doi: 10.1099/mic.0.28217-0.

Karatan, E., Saulmon, M. M., Bunn, M. W. and Ordal, G. W. (2001) 'Phosphorylation of the Response Regulator CheV Is Required for Adaptation to Attractants during Bacillus subtilis Chemotaxis', 276(47), pp. 43618–43626. doi: 10.1074/jbc.M104955200.

Karimova, G., Pidoux, J., Ullmann, A. and Ladant, D. (1998) 'A bacterial two-hybrid system based on a reconstituted signal transduction pathway', 95(May), pp. 5752–5756.

Keilberg, D. and Ottemann, K. M. (2015) 'H. pylori GPS: Modulating host metabolites for location sensing', *Cell Host and Microbe*. Elsevier Inc., 18(2), pp. 135–136. doi: 10.1016/j.chom.2015.07.013.

Kentner, D. and Sourjik, V. (2006) ‘Spatial organization of the bacterial chemotaxis system.’, *Current opinion in microbiology*, 9(6), pp. 619–24. doi: 10.1016/j.mib.2006.10.012.

Kentner, D., Thiem, S., Hildenbeutel, M. and Sourjik, V. (2006) ‘Determinants of chemoreceptor cluster formation in Escherichia coli.’, *Molecular microbiology*, 61(2), pp. 407–17. doi: 10.1111/j.1365-2958.2006.05250.x.

Kirby, J. R. (2009) ‘Chemotaxis-like regulatory systems: unique roles in diverse bacteria.’, *Annual review of microbiology*, 63, pp. 45–59. doi: 10.1146/annurev.micro.091208.073221.

Konovalova, A., Löbach, S. and Søgaard-Andersen, L. (2012) ‘A RelA-dependent two-tiered regulated proteolysis cascade controls synthesis of a contact-dependent intercellular signal in Myxococcus xanthus’, *Molecular Microbiology*, 84(2), pp. 260–275. doi: 10.1111/j.1365-2958.2012.08020.x.

Korolik, V. (2010) ‘Aspartate chemosensory receptor signalling in Campylobacter jejuni’, *Virulence*, 1(5), pp. 414–417. doi: DOI 10.4161/viru.1.5.12735.

Kusters, J. G., van Vliet, A. H. M. and Kuipers, E. J. (2006) ‘Pathogenesis of Helicobacter pylori infection.’, *Clinical microbiology reviews*, 19(3), pp. 449–90. doi: 10.1128/CMR.00054-05.

Lertsethtakarn, P., Draper, J. and Ottemann, K. M. (2012) ‘Chemotactic Signal Transduction in’, in *Two-Component Systems in Bacteria*. Caister Academic Press, pp. 355–370.

Lertsethtakarn, P., Howitt, M. R., Castellon, J., Amieva, M. R. and Ottemann, K. M. (2015) ‘Helicobacter pylori CheZ(HP) and ChePep form a novel chemotaxis-regulatory complex distinct from the core chemotaxis signaling proteins and the flagellar motor’, *Molecular Microbiology*, 97(6), pp. 1063–1078. doi: 10.1111/mmi.13086.

Lertsethtakarn, P. and Ottemann, K. M. (2010) ‘A remote CheZ orthologue retains phosphatase function.’, *Molecular microbiology*, 77(1), pp. 225–35. doi: 10.1111/j.1365-2958.2010.07200.x.

Lertsethtakarn, P., Ottemann, K. M. and Hendrixson, D. R. (2011) 'Motility and chemotaxis in Campylobacter and Helicobacter .', *Annual review of microbiology*, 65, pp. 389–410. doi: 10.1146/annurev-micro-090110-102908.

Li, M. and Hazelbauer, G. L. (2004) 'Cellular stoichiometry of the components of the chemotaxis signaling complex', *Journal of Bacteriology*, 186(12), pp. 3687–3694. doi: 10.1128/JB.186.12.3687-3694.2004.

Li, M. and Hazelbauer, G. L. (2014) 'Selective allosteric coupling in core chemotaxis signaling complexes.', *Proceedings of the National Academy of Sciences of the United States of America*, 2014(6), pp. 1–6. doi: 10.1073/pnas.1415184111.

Li, M., Khursigara, C. M., Subramaniam, S. and Hazelbauer, G. L. (2011) 'Chemotaxis kinase CheA is activated by three neighbouring chemoreceptor dimers as effectively as by receptor clusters', *Molecular Microbiology*, 79(3), pp. 677–685. doi: 10.1111/j.1365-2958.2010.07478.x.

Liu, J., Hu, B., Morado, D. R., Jani, S., Manson, M. D. and Margolin, W. (2012) 'Molecular architecture of chemoreceptor arrays revealed by cryoelectron tomography of Escherichia coli minicells', *Proceedings of the National Academy of Sciences of the United States of America*, 109(3), pp. E1481--E1488. doi: 10.1073/pnas.1200781109.

Locasale, J. W., Shaw, A. S. and Chakraborty, A. K. (2007) 'Scaffold proteins confer diverse regulatory properties to protein kinase cascades.', *Proceedings of the National Academy of Sciences of the United States of America*, 104, pp. 13307–13312. doi: 10.1073/pnas.0706311104.

Lowenthal, A. C., Hill, M., Sycuro, L. K., Mehmood, K., Salama, N. R. and Ottemann, K. M. (2009) 'Functional analysis of the Helicobacter pylori flagellar switch proteins.', *Journal of bacteriology*, 191(23), pp. 7147–56. doi: 10.1128/JB.00749-09.

Lowenthal, A. C., Simon, C., Fair, A. S., Mehmood, K., Terry, K., Anastasia, S. and Ottemann, K. M. (2009) 'A fixed-time diffusion analysis method determines that the three cheV genes of Helicobacter pylori differentially affect motility', pp. 1181–1191. doi: 10.1099/mic.0.021857-0.

Maddock, J. R. and Shapiro, L. (1993) ‘Polar location of the chemoreceptor complex in the Escherichia coli cell.’, *Science (New York, N.Y.)*, 259(5102), pp. 1717–1723. doi: 10.1126/science.8456299.

McClain, M. S., Shaffer, C. L., Israel, D. a, Peek, R. M. and Cover, T. L. (2009) ‘Genome sequence analysis of Helicobacter pylori strains associated with gastric ulceration and gastric cancer.’, *BMC genomics*, 10, p. 3. doi: 10.1186/1471-2164-10-3.

Miller, J. H. (1972) ‘Experiments in Molecular Genetics, Cold Spring Harbor Laboratory Press’, p. Cold Spring Harbor, NY.

Miller, L. D., Russel, Matthew, H. and Alexander, G. (2009) ‘Chapter 3 Diversity in Bacterial Chemotactic Responses and Niche Adaptation’, *Advances in Applied Microbiology*, 66, pp. 53–75.

Mirel, D. B., Estacio, W. F., Mathieu, M., Olmsted, E., Ramirez, J. and Márquez-Magaña, L. M. (2000) ‘Environmental regulation of Bacillus subtilis sigma(D)-dependent gene expression.’, *Journal of bacteriology*, 182(11), pp. 3055–3062.

Mobley Harry L.T, M. G. L. and H. S. L. (2001) *Helicobacter pylori physiology and genetics*, *Proceedings of the Royal Society of Medicine*. ASM Press.

Motif, A. (2008) ‘Nuclear Complex Co-IP Kit’, (54001).

Ortega, D. R. and Zhulin, I. B. (2016) ‘Evolutionary Genomics Suggests That CheV Is an Additional Adaptor for Accommodating Specific Chemoreceptors within the Chemotaxis Signaling Complex’, *PLOS Computational Biology*, 12(2), p. e1004723. doi: 10.1371/journal.pcbi.1004723.

Parkinson, J. S., Hazelbauer, G. L. & Falke, J. J. (2015) ‘Signaling and sensory adaptation in Escherichia coli chemoreceptors: 2015 update.’, *Trends Microbiol.*, 23, pp. 257–266.

Pereira, L. and Hoover, T. R. (2005) ‘Stable accumulation of sigma 54 in Helicobacter pylori requires the novel protein HP0958’, *Journal of Bacteriology*, pp. 4463–4469. doi: 10.1128/JB.187.13.4463-4469.2005.

Piasta, K. N. and Falke, J. J. (2015) ‘Increasing and Decreasing the Ultrastability of Bacterial Chemotaxis Core Signaling Complexes by Modifying Protein − Protein Contacts’, *Biochemistry*, 53(August), pp. 5592–5600. doi: 10.1021/bi500849p.

Piñas, G. E., Frank, V., Vaknin, A. and Parkinson, J. S. (2016) ‘The source of high signal cooperativity in bacterial chemosensory arrays’, *Proceedings of the National Academy of Sciences*, 113(12), p. 201600216. doi: 10.1073/pnas.1600216113.

Pittman, M. S., Goodwin, M. and Kelly, D. J. (2001) ‘Chemotaxis in the human gastric pathogen Helicobacter pylori: different roles for CheW and the three CheV paralogues, and evidence for CheV2 phosphorylation.’, *Microbiology (Reading, England)*, 147, pp. 2493–504.

Polk, D. B. and Peek, R. M. (2010) ‘Helicobacter pylori: gastric cancer and beyond.’, *Nature reviews. Cancer*. Nature Publishing Group, 10(6), pp. 403–14. doi: 10.1038/nrc2857.

Porter, S. L., Wadhams, G. H. and Armitage, J. P. (2011) ‘Signal processing in complex chemotaxis pathways.’, *Nature reviews. Microbiology*. Nature Publishing Group, 9(3), pp. 153–65. doi: 10.1038/nrmicro2505.

Qin, Z., Lin, W., Zhu, S., Franco, A. T. and Liu, J. (2016) ‘Imaging the motility and chemotaxis machineries in *Helicobacter pylori* by cryo-electron tomography’, *Journal of Bacteriology*, (November), p. JB.00695-16. doi: 10.1128/JB.00695-16.

Rader, B. a, Wreden, C., Hicks, K. G., Sweeney, E. G., Ottemann, K. M. and Guillemin, K. (2011) ‘Helicobacter pylori perceives the quorum-sensing molecule AI-2 as a chemorepellent via the chemoreceptor TlpB.’, *Microbiology (Reading, England)*, 157(Pt 9), pp. 2445–55. doi: 10.1099/mic.0.049353-0.

Rao, C. V, Glekas, G. D. and Ordal, G. W. (2008) ‘The three adaptation systems of Bacillus subtilis chemotaxis’, *Trends in microbiology*, 16(10), pp. 480–487. doi: 10.1016/j.tim.2008.07.003.The.

Ringgaard, S., Zepeda-Rivera, M., Wu, X., Schirner, K., Davis, B. M. and Waldor, M. K. (2014) ‘ParP prevents dissociation of CheA from chemotactic signaling arrays and tethers them to a polar anchor.’, *Proceedings of the National Academy of Sciences of the United States of America*, 111(2), pp. E255-64. doi:

10.1073/pnas.1315722111.

Rolig, A. S., Shanks, J., Carter, J. E. and Ottemann, K. M. (2012) 'Helicobacter pylori requires TlpD-driven chemotaxis to proliferate in the antrum', *Infection and Immunity*, 80(10), pp. 3713–3720. doi: 10.1128/IAI.00407-12.

Rosario, M. L., Fredrick, K. L., Ordal, G. W. and Helmann, J. D. (1994) 'Chemotaxis in Bacillus subtilis Requires Either of Two Functionally Redundant CheW Homologs', 176(9).

Sanders, L., Andermann, T. M. and Ottemann, K. M. (2013) 'A supplemented soft agar chemotaxis assay demonstrates the Helicobacter pylori chemotactic response to zinc and nickel', *Microbiology*, 159(1), pp. 46–57. doi: 10.1099/mic.0.062877-0.

Sause, W. E., Castillo, A. R. and Ottemann, K. M. (2012) 'The Helicobacter pylori autotransporter ImaA (HP0289) modulates the immune response and contributes to host colonization.', *Infection and immunity*, 80(7), pp. 2286–96. doi: 10.1128/IAI.00312-12.

Schneider, C. a, Rasband, W. S. and Eliceiri, K. W. (2012) 'NIH Image to ImageJ: 25 years of image analysis', *Nature Methods*. Nature Publishing Group, 9(7), pp. 671–675. doi: 10.1038/nmeth.2089.

Sharma, C. M., Hoffmann, S., Darfeuille, F., Reignier, J., Findeiss, S., Sittka, A., Chabas, S., Reiche, K., Hackermüller, J., Reinhardt, R., Stadler, P. F. and Vogel, J. (2010) 'The primary transcriptome of the major human pathogen Helicobacter pylori.', *Nature*, 464(7286), pp. 250–255. doi: 10.1038/nature08756.

Shaw, A. S. and Filbert, E. L. (2009) 'Scaffold proteins and immune-cell signalling.', *Nature reviews. Immunology*, 9(1), pp. 47–56. doi: 10.1038/nri2473.

Sourjik, V. (2004) 'Receptor clustering and signal processing in E. coli chemotaxis.', *Trends in microbiology*, 12(12), pp. 569–76. doi: 10.1016/j.tim.2004.10.003.

Sourjik, V. and Armitage, J. P. (2010) 'Spatial organization in bacterial chemotaxis.', *The EMBO journal*. Nature Publishing Group, 29(16), pp. 2724–33.

doi: 10.1038/emboj.2010.178.

Soutourina, O. A. and Bertin, P. N. (2003) ‘Regulation cascade of flagellar expression in Gram-negative bacteria’, *FEMS Microbiology Reviews*, 27(4), pp. 505–523. doi: 10.1016/S0168-6445(03)00064-0.

Studdert, C. A. and Parkinson, J. S. (2005) ‘Insights into the organization and dynamics of bacterial chemoreceptor clusters through in vivo crosslinking studies’.

Szurmant, H., Bunn, M. W., Cannistraro, V. J. and Ordal, G. W. (2003) ‘Bacillus subtilis hydrolyzes CheY-P at the location of its action, the flagellar switch.’, *The Journal of biological chemistry*, 278(49), pp. 48611–6. doi: 10.1074/jbc.M306180200.

Terry, K., Go, A. C. and Ottemann, K. M. (2006) ‘Proteomic mapping of a suppressor of non-chemotactic cheW mutants reveals that Helicobacter pylori contains a new chemotaxis protein’, *Molecular Microbiology*, 61(4), pp. 871–882. doi: 10.1111/j.1365-2958.2006.05283.x.

Terry, K., Williams, S. M., Connolly, L. and Ottemann, K. M. (2005) ‘Chemotaxis Plays Multiple Roles during Helicobacter pylori Animal Infection’, 73(2), pp. 803–811. doi: 10.1128/IAI.73.2.803.

Tomb, J. F., White, O., Kerlavage, A. R. and Al., E. (1997) ‘The complete genome sequence of the gastric pathogen Helicobacter pylori’, *Nature*, 388(September), pp. 539–47. doi: 10.1038/41483.

Typas, A. and Sourjik, V. (2015) ‘Bacterial protein networks: properties and functions’, *Nat Rev Micro*. Nature Publishing Group, 13(9), pp. 559–572. doi: 10.1038/nrmicro3508.

Voland, P., Weeks, D. L., Marcus, E. a, Prinz, C., Sachs, G. and Scott, D. (2003) ‘Interactions among the seven Helicobacter pylori proteins encoded by the urease gene cluster.’, *American journal of physiology. Gastrointestinal and liver physiology*, 284(1), pp. G96–G106. doi: 10.1152/ajpgi.00160.2002.

Wadhams, G. H. and Armitage, J. P. (2004) ‘Making sense of it all: bacterial

chemotaxis.', *Nature reviews. Molecular cell biology*, 5(12), pp. 1024–37. doi: 10.1038/nrm1524.

Walukiewicz, H. E., Tohidifar, P., Ordal, G. W. and Rao, C. V. (2014) 'Interactions among the three adaptation systems of Bacillus subtilis chemotaxis as revealed by an in vitro receptor-kinase assay', *Molecular Microbiology*, 93(August), pp. 1104–1118. doi: 10.1111/mmi.12721.

White, C. L., Kitich, A. and Gober, J. W. (2010) 'Positioning cell wall synthetic complexes by the bacterial morphogenetic proteins MreB and MreD.', *Molecular microbiology*, 76(3), pp. 616–33. doi: 10.1111/j.1365-2958.2010.07108.x.

Williams, S. M., Chen, Y. T., Andermann, T. M., Carter, J. E., McGee, D. J. and Ottemann, K. M. (2007) 'Helicobacter pylori chemotaxis modulates inflammation and bacterium-gastric epithelium interactions in infected mice', *Infection and Immunity*, pp. 3747–3757. doi: 10.1128/IAI.00082-07.

Yamaoka, Y. (2008) *Helicobacter pylori: Molecular Genetics and Cellular Biology*. Edited by U. Yoshio Yamaoka Michael E. DeBakey Veterans Affairs Medical Center, TX 77030. Caister Academic Press.

Zeke, A., Lukacs, M., Lim, W. A. and Remenyi, A. (2009) 'Scaffolds: interaction platforms for cellular signalling circuits', *Trends in Cell Biology*, 19(8), pp. 364–374. doi: 10.1016/j.tcb.2009.05.007.

Zhang, K., Liu, J., Tu, Y., Xu, H., Charon, N. W. and Li, C. (2012) 'Two CheW coupling proteins are essential in a chemosensory pathway of Borrelia burgdorferi', *Molecular Microbiology*, 85(4), pp. 782–794. doi: 10.1111/j.1365-2958.2012.08139.x.

Zhao, J. and Parkinson, J. S. (2006) 'Mutational Analysis of the Chemoreceptor-Coupling Domain of the Escherichia coli Chemotaxis Signaling Kinase CheA Mutational Analysis of the Chemoreceptor-Coupling Domain of the Escherichia coli Chemotaxis Signaling Kinase CheA', 188(9), pp. 3299–3307. doi: 10.1128/JB.188.9.3299.